

**HIGH RESOLUTION MOLECULAR BEAM STUDY
OF
ALKALI CYANIDES**

**HIGH RESOLUTION MOLECULAR BEAM STUDY
OF
ALKALI CYANIDES**

PROMOTOR: PROF. DR. A. DYMANUS

CO-REFERENT: DR. W.L. MEERTS

**HIGH RESOLUTION MOLECULAR BEAM STUDY
OF
ALKALI CYANIDES**

PROEFSCHRIFT

TER VERKRIJGING VAN DE GRAAD VAN DOCTOR
IN DE WISKUNDE EN NATUURWETENSCHAPPEN
AAN DE KATHOLIEKE UNIVERSITEIT TE NIJMEGEN
OP GEZAG VAN DE RECTOR MAGNIFICUS
PROF. DR. J.H.G.I. GIESBERS
VOLGENS BESLUIT VAN HET COLLEGE VAN DEKANEN
IN HET OPENBAAR TE VERDEDIGEN
OP DINSDAG 13 DECEMBER 1983
DES NAMIDDAGS TE 4.00 UUR

door

JOHANNES JACOBUS VAN VAALS

geboren te Gilze en Rijen

Graag wil ik op deze plaats iedereen bedanken die heeft bijgedragen tot het slagen van het onderzoek en het tot stand komen van het proefschrift, met name:

de (oud-)leden van de afdeling Atoom- en Molecuulfysica voor de goede samenwerking;

Leo Hendriks, John Holtkamp, Eugène van Leeuwen, Frans van Rijn, Cor Sikkens en Jaap Nieboer voor hun onmisbare en bekwame ondersteuning op elektronisch en technisch gebied;

Alfons Gebbink, die aan het onderzoek heeft meegewerkt tijdens zijn afstudeerperiode

de dienstverlenende afdelingen van de Faculteit der Wiskunde en Natuurwetenschappen, onder leiding van de heren P. Walraven (Instrumentmakerij), H. Verschoor (Service Instrumentmakerij), J. Holten (Glasinstrumentmakerij), W. Verdijk (Illustratie) en H. Spruyt (Fotografie);

het Universitair Rekencentrum voor de geboden faciliteiten;

en heel speciaal Mariël van Dijk.

Dit onderzoek is onderdeel van het research programma van de Stichting voor Fundamenteel Onderzoek der Materie (F.O.M.) en is mogelijk gemaakt door financiële steun van de Nederlandse Organisatie voor Zuiver Wetenschappelijk Onderzoek (Z.W.O.).

Aan mijn ouders

Aan Mariël

CONTENTS

CHAPTER I *Introduction*

1. Background and goal	9
2. The molecular beam electric resonance spectrometer	11
3. Outline of results	15
References	18

CHAPTER II *Theory*

1. Rotational structure	20
2. Hyperfine structure	23
3. Molecular structure	25
References	26

CHAPTER III *Molecular beam electric resonance study of KCN, K¹³CN and KC¹³N*

Abstract	27
1. Introduction	28
2. Experimental	29
3. Theory	30
4. Results	31
5. Structure	36
6. Discussion	37
Appendix	42
References	48

CHAPTER IV-A *Structure of sodium cyanide by molecular beam electric resonance spectroscopy*

Abstract	51
Letter	52
References	56

CHAPTER IV-B *High resolution molecular beam spectroscopy of NaCN and Na¹³CN*

Abstract	57
1. Introduction	58

2. Experimental results	59
3. Structure	65
4. Discussion	66
Appendix	70
References	76

CHAPTER V Rotational spectrum, hyperfine spectrum, and structure of lithium isocyanide

Abstract	78
1. Introduction	79
2. Experimental	80
3. Results	84
4. Discussion	90
References	92

TITEL EN SAMENVATTING 94

CURRICULUM VITAE 96

The following chapters are (modified) versions of publications:

- *CHAPTER III:* J.J. van Vaals, W.L. Meerts, and A. Dymanus; *J. Mol. Spectrosc.*, submitted (1983).
- *CHAPTER IV-A:* J.J. van Vaals, W.L. Meerts, and A. Dymanus; *J. Chem. Phys.* **77**, 5245 (1982).
- *CHAPTER IV-B:* J.J. van Vaals, W.L. Meerts, and A. Dymanus; *Chem. Phys.*, submitted (1983).
- *CHAPTER V:* J.J. van Vaals, W.L. Meerts, and A. Dymanus; *Chem. Phys.*, accepted for publication (1983).

INTRODUCTION

1. BACKGROUND AND GOAL

Until recently the gaseous alkali metal cyanides¹ were assumed to have a linear structure, as established experimentally for hydrogen cyanide² and the cyanogen halides³. From vibrational isotope effects of the alkali metal cyanides in inert gas matrices Ismail *et al.*⁴ concluded the structural configuration of KCN and NaCN to be linear cyanide, and of LiNC linear isocyanide. *Ab initio* calculations on KCN by Pietro *et al.*⁵ and on LiNC by Bak *et al.* and Clementi *et al.*⁶ also predicted a linear cyanide and isocyanide geometry, respectively. Computations of the potential energy surface in the bending direction by Clementi *et al.*⁶ indicated that LiNC has a very low barrier (~0.3 eV) for internal rotation of the Li⁺ cation around the CN⁻ anion. In this case no structural formula is preferred and the bond is called "polytopic". Molecules in vibrational states lying below the barrier will show large amplitude motions. The anharmonicity and the low barrier of the potential energy affect strongly the structure of the rotational and vibrational levels.

A well resolved microwave absorption spectrum of KCN was first observed by Kuijpers *et al.*⁷ in the 100 GHz range. Unexpectedly, this spectrum could not be fitted to a linear rotor model. Microwave absorption measurements in Berlin and molecular beam electric resonance (MBER) experiments in Nijmegen⁸ established that potassium cyanide in the ground vibrational state has a T-shaped structure. However, this structure determination required the assumption of one structural parameter, since the rotational spectrum of only one isotopic species was measured. For a nonsymmetric triatomic molecule rotational information on at least two, and in the case of a linear molecule three, isotopic species is needed to calculate the structure. So, a more accurate and unambiguous structure determination of KCN than performed by Topping *et al.*⁹ is achieved by the observation of the rotational spectra of isotopically substituted species. Since

the experimentally determined structure of KCN is T shaped, whereas the *ab initio* structure of LiNC computed by Clementi *et al.*⁶ is linear, no reliable prediction can be made for the structure of NaCN. A precise structure determination for LiNC is a good test for the *ab initio* calculations⁶ Because no full potential energy surface was computed, and the calculated isomerization energy is very low, even the possibility of a linear cyanide or nonlinear structure cannot be ruled out for LiNC. A decisive structure determination for KCN, NaCN and LiNC will yield valuable information on the potential energy surface and deeper understanding of the weak internal interaction in floppy molecules, which the alkali metal cyanides are expected to be.

So far there is no information available in the literature on any spectrum (microwave, infrared, visible) of the gaseous alkali metal cyanides apart from the results of Kuypers *et al.*⁷ and Topping *et al.*⁸ for potassium cyanide, and the disputed⁴ infrared absorption study by Leroi and Klemperer⁹.

KCN and NaCN are stable compounds, but high temperatures of approximately 1100 K are needed to obtain sufficiently high vapour pressures of about 1 mbar to produce a molecular beam and observe transitions. At such temperatures reactions occur of the alkali metal cyanides with the material of the oven wall, and there is thermal dissociation and polymerization. Earlier attempts by Kuypers and Topping in our laboratory to observe microwave absorption of NaCN in a cell failed. The chemical stability of LiNC is very poor, even at room temperature. Also for this molecule high temperatures of about 1050 K are required, and producing a stable molecular beam is even more difficult than for KCN and NaCN.

In the present investigation the rotational and hyperfine spectra of several isotopic species of potassium cyanide, sodium cyanide and lithium isocyanide are studied by molecular beam electric resonance spectroscopy in the microwave region. This method furnishes high sensitivity at very high resolution, in the order of 10 kHz. The hyperfine structure can be resolved and used to identify a molecule and to study its internal field which depends on the electronic distribution. The seeded beam technique is applied to produce a supersonic expansion through a nozzle of a molecular beam, yielding strong translational, rotational and vibrational cooling. This enhances the intensity of the observed transitions and simplifies the rotational spectra, facilitating the analysis and identification considerably. The material consumption in a seeded beam is very low, which makes it possible to study expensive isotopically enriched samples. The problem of identification of the very complicated hyperfine spectrum is solved by the application of the microwave-microwave double resonance technique.

2. THE MOLECULAR BEAM ELECTRIC RESONANCE SPECTROMETER

The molecular beam electric resonance technique is well established (a review is given, for example, by Zorn and English¹⁰). The principle is illustrated in Fig. 1. The source produces a well defined molecular beam. Molecules traversing the A-, C- and B-field in quantum states with positive Stark effect are forced in the inhomogeneous electric fields present in the A-field (state selector, or polarizer) and B-field (state analyzer) towards the molecular beam axis (trajectories indicated by solid lines in Fig. 1). Those with negative Stark effect are deflected out of the beam (trajectories indicated by dashed lines in Fig. 1). The detector measures the flux of molecules in the beam. So, if in the electric resonance section (C-field) a transition is induced from a state in which the molecules are transmitted by the A- as well as the B-field to a state rejected by the B-field, the number of detected molecules will decrease (flop-out). This technique requires a nonzero electric dipole moment of the molecule.

An outline of the MBER-spectrometer used in the present investigations is presented in Fig. 2. The molecular beam is produced in a supersonic expansion of the alkali metal cyanide molecules diluted (0.1-1%) in argon with a backing pressure of about 1 bar through the 130 μm nozzle of the high temperature double chamber oven. A stainless steel oven of the type described by Törning *et al.*⁹ was employed for the experiments on KCN and NaCN. At the high temperatures of typically 1100 K for the supply chamber of the oven, necessary to obtain about 1 mbar vapour pressure of the alkali cyanides, and 1300 K for the nozzle chamber, required to avoid clogging of the nozzle, reactions of the molecules with the oven wall occur and decomposition, thermal dissociation and polymerization impede the production of a molecular beam. For NaCN, these problems were more serious than for KCN, and it took several weeks of running to pacify the oven adequately to maintain a stable beam during a few hours. Since LiNC is known to be very unstable, for this molecule a new double cham-

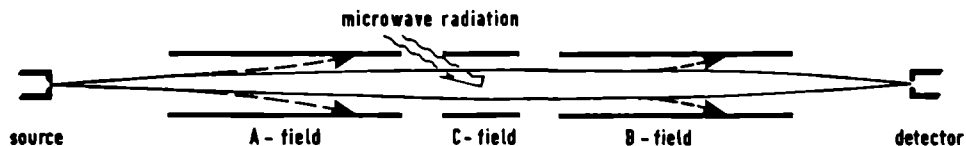


Fig. 1. Principle of the molecular beam electric resonance technique.

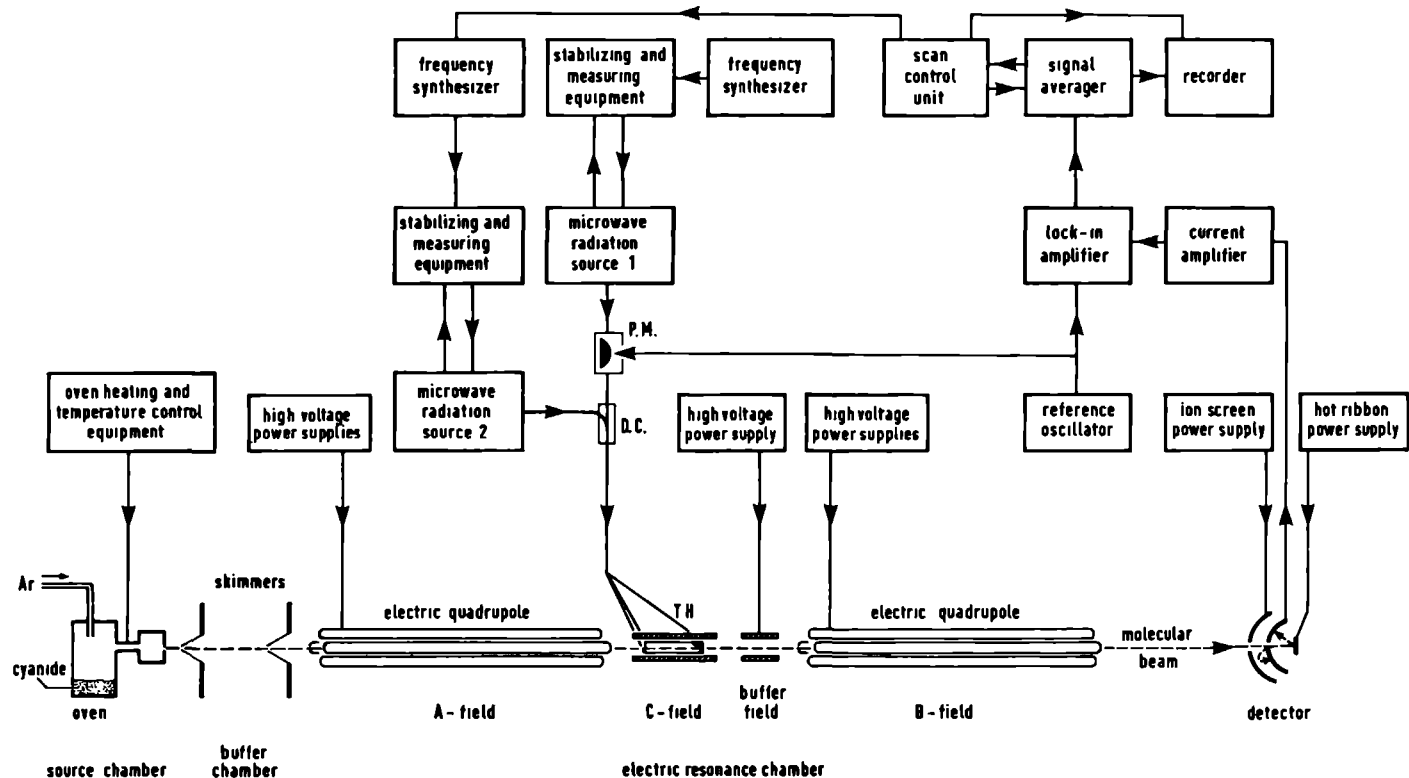


Fig. 2. Outline of the spectrometer. The source and buffer chambers are pumped by a 6000 l/s and 1000 l/s oil diffusion pump, respectively, with water cooled baffles; the vacuum chamber containing the electric

resonance section and the detector is pumped by two 700 l/s oil diffusion pumps with baffles cooled by liquid nitrogen. P.M.: power modulator; D.C.: directional coupler; T.H.: transmitting horn.

ber oven was developed, made of tantalum (a schematic view of the oven is presented in Chapter V, Section 2). This was a very successful attack of the problem, and essential for the production of a stable molecular beam of LiNC molecules.

The oven is located in the source chamber (pressure at operating conditions typically 2×10^{-4} mbar). The divergence of the beam is limited by a conical skimmer with an aperture of 1.36 mm. A buffer chamber (pressure of 5×10^{-6} mbar) separates the source chamber from the electric resonance section, which is isolated from the buffer chamber by a second skimmer with an aperture of 2 mm. The A-, C- and B-fields and the detector are located in the electric resonance chamber (pressure of 1×10^{-7} mbar).

The state selection in the A- and B-fields is performed by 34 cm long electric quadrupoles. The cylindrical electrodes are 10 mm in diameter and are mounted on perspex rings to form an inhomogeneous electric field with a diameter ($\approx 2r_0$) of 10 mm. The applied potential difference ($\approx 2V_0$) between two adjacent rods can be as high as 40 kV before breakdown occurs. In such a field molecules with a permanent electric dipole moment μ will experience an external force F_r in the radial direction given by:

$$F_r = -(\partial W / \partial E)(\partial E / \partial r) = -\mu_{\text{eff}}(2V_0 / r_0^2), \quad (1)$$

where W is the Stark energy, E is the electric field strength and μ_{eff} is the effective dipole moment, which depends on E and on the quantum state of the molecule. The force is directed towards the state selector axis for $\mu_{\text{eff}} > 0$ (positive Stark effect) and away from it for $\mu_{\text{eff}} < 0$ (negative Stark effect).

In the buffer field a homogeneous electric field can be applied in order to preserve the space quantization of molecular states. Due to lack of space no buffer field could be installed between the A- and C-field.

The C-field consists of two parallel metal plates. Microwaves are irradiated through a transmitting horn¹¹ and a Rexolite lens in order to produce a plane travelling wavefront. The radiation propagates between the plates perpendicularly to the molecular beam axis. Standing waves, which can distort the spectral lineshape are avoided by an absorber at the end of the transmission line, which prevents reflections of the microwave radiation.

The detector is of the surface ionization type with an effective aperture of 3×3 mm. The iridium ribbon of the detector is oxygenated before each run and 100% detection efficiency is achieved for potassium, sodium and lithium compounds. An ion screen is placed in front of the collector, and is kept at a po-

tential sufficiently high to repulse back ions leaving the hot iridium ribbon and escaping through the aperture in the collector. This arrangement increases the signal with 30%.

A simplified diagram of the microwave and detection system in the microwave-microwave double resonance set-up is shown in Fig 2. Two microwave radiation sources [OKI klystrons or Varian backward wave oscillators(BWO)] are independently frequency stabilized by phase locking to Hewlett-Packard 8660B and 5105A synthesizers. For frequencies higher than 40 GHz, an intermediate X-band oscillator was used to facilitate locking. Oscillator 1 is kept at a fixed frequency corresponding to a specific hyperfine transition of rotational transition X , and its power is 100% modulated at the frequency (20 Hz) of the reference oscillator. The frequency of oscillator 2 is scanned around the frequency of another rotational transition (Y). The rotational transitions X and Y should have one rotational energy level in common. The hyperfine spectrum of transition Y is now detected as a change in the intensity of the monitored hyperfine component of rotational transition X . As a consequence of additional selection rules, the observed spectrum is simplified considerably compared with a single resonance measurement of the hyperfine structure of transition Y .

The spectral recordings are obtained by connecting a Keithley 427 current amplifier to the collector of the detector. After suppression of the background current due to the total beam, the signal is amplified and fed into a PAR 120 lock-in amplifier. If required, a Hewlett-Packard 5480B signal analyser is interfaced with the scan control unit to improve the signal-to-noise ratio by averaging techniques.

Since the C-field consists of a non-resonant structure, the spectrometer can be used easily over a wide frequency range (from 10 MHz to 100 GHz). We performed measurements in the frequency region 9-54 GHz. The spectral linewidth in the microwave region is determined primarily by the transit time of a molecule through the resonance region and is typically 20-30 kHz. Searching over a large spectral range within a reasonable sweep time is possible because the instrumental linewidth can be broadened artificially to about 3 MHz without loss of sensitivity by white noise frequency modulation¹² of the microwave radiation source. The drawbacks of the MBER method are the need of a rather complicated instrumentation and the restriction to transitions of polar molecules between states obeying strict selection rules.

3. OUTLINE OF RESULTS

The rotational and hyperfine spectra of KCN, $K^{13}\text{CN}$, $KC^{15}\text{N}$, NaCN, Na^{13}CN , LiNC and $^6\text{LiNC}$ in the ground vibrational and electronic state were measured between 9 and 54 GHz. Potassium and sodium cyanide are near-prolate asymmetric rotors, and for both molecules a-type (induced by the a component of the electric dipole moment μ_a) and b-type (induced by μ_b) transitions were observed. The rotational spectrum of lithium isocyanide is that of a linear rotor and therefore much simpler than of KCN and NaCN.

The hyperfine spectra of all three molecules are very complex because two nuclei with rather large nuclear spins contribute to the hyperfine structure with couplings of comparable strength. Each rotational level is split, on the average, into twelve hyperfine sublevels. This gives rise to about seventy allowed hyperfine transitions between two rotational levels according to the selection rule $\Delta F=0, \pm 1$, where F represents the total angular momentum. Only a limited number of those allowed transitions is actually observed as a consequence of focustion properties.

We succeeded in analyzing and identifying all the observed rotational and hyperfine transitions for all the molecules studied. Many rotational and hyperfine constants could be evaluated accurately.

The molecular parameters are determined in least-squares fits of observed quantities (e.g. transition frequencies). The computer programs used minimize χ^2 , defined as:

$$\chi^2 = \sum_i [(x_{i,\text{obs}} - x_{i,\text{calc}}) / \Delta x_i]^2, \quad (2)$$

where $x_{i,\text{obs}}$, $x_{i,\text{calc}}$ and Δx_i represent the value of the i^{th} observed and calculated quantity and its uncertainty. The variance σ of a fit is:

$$\sigma = [\chi^2 / (n-m)]^{\frac{1}{2}}, \quad (3)$$

with n the number of observed quantities and m the number of parameters in the fit. The reported uncertainties in the results are three times the calculated standard deviations to insure a 90% confidence limit.

The effective structures of KCN, NaCN and LiNC in the ground vibrational state are calculated from the moments of inertia and presented schematically in

Fig. 3. For KCN also the substitution structure could be evaluated since for this molecule three isotopic species were studied.

The dramatic difference of the structure of LiNC compared with the structures of KCN and NaCN has been explained by Essers *et al.*¹³ from the subtle balance between a short-range component (dominated by the exchange repulsion and favouring a T-shaped structure) and a long-range component (dominated by the Coulomb attraction and favouring a linear cyanide structure) of the interaction energy between the alkali metal and the CN group. The behaviour of these components resembles the situation sketched in Fig. 4 and is qualitatively the same for all three alkali cyanides. The differences in the shape of the final potential energy surface in the bending direction is the result of quantitative differences in the interaction components (see Fig. 5), and yields for KCN and NaCN a T-shaped structure and for LiNC a linear isocyanide configuration. The accurate experimental determination of the structures has well located the bottoms of the intermolecular potentials for the alkali cyanides.

The experimental geometries are in gratifying agreement with the results of most of the recent *ab initio* calculations on KCN^{14,15}, NaCN¹⁵ and LiNC^{13,16} dealing with potential energy surfaces, equilibrium structures and

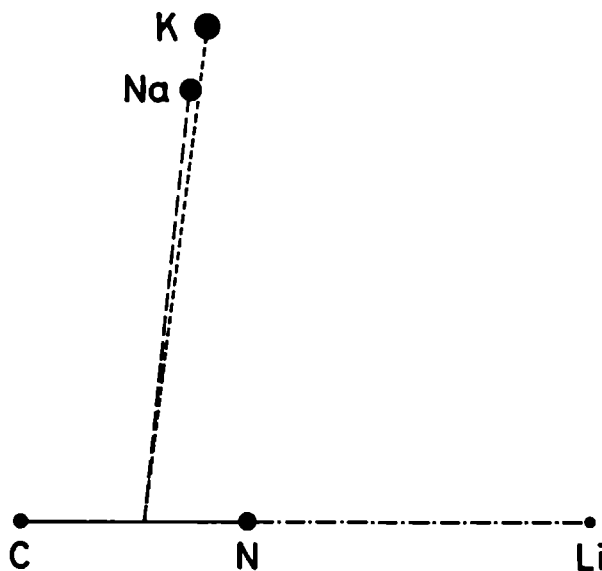


Fig. 3. The effective structures of potassium cyanide, sodium cyanide and lithium isocyanide in the ground vibrational state.

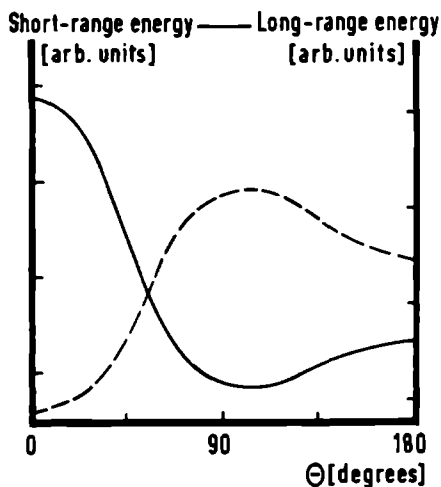


Fig. 4. Typical picture of short-range energy (full line) and long-range energy (dashed line) for alkali cyanides.

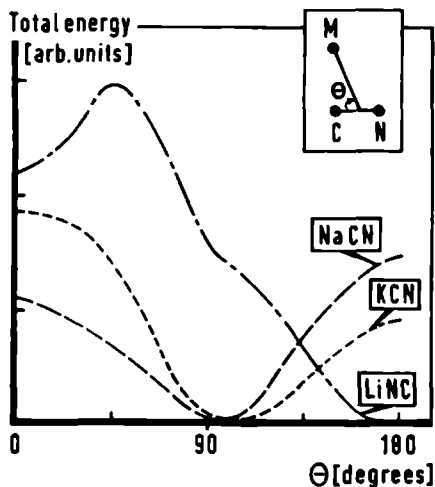


Fig. 5. Typical bending potential energy surfaces for KCN, NaCN and LiNC.

ro-vibrational spectra and frequently stimulated by our experimental investigations. There is still disagreement among the various calculations of the height of the energy barriers, with values ranging from 300 cm^{-1} to 3000 cm^{-1} for the different barriers. The computed energies are strongly affected by the quality of the basis sets used in the SCF calculations and by the inclusion of correlation energy¹⁷, as is illustrated clearly by Marsden¹⁵.

From the evaluated principal hyperfine quadrupole coupling constants and CN bond length, we conclude that in gaseous KCN and NaCN the CN group approximately can be considered as a free CN^- ion. This corresponds to the almost complete ionic character of the "polytopic bond" described by Clementi *et al.*⁶ However, because the observed rotational spectra could still be described properly by a semirigid rotor model, specific structures could be assigned in the traditional sense, about which the molecules exhibit large amplitude motions of up to 15° in the bending direction. As a consequence of the low energy barriers, moderate vibrational excitation will increase this amplitude and change the effective structure drastically.

REFERENCES

- ¹In this work the alkali metal cyanides are denoted by MCN (where M represents the alkali metal), whatever the structure may be, and the atomic symbol designates the most abundant isotope, unless specified otherwise.
- ²J.W. Simmons, W.E. Anderson, and W. Gordy, *Phys. Rev.* **77**, 77 (1950); *Phys. Rev.* **86**, 1055 (1952); R.A. Creswell, E.F. Pearson, M. Winnewisser, and G. Winnewisser, *Z. Naturforsch.* **31a**, 221 (1976).
- ³A.G. Smith, H. Ring, W.V. Smith, and W. Gordy, *Phys. Rev.* **74**, 370 (1948); C.H. Townes, A.N. Holden, and R.F. Merritt, *Phys. Rev.* **74**, 1113 (1948); J.K. Tyler, and J. Sheridan, *Trans. Faraday Soc.* **59**, 2661 (1963).
- ⁴Z.K. Ismail, R.H. Hauge, and J.L. Margrave, *J. Chem. Phys.* **57**, 5137 (1972); *J. Mol. Spectrosc.* **45**, 304 (1973).
- ⁵W.J. Pietro, B.A. Levi, W.J. Hehre, and R.F. Stewart, *Inorg. Chem.* **19**, 2225 (1980).
- ⁶B. Bak, E. Clementi, and R.N. Kortzeborn, *J. Chem. Phys.* **52**, 764 (1970); E. Clementi, H. Kistenmacher, and H. Popkie, *J. Chem. Phys.* **58**, 2460 (1973).
- ⁷P. Kuijpers, T. Törring, and A. Dymanus, *Chem. Phys. Lett.* **42**, 423 (1976).
- ⁸T. Törring, J.P. Bekooy, W.L. Meerts, J. Hoeft, E. Tiemann, and A. Dymanus, *J. Chem. Phys.* **73**, 4875 (1980).
- ⁹G.E. Leroi, and W. Klemperer, *J. Chem. Phys.* **35**, 774 (1961).
- ¹⁰J.C. Zorn, and T.C. English, in: *Advances in Atomic and Molecular Physics*, Volume 9, eds. D. Bates, and I. Estermann (Academic Press, New York, 1973).
- ¹¹H. Dijkerman, W. Flegel, G. Gräff, and B. Mönter, *Z. Naturforsch.* **27a**, 100 (1972).
- ¹²W.L. Meerts, J.P. Bekooy, and A. Dymanus, *Mol. Phys.* **37**, 425 (1979).
- ¹³R. Essers, J. Tennyson, and P.E.S. Wormer, *Chem. Phys. Lett.* **89**, 223 (1982).
- ¹⁴P.E.S. Wormer, and J. Tennyson, *J. Chem. Phys.* **75**, 1245 (1981); J. Tennyson, and B.T. Sutcliffe, *Mol. Phys.* **46**, 97 (1982); J. Tennyson, and A. van der Avoird, *J. Chem. Phys.* **76**, 5710 (1982); J. Tennyson, and B.T. Sutcliffe, *J. Chem. Phys.* **77**, 4061 (1982).

- ¹⁵M.L. Klein, J.D. Goddard, and D.G. Bounds, *J. Chem. Phys.* **75**, 3909 (1981); C.J. Marsden, *J. Chem. Phys.* **76**, 6451 (1982); private communication.
- ¹⁶L.T. Redmon, G.D. Purvis, III, and R.J. Bartlett, *J. Chem. Phys.* **72**, 986 (1980); A. Schmiedekamp, C.W. Bock, and P. George, *J. Mol. Struct.* **67**, 107 (1980); G.H.L.A. Brocks, and J. Tennyson, *J. Mol. Spectrosc.* **99**, 263 (1983).
- ¹⁷C.E. Dykstra, *Ann. Rev. Phys. Chem.* **32**, 25 (1981).

THEORY

1. ROTATIONAL STRUCTURE

For a semirigid linear polyatomic molecule the rotational Hamiltonian can be written as:

$$H=H_o+H_c, \quad (1)$$

where H_o represents the contribution for a rigid rotor and H_c describes the centrifugal distortion energy. To second order the energy of the molecule in the state with angular momentum J is given by¹:

$$E_J=BJ(J+1)-DJ^2(J+1)^2+HJ^3(J+1)^3, \quad (2)$$

where B is the rotational constant, D is the centrifugal distortion constant and H is the second-order distortion constant.

The theory of the rotational energy for a semirigid asymmetric top molecule is considerably more complex¹⁻³. Only a short summary is given here. The Hamiltonian can be written in a formal way as:

$$H=H_r+H_d, \quad (3)$$

$$\text{with: } H_r=AP_a^2+BP_b^2+CP_c^2, \quad (4)$$

$$H_d=\frac{1}{4}\sum_{\alpha,\beta,\gamma,\delta}\tau_{\alpha\beta\gamma\delta}P_\alpha P_\beta P_\gamma P_\delta. \quad (5)$$

Herein A, B and C are the τ -free rotational constants and $\tau_{\alpha\beta\gamma\delta}$ the quartic distortion constants with $\alpha, \beta, \gamma, \delta = a, b, c$, the inertial axes. Because of the noncommuting character of the rotational angular momentum components P_α , there are 81 terms in the sum of Eq. (5). However, many distortion constants are equiv-

alent and many will not contribute to first-order (for molecules with orthorhombic symmetry even to any order). This results in only nine different quartic distortion constants:

$$\tau_{\alpha\alpha\alpha\alpha}, \tau_{\alpha\alpha\beta\beta} = \tau_{\beta\beta\alpha\alpha}, \tau_{\alpha\beta\alpha\beta} = \tau_{\alpha\beta\beta\alpha} = \tau_{\beta\alpha\beta\alpha} = \tau_{\beta\alpha\alpha\beta} \quad (\alpha \neq \beta) \quad (6)$$

Furthermore, from commutation relations for the P_{α} 's and a redefinition of the rotational and distortion constants¹ it can be shown that the distortion energy to first-order complies with only six independent quartic distortion constants. Finally, this number can be reduced to five by the application of a unitary transformation, yielding Watson's reduced Hamiltonian². In the notation of Kirchhoff this Hamiltonian, with higher-order distortion terms up to P^6 , is:

$$\begin{aligned} \tilde{H} = & \tilde{A}P_a^2 + \tilde{B}P_b^2 + \tilde{C}P_c^2 \\ & - \Delta_J P^4 - \Delta_{JK} P^2 P_a^2 - \Delta_K P_a^4 \\ & - 2\delta_J P^2 (P_b^2 - P_c^2) - \delta_K [P_a^2 (P_b^2 - P_c^2) + (P_b^2 - P_c^2) P_a^2] \\ & + H_J P^6 + H_{JK} P^4 P_a^2 + H_{KJ} P^2 P_a^4 + H_K P_a^6 \\ & + 2h_J P^4 (P_b^2 - P_c^2) + h_{JK} P^2 [P_a^2 (P_b^2 - P_c^2) + (P_b^2 - P_c^2) P_a^2] \\ & + h_K [P_a^4 (P_b^2 - P_c^2) + (P_b^2 - P_c^2) P_a^4]. \end{aligned} \quad (7)$$

We employed in the computer program for the rotational spectrum of an asymmetric-top molecule the matrix elements for the Hamiltonian \tilde{H} , given by Kirchhoff³. To facilitate comparison with other work, the parameters that could be fitted were taken: A'' , B'' , C'' (the rotational constants); either Δ_J , Δ_{JK} , Δ_K , δ_J , δ_K or τ_{aaaa} , τ_{bbbb} , τ_{cccc} , τ_1 , τ_2 (the quartic distortion constants); and H_J , H_{JK} , H_{KJ} , H_K , h_J , h_{JK} , h_{KJ} , h_K (the sextic distortion constants). The various rotational and quartic distortion constants are related to each other by the following equations¹:

$$\tilde{A} = A'' + 2\Delta_J, \quad (8)$$

$$\tilde{B} = B'' + 2\Delta_J + \Delta_{JK} - 2\delta_J - 2\delta_K, \quad (9)$$

$$\tilde{C} = C'' + 2\Delta_J + \Delta_{JK} + 2\delta_J + 2\delta_K; \quad (10)$$

$$\tau_{aaaa} = -\tau_{bbbb} - \tau_{cccc} + \tau_1 - 4\Delta_K, \quad (11)$$

$$\tau_{bbbb} = -4\Delta_J - 8\delta_J, \quad (12)$$

$$\tau_{cccc} = -\tau_{bbbb} - 8\Delta_J, \quad (13)$$

$$\tau_1 = \frac{3}{2}(\tau_{bbbb} + \tau_{cccc}) - 4\Delta_{JK}, \quad (14)$$

$$\tau_2 = \frac{1}{2}(A'' + B'' + C'')^{-1} [\tau_{bbbb}'(A'' - B'') + \tau_{cccc}'(A'' - C'') + \tau_1(B'' + C'') + 8\delta_K(B'' - C'')]. \quad (15)$$

The τ -planarity defect indicates how well the planarity conditions³ are satisfied and is defined by:

$$\Delta\tau = \tau_{\text{CCCC}}' - \tau_2 - [C''/(A''+B'')](\tau_2 - \tau_1). \quad (16)$$

The number of independent quartic centrifugal distortion constants can be reduced to four by invoking the planarity conditions. It is then possible to calculate³ the τ -free rotational constants (A, B, C) and the τ 's (e.g. τ_{aaaa}' , τ_{bbbb}' , τ_{aabb}' , τ_{abab}'). However, since the planarity conditions are usually not completely obeyed ($\Delta\tau \neq 0$), the result is ambiguous and depends on which four distortion constants are selected out of the set τ_{aaaa}' , τ_{bbbb}' , τ_{cccc}' , τ_1 , τ_2 to evaluate the constants A, B, C, and the unprimed τ 's.

The experimentally determined distortion constants provide information on the quadratic force field of the intermolecular potential, according to the relation:

$$\tau_{\alpha\beta\gamma\delta} = R (|I_{\alpha\alpha} I_{\beta\beta} I_{\gamma\gamma} I_{\delta\delta}|)^{-1} \sum_{i,j} (J_{\alpha\beta}^i)^{-1} (f^{-1})_{ij} (J_{\gamma\delta}^j), \quad (17)$$

where the proportionality constant $R = -338.476$ when the elements of the inertia matrix I are in $\text{amu}\text{\AA}^2$, the partial derivatives $J_{\alpha\beta}^i \equiv \partial I_{\alpha\beta} / \partial S_i$ with respect to the internal coordinate S_i in $\text{amu}\text{\AA}$, the force constants f_{ij} in $\text{mdyne}/\text{\AA}$ and the distortion constants $\tau_{\alpha\beta\gamma\delta}$ in MHz. The inertial defect ΔI is given by:

$$\Delta I = (h/8\pi^2)(1/C - 1/B - 1/A), \quad (18)$$

and can also be used to determine the force field, since it can be expressed¹ in terms of the vibrational frequencies ω_s and the Coriolis coupling constants $\zeta_{ss'}$. The latter constants are related to the force field constants. A computer program was constructed to determine the force field from distortion constants and inertial defects in which data from several isotopic species could be fitted to obtain the constants.

The rotational states of an asymmetric-top molecule are indicated by the angular momentum J and the pseudo quantum numbers K_{-1} and K_1 . The electric dipole moment μ_c is zero in the near-prolate rotors KCN and NaCN. Consequently the only allowed transitions are a-type (due to μ_a) with selection rules $\Delta J = 0, \pm 1$, $\Delta K_{-1} = 0, \pm 2, \dots$, $\Delta K_1 = \pm 1, \pm 3, \dots$, and b-type (due to μ_b) with selection rules $\Delta J = 0, \pm 1$, $\Delta K_{-1} = \pm 1, \pm 3, \dots$, $\Delta K_1 = \pm 1, \pm 3, \dots$.

2. HYPERFINE STRUCTURE

The Hamiltonian for the hyperfine interaction in molecules with two nuclei with nonzero spins and couplings of comparable strength can be given formally by:

$$H = H_{Q_1} + H_{Q_2} + H_{I_1J} + H_{I_2J} + H_{I_1I_2}. \quad (19)$$

Here $H_{Q_1} + H_{Q_2}$ contains the quadrupole, $H_{I_1J} + H_{I_2J}$ the spin-rotation, and $H_{I_1I_2}$ the spin-spin interaction. Only the direct, or nuclear, spin-spin interaction is considered; the much smaller indirect, or electron coupled, spin-spin interaction is neglected.

In the representation used, the nucleus with spin I_1 is coupled first to the molecular rotational angular momentum J to form a resultant F_1 ; then the nucleus with spin I_2 is coupled with F_1 to form the total angular momentum F . We constructed a computer program for the hyperfine interaction based on the Hamiltonian of Eq. (19). The Hamiltonian matrix is diagonalized in this program and the energy levels thus obtained are labeled by the quantum number J and F , and by a pseudo spin quantum number ϵ . For a given J and F , the state lowest in energy is indicated by $\epsilon=1$ and the higher states are denoted by $\epsilon=2,3,\dots$ in the order of increasing energy.

The matrix elements are derived from the general expressions given by Thaddeus *et al.*⁴ and are given in Eqs. (20) through (29) for the specific case of two interacting nuclei. In the following, eQq_{gg} , c_{gg} and d_{gg} are the quadrupole, spin-rotation and spin-spin coupling constants with reference to the inertial axes $g=a,b,c$; $\langle P_g^2 \rangle$ represents the average value of P_g^2 of the unperturbed asymmetric rotor in the rotational level J_{K_{-1}, K_1} , where P_g is the component of the angular momentum of rotation along the g axis; $L=1,2$ designates the two nuclei and Σ indicates a summation over $g=a,b,c$.

The matrix elements for the quadrupole interaction are given by:

$$\begin{aligned} &\langle J, I_1, F_1, I_2, F | H_{Q_1} | J, I_1, F_1, I_2, F \rangle = \\ &(-1)^{J+I_1+F_1} (eQq_{g_1})_1 \\ &\times \left[\frac{(2J+1)(2J+2)(2J+3)(2I_1+1)(2I_1+2)(2I_1+3)}{8J(2J-1)} \right]^{\frac{1}{2}} \begin{Bmatrix} F_1 & I_1 & J \\ 2 & J & I_1 \end{Bmatrix}, \quad (20) \end{aligned}$$

$$\begin{aligned}
& \langle J, l_1, F_1', l_2, F | H_{Q_2} | J, l_1, F_1, l_2, F \rangle = \\
& (-1)^{J+l_1+l_2+2F_1+F} (eQq_J)_2 \\
& \times \left[\frac{(2J+1)(2J+2)(2J+3)(2F_1'+1)(2F_1+1)(2l_2+1)(2l_2+2)(2l_2+3)}{8J(2J-1) \quad 8l_2(2l_2-1)} \right]^{\frac{1}{2}} \\
& \times \begin{Bmatrix} l_1 & J & F_1 \\ 2 & F_1' & J \end{Bmatrix} \begin{Bmatrix} F & l_2 & F_1 \\ 2 & F_1' & l_2 \end{Bmatrix}, \quad (21)
\end{aligned}$$

$$\text{with: } (eQq_J)_L = \frac{2}{(J+1)(2J+3)} \Sigma eQq_{gg}(L) \langle P_g^2 \rangle. \quad (22)$$

The matrix elements for the spin-rotation interaction are given by:

$$\langle J, l_1, F_1, l_2, F | H_{1J} | J, l_1, F_1, l_2, F \rangle = (c_J)_1 H11J(F_1), \quad (23)$$

$$\langle J, l_1, F_1', l_2, F | H_{1J} | J, l_1, F_1, l_2, F \rangle = (c_J)_2 H12J(F_1', F_1), \quad (24)$$

$$\text{with: } (c_J)_L = \frac{1}{J(J+1)} \Sigma c_{gg}(L) \langle P_g^2 \rangle, \quad (25)$$

$$\begin{aligned}
& H11J(F_1) \equiv \\
& (-1)^{J+l_1+F_1} [J(J+1)(2J+1)l_1(l_1+1)(2l_1+1)]^{\frac{1}{2}} \\
& \times \begin{Bmatrix} F_1 & l_1 & J \\ 1 & J & l_1 \end{Bmatrix}, \quad (26)
\end{aligned}$$

$$\begin{aligned}
& H12J(F_1', F_1) \equiv \\
& (-1)^{1+J+l_1+l_2+2F_1+F} [J(J+1)(2J+1)(2F_1'+1)(2F_1+1)l_2(l_2+1)(2l_2+1)]^{\frac{1}{2}} \\
& \times \begin{Bmatrix} l_1 & J & F_1 \\ 1 & F_1' & J \end{Bmatrix} \begin{Bmatrix} F & l_2 & F_1 \\ 1 & F_1' & l_2 \end{Bmatrix}. \quad (27)
\end{aligned}$$

The matrix elements for the spin-spin interaction are given by:

$$\begin{aligned}
& \langle J, l_1, F_1', l_2, F | H_{1l_2} | J, l_1, F_1, l_2, F \rangle = \\
& \frac{2}{J(2J-1)(J+1)(2J+3)} \Sigma d_{gg} \langle P_g^2 \rangle \\
& \times \left\{ \frac{1}{2} [H12J(F_1', F_1)H11J(F_1) + H11J(F_1')H12J(F_1', F_1)] - H1112(F_1', F_1) \right\}, \quad (28)
\end{aligned}$$

$$\begin{aligned}
\text{with: } & H_{1112}(F_1', F_1) \equiv (-1)^{1+J+l_1+l_2+F_1'+F_1+F_J(J+1)} \\
& \times [l_1(l_1+1)(2l_1+1)(2F_1'+1)(2F_1+1)(l_2(l_2+1)(2l_2+1))]^{\frac{1}{2}} \\
& \times \begin{Bmatrix} J & l_1 & F_1 \\ 1 & F_1' & l_1 \end{Bmatrix} \begin{Bmatrix} F & l_2 & F_1 \\ 1 & F_1' & l_2 \end{Bmatrix}.
\end{aligned} \tag{29}$$

All matrix elements considered are diagonal in J and F . The matrix elements for H_{Q_1} and $H_{l_1 J}$ are nonvanishing if $\Delta F_1 \equiv |F_1' - F_1| = 0$, for $H_{l_2 J}$ and $H_{l_1 l_2}$ if $\Delta F_1 = 0, \pm 1$, and for H_{Q_2} if $\Delta F_1 = 0, \pm 1, \pm 2$.

3. MOLECULAR STRUCTURE

Two types of structures could be evaluated from the experimental data: the effective structure for the ground vibrational state, calculated from the moments of inertia; and the substitution structure, derived from the differences in the moments of inertia for several isotopic species. To evaluate a structure it is required to assume that molecular structural parameters do not change with isotopic substitution.

The effective structure can be calculated from the following relations for the moments of inertia:

$$I_a = \sum_i m_i b_i^2, \quad I_b = \sum_i m_i a_i^2, \quad I_c = \sum_i m_i (a_i^2 + b_i^2), \tag{30}$$

where I_a , I_b , I_c are the moments of inertia and m_i , a_i and b_i are the mass and coordinates of the nucleus i in the principal axes system (the c axis is perpendicular to the molecular plane. Because only two of the moments of inertia of a rigid planar molecule are independent ($I_c = I_a + I_b$; in the non-rigid case $I_c \approx I_a + I_b$), the evaluation of the effective structure for a nonlinear nonsymmetric triatomic molecule requires data from at least two isotopic species. Ambiguities in the structural calculations are introduced if different sets of moments of inertia and isotopic species are used. This limits the accuracy of the derived structure and is a consequence of zero-point vibrational effects.

For a linear nonsymmetric triatomic molecule the rotational structure is described by only one rotational constant, and, consequently, at least three isotopic species are required to calculate the effective structure unambiguously.

The substitution structure can be calculated from Kraitchman's equations⁵. According to these relations, the coordinates a and b of the substituted nucleus in the principal axes system of the moments of inertia with respect to the centre of mass for the parent isotopic species are given in the case of a planar asymmetric-top molecule by:

$$a^2 = \mu^{-1} \Delta I_b [1 + \Delta I_a / (I_a - I_b)], \quad (31)$$

$$b^2 = \mu^{-1} \Delta I_a [1 + \Delta I_b / (I_b - I_a)], \quad (32)$$

with the reduced mass $\mu \equiv M\Delta m / (M + \Delta m)$, and $\Delta I_a \equiv I_a' - I_a$ and $\Delta I_b \equiv I_b' - I_b$. Herein M, I_a , I_b and $M + \Delta m$, I_a' , I_b' are the mass and the moments of inertia of the parent isotopic species and the isotopically substituted species, respectively. If one atom is not substituted or located close to a principal axes (in which case Kraitchman's equations produce large uncertainties), its position can be calculated from the first-moment (i.e. centre of mass) conditions:

$$\sum_i m_i a_i = 0 \quad \text{and} \quad \sum_i m_i b_i = 0, \quad (33)$$

where m_i , a_i and b_i are the masses and (substitution) coordinates of the nuclei in the principal axes system of the parent isotopic species. The effects of zero-point vibrations tend to cancel in the calculation of structural parameters with Kraitchman's equations. The isotopic substitution method yields a structure which is closer to the equilibrium structure (corresponding to the hypothetical vibrationless state) than the effective structure.

REFERENCES

- ¹W. Gordy, and R.L. Cook, *Microwave Molecular Spectra* (Interscience, New York, 1970).
- ²J.K.G. Watson, *J. Chem. Phys.* **46**, 1935 (1967); *J. Chem. Phys.* **48**, 4517 (1968).
- ³W.H. Kirchhoff, *J. Mol. Spectrosc.* **41**, 333 (1972).
- ⁴P. Thaddeus, L.C. Krisher, and J.H.N. Loubser, *J. Chem. Phys.* **40**, 257 (1964).
- ⁵J. Kraitchman, *Amer. J. Phys.* **21**, 17 (1953).

MOLECULAR BEAM ELECTRIC RESONANCE STUDY

OF KCN, K¹³CN AND KC¹⁵N

ABSTRACT

The microwave spectra of the isotopic species K¹³CN and KC¹⁵N have been observed by molecular beam electric resonance spectroscopy, using the seeded beam technique. For both isotopic species we observed about 20 rotational transitions in the frequency range 9 to 38 GHz originating in the ground vibrational state. We fitted the observed transitions to an asymmetric rotor model and determined the three rotational, as well as the five quartic and three sextic centrifugal distortion constants.

The hyperfine spectrum of KCN has been unravelled with the help of microwave-microwave double resonance techniques. One hundred and forty hyperfine transitions in eleven rotational transitions have been assigned. We also studied the hyperfine structure of K¹³CN and KC¹⁵N. For all three isotopic species the quadrupole coupling constants and some spin-rotation coupling constants could be deduced.

The rotational constants of the ¹³C and ¹⁵N isotopically substituted species of potassium cyanide combined with those of the normal isotopic species (determined more accurate in this work) allowed an accurate and unambiguous determination of the structure, which was confirmed to be T shaped. Both the effective structure of the ground vibrational state and the substitution structure were evaluated. The results for the effective structural parameters are: $r_{\text{CN}} = 1.169(3)$ Å, $r_{\text{KC}} = 2.716(9)$ Å, $r_{\text{KN}} = 2.549(9)$ Å.

The values obtained for the principal hyperfine coupling constant $eQq_z(\text{N})$, the angle between the CN-axis and z_{N} , and the bond length r_{CN} indicate that in gaseous potassium cyanide the CN group can be considered as an almost unperturbed CN⁻ ion.

1. INTRODUCTION

Gaseous alkali metal cyanides¹ are floppy molecules. They possess large zero-point bending motion amplitudes²⁻⁴ of up to 15° . The potential energy barrier in the bending direction is small (less than 0.3 eV)²⁻⁵ and vibrational excitation can change the structure of the molecule drastically. At high temperatures it will even be possible for the M^+ cation to orbit around the CN^- anion. Because in this case no unique structure can be assigned, Clementi *et al.*⁵ named this type of bonding for LiNC "polytopic". The Born-Oppenheimer approximation breaks down since the motions of electrons and nuclei are strongly coupled, and the ro-vibrational spectrum of the molecule cannot be described with a (semi)rigid rotor or small amplitude vibrator model. Studies of the alkali metal cyanides give a more complete understanding of molecules with weak internal interaction.

Until recently the structure of the KCN, NaCN and LiNC molecules was assumed to be linear. For KCN, a linear cyanide configuration was deduced by Ismail *et al.*⁶ from vibrational isotope effects of potassium cyanide in inert gas matrices, and by Pietro *et al.*⁷ from *ab initio* calculations. Kuijpers *et al.*⁸ reported the first successful observation of the microwave absorption spectrum of KCN between 85 and 107 GHz. It was, however, not possible to determine the structure, since a tentative fit of some observed lines to a linear rotor model resulted in improbable structural parameters. A correct identification was impeded by the appearance of at least eleven vibrational states in the observed rotational spectrum. However, Törring *et al.*⁹ established experimentally that the most stable structure of KCN in the ground vibrational state is T shaped. Since only one, the most abundant, isotopic species was measured, no precise structure could be deduced.

In the current work, we present a more accurate and unambiguous structure determination of KCN using isotopic substitution. The microwave spectra between 12 and 38 GHz of the ^{13}C and ^{15}N isotopically substituted species of potassium cyanide in the ground vibrational state were measured by molecular beam electric resonance spectroscopy. The seeded beam technique was used to obtain translational, rotational and vibrational relaxation. For both isotopic species we observed about 20 rotational transitions which were fitted to an asymmetric rotor model. We determined the rotational, the five quartic and three sextic distortion constants.

The hyperfine structure of KCN was resolved and identified with the help of microwave-microwave double resonance. One hundred and forty hyperfine transitions in eleven rotational transitions have been assigned. In combination with the results of Törring *et al.*⁹, we deduced more accurate rotational constants of KCN. The hyperfine spectra of $K^{13}CN$ and $KC^{15}N$ were also unravelled. For all three isotopic species we determined the hyperfine quadrupole coupling constants eQq_{aa} and eQq_{bb} for both potassium and (except for $KC^{15}N$) nitrogen, and some spin-rotation coupling constants.

The rotational constants of all three isotopic species allowed for an unambiguous and accurate structure determination of KCN, which we confirmed to be T shaped. Both the effective structure of the ground vibrational state and the substitution structure were evaluated.

2. EXPERIMENTAL

The measurements were performed with the molecular beam electric resonance (MBER) spectrometer described elsewhere^{10,11}. The experimental conditions are essentially the same as used by Törring *et al.*⁹. The supply and the nozzle chamber temperatures of the stainless steel double chamber oven were kept at 1150 K and 1350 K, respectively. According to Simmons *et al.*¹², the supply chamber temperature corresponds to a vapour pressure of monomeric potassium cyanide of about 4 mbar. The stagnation pressure of the carrier gas argon used to produce a seeded beam was 0.6-1 bar. The strong translational, rotational and vibrational cooling obtained in this way simplified the spectra and enhanced the intensity of the observed transitions considerably by concentrating the population in the low J states of the ground vibrational state⁹. This resulted in a signal-to-noise ratio for the strongest lines of 40 at an integration time of 1 s. The observed linewidth was about 30 kHz. The frequencies of the observed microwave transitions are determined with an accuracy of typically a few kHz.

An additional advantage of the seeded beam technique (over e.g. microwave absorption spectroscopy) is a very low material consumption (less than 1 g in 15 hours), which made it possible to study expensive isotopically enriched samples of $K^{13}CN$ (90%) and $KC^{15}N$ (95%).

3. THEORY

The Hamiltonian for the hyperfine quadrupole, spin-rotation and spin-spin interaction in molecules with two nuclei with nonzero spins may be written in a formal way as:

$$H = H_{Q_1} + H_{Q_2} + H_{I_1J} + H_{I_2J} + H_{I_1I_2}. \quad (1)$$

Here $H_{Q_1} + H_{Q_2}$ contains the quadrupole, $H_{I_1J} + H_{I_2J}$ the spin-rotation, and $H_{I_1I_2}$ the spin-spin interaction.

We applied the general expressions given by Thaddeus *et al.*¹³ to obtain the matrix elements of the hyperfine Hamiltonian for the specific case of two interacting nuclei¹¹.

The quadrupole coupling constants eQq_{gg} , the spin-rotation coupling constants c_{gg} and the spin-spin coupling constants d_{gg} with reference to the inertial axes $g=a,b,c$ are defined as follows:

$$eQq_{gg} \equiv eQV_{gg}, \quad (2)$$

$$c_{gg} \equiv N_{gg} + E_{gg}, \quad (3)$$

$$d_{gg} \equiv g_1 g_2 \mu_N^2 r_{12}^{-5} (-3(r_{12})_g^2 + r_{12}^2), \quad (4)$$

where V_{gg} , N_{gg} and E_{gg} are given by Thaddeus *et al.*¹³, e is the electronic charge, Q is the nuclear electric quadrupole moment, g_1 and g_2 are the nuclear g -factors, μ_N is the nuclear magneton, and $(r_{12})_g$ is the projection of the internuclear distance r_{12} on the inertial axis g .

We constructed a computer program for the hyperfine interaction in molecules with two nuclei possessing couplings of comparable strength, employing the Hamiltonian given by Eq. (1). The following coupling scheme was used:

$$\underline{F}_1 = \underline{J} + \underline{I}_1 \quad \text{and} \quad \underline{F} = \underline{F}_1 + \underline{I}_2, \quad (5)$$

where \underline{I}_1 and \underline{I}_2 are the nuclear spins, \underline{J} is the molecular rotational angular momentum, and \underline{F} is the total angular momentum.

After diagonalization, the energy states are labeled by the quantum numbers J and F , and by a pseudo spin quantum number ϵ . For a given J and F ,

the state lowest in energy is denoted with $\epsilon=1$; the states higher in energy are labeled $\epsilon=2,3,\dots$ consecutively.

The quadrupole and spin-spin coupling constants satisfy Laplace's equation:

$$eQq_{aa} + eQq_{bb} + eQq_{cc} = 0, \quad (6)$$

$$d_{aa} + d_{bb} + d_{cc} = 0. \quad (7)$$

These constraints are imposed in the calculation. For this reason eQq_{cc} and d_{cc} are omitted in the list of constants.

4. RESULTS

The analysis of the hyperfine spectrum of the asymmetric rotor molecule potassium cyanide is quite complex because in one rotational transition there are typically about 70 allowed hyperfine transitions (according to the selection rule $\Delta F=0,\pm 1$) in a frequency region of about 3 MHz. As a consequence of apparatus focustion properties we only observed a limited number of hyperfine transitions in a given rotational transition.

The problem of identification was solved by the application of microwave-microwave double resonance. This technique was used to analyze the hyperfine spectrum of the a-type (i.e. associated with the electric dipole moment μ_a) $2_{0,2} \rightarrow 1_{0,1}$ and the b-type (i.e. associated with the electric dipole moment μ_b) $1_{1,1} \rightarrow 2_{0,2}$ rotational transition of KCN. A microwave radiation source was scanned around the frequency of the rotational transition while we monitored specific hyperfine components of the $1_{0,1} \rightarrow 0_{0,0}$ and the $2_{0,2} \rightarrow 1_{0,1}$ rotational transition, respectively. In this way a decisive identification was effected. Adding step by step more transitions to the least-squares fit for the hyperfine interaction, we were able to assign all observed hyperfine transitions. The same procedure was applied for $K^{13}CN$ and $KC^{15}N$. For these molecules we started with the hyperfine coupling constants ascertained for KCN. By this approach a positive identification was possible without the help of double resonance spectroscopy. We observed and identified for KCN 140, for $K^{13}CN$ 68, and for $KC^{15}N$ 88 hyperfine transitions in 11, 16 and 20 rotational transitions, respectively (see the Appendix).

The best fit values¹⁴ for the determinable hyperfine coupling constants of KCN, K¹³CN and KC¹⁵N in the ground vibrational state are presented in Table I. The quality of the least-squares fit can be judged¹⁵ from $\sigma=0.44$, $\sigma=0.48$ and $\sigma=0.34$, respectively. The nuclear spin of ¹⁵N is $\frac{1}{2}$, so there is no quadrupole interaction due to this nucleus in KC¹⁵N. For all three isotopic species the spin-rotation coupling constants of the potassium nucleus and the spin-rotation coupling constant $c_{bb}(N)$ of the nitrogen nucleus could not be determined significantly and were constrained in the fit at zero, as was $c_{aa}(N)$ for K¹³CN and KC¹⁵N. The spin-spin coupling constants $d_{aa}(K-N)$ and $d_{bb}(K-N)$ were fixed in the least-squares fit at the values calculated from the effective geometry using Eq. (4).

In K¹³CN all three nuclei possess nonzero spin. The nuclear spin $\frac{1}{2}$ of ¹³C gives rise to an additional splitting of the hyperfine transitions due to its spin-rotation and spin-spin interaction. This effect is only marginal, since there was no observable splitting or broadening of the measured hyperfine transitions. This justifies the assumption that the nuclear spin of ¹³C can be neglected in the fit of the observed hyperfine spectrum.

The hyperfine quadrupole coupling constants are discussed in detail in section 6.

The frequencies ν_0 of the hyperfine-free origins of the rotational transitions are also evaluated in the fit of the hyperfine structure, and are listed in Table II for the three isotopic species. These rotational frequencies were fitted by a

Table I. Hyperfine coupling constants¹⁴ for the ground vibrational state of KCN, K¹³CN and KC¹⁵N.

Constant	KCN	K ¹³ CN	KC ¹⁵ N	Unit
$eQq_{aa}(K)$	-5.605(5)	-5.589(21)	-5.614(8)	MHz
$eQq_{bb}(K)$	2.594(11)	2.594(25)	2.606(7)	MHz
$eQq_{aa}(N)$	1.921(4)	1.909(9)	-	MHz
$eQq_{bb}(N)$	-4.041(15)	-4.019(11)	-	MHz
$c_{aa}(N)$	9.7(6.2)	-	-	kHz
$c_{cc}(N)$	0.70(58)	0.62(50)	1.02(59)	kHz
$d_{aa}(K-N)$	-0.0454	-0.0450	0.0640	kHz
$d_{bb}(K-N)$	0.0209	0.0205	-0.0296	kHz

Table II. Frequencies (in MHz) of the observed^a and calculated hyperfine-free origins of the rotational transitions of KCN, K¹³CN and K¹⁵N in the ground vibrational state.

Isotope	J'	K ₋₁ '	K ₁ '	J''	K ₋₁ ''	K ₁ ''	Type	Obs.frequency	Obs.-calc.
KCN	1	0	1	0	0	0	a	9475.4865(30)	0.0045
	2	0	2	1	0	1	a	18948.5547(30)	0.0018
	3	0	3	2	0	2	a	28416.8015(20)	-0.0009
	4	0	4	3	0	3	a	37877.8223(20)	-0.0007
	8	1	7	8	1	8	a	14529.2077(70)	0.0017
	9	1	8	9	1	9	a	18157.1001(80)	-0.0032
	4	2	3	3	2	2	a	37886.9672(80)	0.0047
	1	1	1	2	0	2	b	34375.9059(30)	0.0007
	2	1	2	3	0	3	b	24504.6206(30)	0.0006
	3	1	3	4	0	4	b	14443.3633(30)	-0.0008
K ¹³ CN	7	0	7	6	1	6	b	16795.7519(70)	-0.0008
	2	0	2	1	0	1	a	18465.8935(90)	0.0018
	4	0	4	3	0	3	a	36912.2301(40)	0.0003
	8	1	7	8	1	8	a	14343.9584(70)	0.0032
	9	1	8	9	1	9	a	17925.3794(60)	-0.0018
	19	2	17	19	2	18	a	13059.473(20)	-0.0148
	20	2	18	20	2	19	a	15781.880(20)	0.0196
	21	2	19	21	2	20	a	18864.081(20)	-0.0057
	1	1	1	2	0	2	b	32700.0794(90)	-0.0028
	3	1	3	4	0	4	b	13263.7935(70)	-0.0006
	7	0	7	6	1	6	b	17208.5231(60)	-0.0009
	11	2	10	12	1	11	b	27986.980(18)	0.0029
	12	2	11	13	1	12	b	16268.537(19)	-0.0034
	17	1	16	16	2	15	b	32244.202(20)	0.0004
21	3	19	22	2	20	b	36812.959(20)	0.0010	
23	3	21	24	2	22	b	12520.298(20)	-0.0017	
26	2	24	25	3	23	b	12824.249(20)	-0.0007	
K ¹⁵ N	2	0	2	1	0	1	a	18564.6047(40)	0.0018
	3	0	3	2	0	2	a	27840.7939(40)	0.0009
	4	0	4	3	0	3	a	37109.6539(30)	0.0010
	8	1	7	8	1	8	a	14409.3837(60)	-0.0002
	9	1	8	9	1	9	a	18007.3133(80)	0.0031
	11	1	10	11	1	11	a	26391.7895(80)	0.0057
	12	1	11	12	1	12	a	31174.6757(80)	-0.0003
	13	1	12	13	1	13	a	36348.0219(80)	-0.0045
	19	2	17	19	2	18	a	13099.9462(40)	-0.0029
	20	2	18	20	2	19	a	15832.1421(40)	0.0008
	21	2	19	21	2	20	a	18925.9161(40)	0.0013
	23	2	21	23	2	22	a	26260.1079(40)	0.0006
	24	2	22	24	2	23	a	30524.6567(40)	-0.0012
	1	1	1	2	0	2	b	32939.0431(30)	-0.0017
	7	0	7	6	1	6	b	17235.2403(40)	-0.0031
	11	2	10	12	1	11	b	28330.3342(70)	0.0003
	12	2	11	13	1	12	b	16548.3697(70)	0.0012
	17	1	16	16	2	15	b	32230.0446(90)	0.0021
21	3	19	22	2	20	b	37305.990(16)	0.0004	
26	2	24	25	3	23	b	12615.525(10)	-0.0028	

^aThe observed frequencies¹⁴ are evaluated in the least-squares fit of the observed hyperfine spectrum.

Table III. Rotational constants¹⁴ for the ground vibrational state of KCN, K¹³CN and KC¹⁵N.

Constant	KCN	K ¹³ CN	KC ¹⁵ N	Unit
A''	58265.8452(35)	55984.083(15)	56347.208(6)	MHz
B''	4940.0540(4)	4816.796(3)	4842.403(2)	MHz
C''	4536.2176(5)	4418.098(4)	4441.900(3)	MHz
τ_{aaaa}'	-5.360(12)	-5.28(7)	-4.65(6)	MHz
τ_{bbbb}'	-0.02699(2)	-0.0266(2)	-0.0254(2)	MHz
τ_{cccc}'	-0.01882(4)	-0.0184(3)	-0.0178(2)	MHz
τ_1	-1.55628(63)	-1.4294(68)	-1.5369(61)	MHz
τ_2	-0.12089(6)	-0.1131(7)	-0.1198(6)	MHz
H _{JK}	-4.71(14)	-4.3(4)	-4.18(7)	Hz
H _{KJ}	95(3)	96(19)	89(8)	Hz
h _{JK}	-2.4(2.1)	-7.5(3.0)	-3.6(8)	Hz
$\Delta\tau$	-0.95(2)	-0.89(6)	-0.88(2)	kHz

least-squares method to an asymmetric rotor model based on Watson's reduced Hamiltonian¹⁶. The variance¹⁵ σ for the fit of the rotational spectrum of KCN, K¹³CN and KC¹⁵N was 0.36, 0.60 and 0.60, respectively. For KCN, the frequencies given in Table II were combined with the frequencies of the rotational transitions assigned by Törring *et al.*⁹. The rotational transitions of K¹³CN and KC¹⁵N were identified by the observed hyperfine structure, their optimum voltages for the state selector fields, and their optimum microwave radiation power. For all three isotopic species, we were able to fit the three rotational constants A'', B'' and C'', the five quartic centrifugal distortion constants τ_{aaaa}' , τ_{bbbb}' , τ_{cccc}' , τ_1 and τ_2 , as well as three sextic centrifugal distortion constants: H_{JK}, H_{KJ} and h_{JK}. The remaining four sextic distortion constants H_J, H_K, h_J and h_K were constrained at zero. The results are presented in Table III. The present more accurate results for KCN agree very well with the values obtained by Törring *et al.*⁹. This is not surprising because preliminary values for the hyperfine free ν_0 frequencies obtained by Vaals *et al.*¹⁷ were already used in their fit.

In the least-squares fit of the rotational spectra the planarity conditions for the τ 's were not invoked¹⁸. This is a correct approach, since there are five τ 's

Table IV. Derived molecular constants for the ground vibrational state of KCN, K¹³CN and KC¹⁵N.

Constant	KCN	K ¹³ CN	KC ¹⁵ N	Unit
From τ_1 and τ_2 , assuming planarity:				
A	58265.3905	55983.660	56346.771	MHz
B	4939.6565	4816.430	4842.012	MHz
C	4536.0698	4417.967	4441.747	MHz
τ_{aaaa}	-5.360	-5.28	-4.65	MHz
τ_{bbbb}	-0.02699	-0.0266	-0.0254	MHz
τ_{aabb}	0.14827	0.1499	0.1198	MHz
τ_{abab}	-0.88762	-0.8255	-0.8540	MHz
ΔI	0.4291	0.4364	0.4365	amuÅ ²
From τ_1 and τ_{cccc} , assuming planarity:				
A	58265.4330	55983.699	56346.809	MHz
B	4939.6602	4816.434	4842.015	MHz
C	4536.0450	4417.944	4441.724	MHz
τ_{aaaa}	-5.360	-5.28	-4.65	MHz
τ_{bbbb}	-0.02699	-0.0266	-0.0254	MHz
τ_{aabb}	0.05575	0.0650	0.0363	MHz
τ_{abab}	-0.80206	-0.7471	-0.7769	MHz
ΔI	0.4298	0.4371	0.4372	amuÅ ²
From the τ -free rotational constants:				
I_a	8.67374(5)	9.02726(5)	8.96908(5)	amuÅ ²
I_b	102.3105(30)	104.9281(30)	104.3737(30)	amuÅ ²
I_c	111.4137(30)	114.3920(30)	113.7796(30)	amuÅ ²

independently determinable and the τ -planarity defect¹⁸ $\Delta\tau$, given in Table III, is very large. This indicates that potassium cyanide shows large amplitude motions.

In Table IV we list the τ -free rotational constants A, B and C and the centrifugal distortion constants τ_{aaaa} , τ_{bbbb} , τ_{aabb} and τ_{abab} . These molecular parameters were derived under the assumption of planarity¹⁸ using τ_1 and τ_2 , or τ_1 and τ_{cccc} , respectively. The inertial defects $\Delta I = (h/8\pi^2)(1/C - 1/B - 1/A)$ are also listed in Table IV.

The effective moments of inertia I_a , I_b and I_c in the ground vibrational state were evaluated¹⁹ from the τ -free rotational constants using the well known relations $I_a = h/8\pi^2A$, $I_b = h/8\pi^2B$ and $I_c = h/8\pi^2C$. The results are given in Table IV.

5. STRUCTURE

The structure of a nonsymmetric, nonlinear triatomic molecule can be derived accurately from the moments of inertia of at least two isotopic species. So we are now in the position to remove the ambiguity in the structure derived by Törring *et al.*⁹. We fitted I_a , I_b and I_c of KCN, K¹³CN and K¹⁵N to determine the effective structure of potassium cyanide in the ground vibrational state. The result is presented in Table V, and corresponds to "structure B" of Törring *et al.*⁹.

All possible combinations of pairs of moments of inertia of two isotopic species yield structural parameters well within the uncertainties given in Table V. Only when I_a is left out, there is a significant deviation of the structural parameters of up to 0.03 Å for the CN bond length. This is caused by the fortuity that $|a_i| = r_i \equiv (a_i^2 + b_i^2)^{1/2}$ for all three nuclei, especially for potassium where $|a_i| - r_i = 0.00007$ Å. We define a_i , b_i as the coordinates of the nucleus i in the principal axes system. Since $I_b = \sum_i m_i a_i^2$ and $I_c = \sum_i m_i b_i^2$, the calculated structure is inaccurate if $I_a = \sum_i m_i b_i^2$ is excluded from the fit. The small inconsistency of structures calculated from different combinations of I 's and different pairs of isotopic species is a consequence of zero-point vibrations, illustrated by the finite τ -planarity and inertial defect.

The substitution structure, given in Table V, is obtained using Kraitchman's equations²⁰. For the location of the carbon and the nitrogen nucleus, we applied these equations on the observed isotope shifts in the moments of inertia of the ¹³C and ¹⁵N isotopically substituted molecular species. Since we did not observe the spectrum of the ⁴¹KCN molecule, the coordinates of the potassium nucleus were determined by invoking the first-moment (i.e. centre of mass) condition²¹. It is favourable to determine the position of the potassium nucleus in this way because it is located very close to a principal axis ($b_K = -0.012$ Å). In such cases Kraitchman's equations cannot be used for accu-

Table V. Effective structural parameters¹⁴ for the ground vibrational state and substitution structural parameters (in Å) for potassium cyanide.

	r_{CN}	r_{KC}	r_{KN}
effective structure	1 169(3)	2 716(9)	2 549(9)
substitution structure	1 174(2)	2 711(5)	2 532(5)

rate coordinate calculations. However, when the first-moment condition is used, the error in the position is independent of the coordinate value.

The uncertainties in the substitution structural parameters are estimated from the value of the inertial defect and from comparison with other molecules²². It was shown by Costain²³ that the zero-point vibrational effects tend to cancel in the calculation of the substitution structure, which is expected^{23,24} to be closer to the equilibrium structure than the effective structure.

The values of the structural parameters r_{KC} and r_{KN} are larger for the effective than for the substitution structure. This can be understood from the same considerations as used for the bond length in a diatomic molecule²² with stretch vibration (K-[CN]). The value of r_{CN} , however, decreases. This can be explained from the large bending vibration, which can be considered as a wagging of the C-N axis. The stretch vibrations can be neglected, and the value of the effective bond length is the result for the "effective" projection of the vibrating C and N nuclei on the equilibrium position of the C-N axis.

6. DISCUSSION

The measurements of Törring *et al.*⁹ and the experiments described in the current work and presented before¹⁷, showed that the structure of potassium cyanide is T shaped. This unusual structure stimulated *ab initio* calculations of the potential energy surface for both potassium^{2,3} and sodium cyanide³, as well as for lithium isocyanide^{4,25}. We established experimentally that also the structure of NaCN is T shaped²⁵, and that LiNC has a linear isocyanide structure¹⁰.

Table VI. Summary of results of *ab initio* calculations on KCN. The hyperfine coupling constants²⁷ are given for the *ab initio* structure, and in brackets for the experimental structure (see text).

Constant	Wormer <i>et al.</i> ²	Klein <i>et al.</i> ³	Marsden ³	Unit
E(KCN)	2020	2280	1090	cm ⁻¹
E(KNC)	494	600	1170	cm ⁻¹
r_{CN}	1.157	1.153	1.14	Å
r_{KC}	2.906	2.850	2.80	Å
r_{KN}	2.582	2.616	2.65	Å
eQq_{aa} (K)	-5.582(-5.670)	-4.638(-4.940)	-	MHz
eQq_{bb} (K)	2.633(2.721)	1.753(2.055)	-	MHz
eQq_{aa} (N)	1.513(1.913)	1.758(1.896)	-	MHz
eQq_{bb} (N)	-3.458(-3.858)	-3.758(-3.896)	-	MHz

In Table VI are listed some results of *ab initio* calculations on KCN. We define E(KCN) and E(KNC) as the energies of the linear cyanide and isocyanide configurations, respectively, relative to the energy of the T-shaped configuration. Though there is an explicit discrepancy for the various theoretical predictions of E(KCN) and E(KNC), the agreement between the calculated results for the structure and the accurate experimental values is gratifying.

The hyperfine quadrupole coupling constants given in Table VI are obtained²⁷ from the *ab initio* field gradients by a transformation of the calculated quadrupole coupling matrices to the principal inertia axes system of the *ab initio* structures. In brackets, we have shown the results for a transformation to the principal inertia axes system of the experimental effective structure. A comparison of the listed values for the quadrupole coupling constants with the experimental results given in Table I shows that the constants with respect to the experimental structure are in better agreement than the values with respect to the *ab initio* structure. The agreement is very good for the field gradients calculated by Wormer *et al.*², if transformed to the experimental structure.

Since we determined the quadrupole coupling constants eQq_{aa} and eQq_{bb} in more than one isotopic species, the principal elements eQq_{x} (K), eQq_{z} (K) and eQq_{x} (N), eQq_{z} (N) of the quadrupole coupling tensors for potassium and nitrogen can be evaluated²⁸. The results are presented in Table VII, including the

Table VII. Principal hyperfine quadrupole coupling constants¹⁴ for potassium cyanide in the ground vibrational state.

Constant	Potassium	Nitrogen	Unit
eQq_x	2.637(9)	1.995(23)	MHz
eQq_z	-5.645(10)	-4.110(25)	MHz
η	0.066(4)	0.029(13)	
$\theta(a, z)$	-4.0(7)	83.7(1.0)	degree
$\theta(z, C-N)$	85.9(7)	-1.8(1.0)	degree

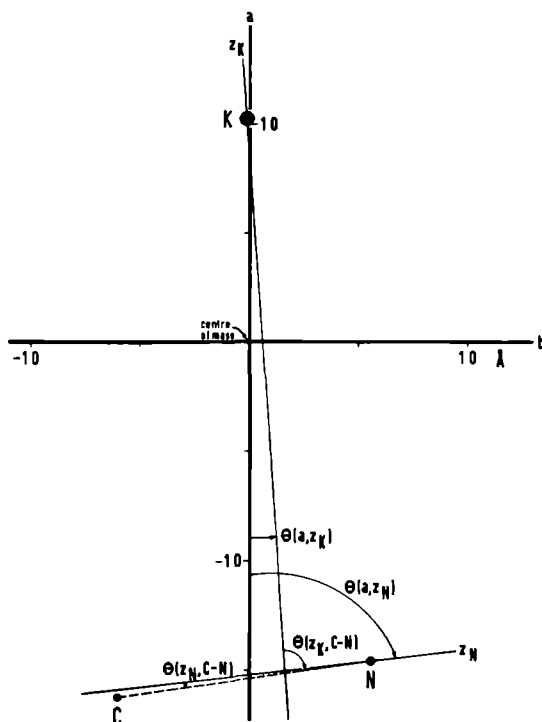


Fig. 1. Orientation of the principal axes of inertia (a,b,c) and the principal axes of the field gradient (x,y,z) in the potassium cyanide molecule. The c and y axes coincide and are perpendicular to the molecular plane. The subscripts K and N are added to clarify the distinction between the potassium and the nitrogen quadrupole principal axes.

asymmetry parameter $\eta = (eQq_x - eQq_y) / eQq_z$. In Fig. 1 is shown the orientation of the principal inertial (a, b, c) and quadrupole (x, y, z) axes. The axis y coincides with the c axis. The principal axis z is chosen as the axis for which the coupling of the nucleus approximately has axial symmetry. In Table VII are listed also the angles between the z axis of the principal quadrupole system for potassium and nitrogen, z_K and z_N , respectively, and the principal inertial axis a and the C-N axis, respectively.

As a consequence of the almost completely ionic bonding²⁹, and the large distance of the potassium nucleus to the CN group, we expect that the CN group can be considered as a free CN^- ion. This picture is supported by the following arguments. The determined asymmetry parameters η indicate that the couplings are practically axial symmetric ($eQq_x = eQq_y = -\frac{1}{2}eQq_z$). For nitrogen, the z axis almost coincides with the C-N axis. So the coupling at the nitrogen nucleus is approximately symmetric about the bond axis between the carbon and the nitrogen. Furthermore, the value for $eQq_z(N)$ is close to the quadrupole coupling constant $eQq(N) = -4.090$ MHz evaluated²⁷ from the field gradient for the free CN^- ion obtained by Wormer³⁰ in a SCF calculation using 54 contracted Gaussian type orbitals at $r_{CN} = 1.174$ Å. Finally, we expect the equilibrium CN bond length in KCN to be close to the equilibrium value³¹ of $r_{CN} = 1.173(2)$ Å in the CN^- ion. There is indeed a very good correspondence between this value and the substitution bond length $r_{CN} = 1.174(2)$ Å given in Table V.

Ab initio calculations^{32,33} of the ro-vibrational spectrum of KCN suffer from serious inaccuracies when the *ab initio* potential is used. If, however, the *ab initio* potential energy surface is shifted to the experimental geometry³², the difference between the theoretical and observed spectrum diminishes dramatically. From the inertial defects ΔI , listed in Table IV, we can estimate²² the bending vibrational frequencies $\omega_2 = h/2\pi^2\Delta I$, yielding 157(30), 154(30) and 154(30) cm^{-1} for KCN, $K^{13}CN$ and $KC^{15}N$, respectively. This is in gratifying agreement with the results from matrix-isolation studies⁶ (139 cm^{-1}) and *ab initio* calculations^{32,33} (116-120 cm^{-1}), but in disagreement with the frequency $\omega_2 = 207(20)$ cm^{-1} obtained by Leroi and Klemperer³⁴ from infrared absorption studies. Tennyson and Sutcliffe³² suggested that the observed absorption corresponds to a bending overtone. This is not very probable, since it can be deduced from intensity considerations that the symmetric stretching mode ω_1 also should have been observed by Leroi and Klemperer³⁴, which was not the case. The interpretation of Ismail *et al.*⁶, that the spectrum of KOCN and not KCN is observed in the infrared absorption cell, seems more likely.

An effort to evaluate the quadratic force constants from the quartic distortion constants determined from the rotational spectrum was unsuccessful. Even the inclusion of the inertial defect and the vibrational frequencies from matrix-isolation studies⁶, did not yield a stable solution. This is a consequence of the large anharmonicity of the potential energy surface^{2, 3, 32, 33}

The discrepancies in the thermodynamic data for potassium cyanide^{6, 12, 35} from mass spectrometric studies and calculations based on the second and third law, can be explained by analogous arguments. In all calculations an incorrect structure, usually linear, of KCN was assumed. However, by moderate thermal excitation the K^+ cation can tunnel through the low bending potential barriers, or even orbit around the CN^- anion. Consequently for a range of temperatures no specific structure or vibrational frequencies can be assigned.

The rotational spectrum of KCN in the ground vibrational state can still properly be described by the semirigid rotor model. The low bending vibrational frequency ω_2 , however, indicates that the molecule is very floppy. Since the potential energy barriers in the bending direction $E(KCN)$ and $E(KNC)$ are very low, only a few excitations of the bending vibration will change the effective structure and increase the bending vibrational amplitude considerably. The bonding becomes then more and more "polytopic" and a new description of the rotation-vibration spectrum^{32, 33, 36} is necessary. An experimental investigation of KCN, NaCN and LiNC in vibrational excited states is planned in our laboratory. Hopefully, this will yield detailed information on the ro-vibrational spectrum and will give a decisive result for the values of $E(KCN)$ and $E(KNC)$, now disputed (see Table VI) by various *ab initio* calculations.

ACKNOWLEDGMENT

The authors wish to express their gratitude to Dr. P.E.S. Wormer for calculating the field gradient at the nitrogen nucleus in the CN^- ion and kindly allowing us to publish his result. They thank Dr. J.P. Bekooij for his continuing interest and the many helpful discussions that we have enjoyed with him. This work is part of the research program of the Stichting voor Fundamenteel Onderzoek der Materie (F.O.M.) and has been made possible by financial support from the Nederlandse Organisatie voor Zuiver Wetenschappelijk Onderzoek (Z.W.O.).

APPENDIX

Frequencies (in MHz) of the observed and calculated hyperfine transitions of KCN in the ground vibrational state. Transitions measured using the microwave-microwave double resonance technique are marked •. The corresponding hyperfine components monitored to observe the double resonance spectrum are marked †.

$F_{\epsilon}^{\prime} \rightarrow F_{\epsilon}^{\prime\prime}$	Obs. frequency	Obs.-calc.	$F_{\epsilon}^{\prime} \rightarrow F_{\epsilon}^{\prime\prime}$	Obs. frequency	Obs.-calc.
Rotational transition $1_{0,1} \rightarrow 0_{0,0}$:					
$7/2_1 \rightarrow 5/2_1$	9475.6680(60)	-0.0031	$7/2_1 \rightarrow 7/2_2$	28414.9398(30)	0.0025
$5/2_2 \rightarrow 5/2_1$	9476.1140(60)†	-0.0015	$9/2_1 \rightarrow 9/2_1$	28415.2151(60)	-0.0034
$1/2_2 \rightarrow 1/2_1$	9476.9100(30)†	0.0008	$9/2_1 \rightarrow 9/2_2$	28415.4859(80)	0.0024
$3/2_3 \rightarrow 3/2_1$	9477.0510(30)†	0.0003	$5/2_1 \rightarrow 3/2_2$	28415.4859(80)	0.0016
Rotational transition $2_{0,2} \rightarrow 1_{0,1}$:					
$3/2_3 \rightarrow 3/2_3$	18948.4376(60)•	-0.0016	$7/2_2 \rightarrow 7/2_2$	28415.6728(80)	-0.0001
$1/2_2 \rightarrow 3/2_3$	18948.5350(60)•	-0.0020	$7/2_1 \rightarrow 9/2_1$	28415.7663(60)	0.0016
$3/2_3 \rightarrow 1/2_2$	18948.5795(60)•	-0.0013	$3/2_1 \rightarrow 5/2_3$	28415.8940(60)	-0.0047
$1/2_2 \rightarrow 1/2_2$	18948.6781(60)•	-0.0004	$1/2_1 \rightarrow 1/2_2$	28416.0023(40)	-0.0005
$7/2_2 \rightarrow 5/2_2$	18948.7321(80)•	-0.0055	$1/2_1 \rightarrow 3/2_3$	28416.0986(40)	-0.0019
$5/2_1 \rightarrow 3/2_1$	18949.176(10)	-0.0046	$3/2_1 \rightarrow 3/2_2$	28416.1778(40)	0.0019
$7/2_2 \rightarrow 7/2_1$	18949.176(10)	-0.0061	$5/2_3 \rightarrow 3/2_3$	28416.4406(50)	-0.0004
$5/2_2 \rightarrow 5/2_1$	18949.512(12)	-0.0038	$3/2_2 \rightarrow 1/2_2$	28416.7313(60)	-0.0002
$3/2_2 \rightarrow 5/2_1$	18949.7210(90)†	-0.0010	$7/2_3 \rightarrow 9/2_1$	28416.8134(60)	0.0001
$3/2_3 \rightarrow 3/2_2$	18949.9902(60)	0.0036	$9/2_1 \rightarrow 7/2_1$	28416.8254(60)	0.0030
$3/2_2 \rightarrow 3/2_1$	18950.2345(90)	0.0006	$3/2_2 \rightarrow 3/2_3$	28416.8299(80)	0.0006
$5/2_3 \rightarrow 3/2_1$	18950.5099(90)	-0.0012	$5/2_1 \rightarrow 3/2_1$	28416.8299(80)	-0.0024
$1/2_2 \rightarrow 1/2_1$	18950.8601(30)†	0.0007	$9/2_2 \rightarrow 7/2_2$	28416.8835(80)	-0.0023
$3/2_3 \rightarrow 5/2_1$	18951.0903(30)†	0.0013	$5/2_2 \rightarrow 5/2_2$	28416.9143(60)	-0.0024
$3/2_3 \rightarrow 3/2_1$	18951.6037(90)	0.0028	$7/2_2 \rightarrow 7/2_1$	28417.5618(80)	0.0038
$1/2_2 \rightarrow 3/2_1$	18951.7006(90)	0.0020	$5/2_2 \rightarrow 5/2_1$	28417.7681(60)	0.0039
Rotational transition $3_{0,3} \rightarrow 2_{0,2}$:					
$3/2_1 \rightarrow 1/2_2$	28414.7135(30)	0.0023	$5/2_2 \rightarrow 3/2_1$	28418.0634(80)	0.0046
$5/2_1 \rightarrow 7/2_2$	28414.7557(30)	0.0015	$7/2_3 \rightarrow 7/2_1$	28418.1529(80)	0.0007
$3/2_1 \rightarrow 3/2_3$	28414.8070(30)	-0.0019	$9/2_2 \rightarrow 7/2_1$	28418.7759(60)	0.0049
			$1/2_1 \rightarrow 3/2_1$	28418.8164(60)	0.0009

$F_{\epsilon} \rightarrow F_{\epsilon}''$	Obs. frequency	Obs. -calc.	$F_{\epsilon} \rightarrow F_{\epsilon}''$	Obs. frequency	Obs. -calc.
$5/2_3 \rightarrow 5/2_1$	28418.8603(80)	-0.0011	$21/2_2 \rightarrow 21/2_1$	18159.5175(80)	-0.0005
$5/2_3 \rightarrow 7/2_1$	28418.9640(60)	0.0010	$21/2_2 \rightarrow 19/2_1$	18159.9819(80)	-0.0009
Rotational transition $4_{0,4} \rightarrow 3_{0,3}$:			Rotational transition $4_{2,3} \rightarrow 3_{2,2}$:		
$3/2_1 \rightarrow 3/2_2$	37877.0211(80)	-0.0006	$7/2_3 \rightarrow 9/2_2$	37877.3342(80)	0.0058
$9/2_3 \rightarrow 9/2_2$	37877.2157(80)	0.0024	$5/2_2 \rightarrow 7/2_2$	37877.5307(80)	-0.0058
$7/2_1 \rightarrow 7/2_1$	37877.416(10)	0.0064	Rotational transition $1_{1,1} \rightarrow 2_{0,2}$:		
$3/2_1 \rightarrow 5/2_3$	37877.416(10)	0.0056	$3/2_1 \rightarrow 1/2_2$	34372.9843(30)•	-0.0013
$7/2_3 \rightarrow 5/2_3$	37877.6512(50)	0.0005	$3/2_1 \rightarrow 3/2_3$	34373.0840(40)•	0.0007
$5/2_2 \rightarrow 3/2_2$	37877.7484(80)	0.0020	$1/2_1 \rightarrow 1/2_2$	34373.4004(50)•	-0.0015
$3/2_1 \rightarrow 1/2_1$	37877.7484(80)	-0.0021	$5/2_1 \rightarrow 3/2_3$	34373.4515(70)•	0.0023
$7/2_3 \rightarrow 9/2_2$	37877.8389(80)	-0.0039	$1/2_1 \rightarrow 3/2_3$	34373.5004(50)•	0.0008
$11/2_1 \rightarrow 9/2_1$	37877.8389(80)	-0.0031	$5/2_1 \rightarrow 7/2_2$	34374.0842(30)	-0.0019
$11/2_2 \rightarrow 9/2_2$	37877.8640(30)	-0.0023	$3/2_1 \rightarrow 5/2_3$	34374.1732(50)	0.0001
$5/2_2 \rightarrow 5/2_3$	37878.1360(30)	0.0013	$3/2_1 \rightarrow 3/2_2$	34374.4509(70)•	0.0006
$11/2_2 \rightarrow 11/2_1$	37878.4507(50)	0.0015	$1/2_2 \rightarrow 3/2_3$	34374.4792(60)•	0.0024
$3/2_1 \rightarrow 5/2_2$	37878.503(12)	-0.0041	$3/2_2 \rightarrow 1/2_2$	34374.5771(70)•	0.0025
$7/2_2 \rightarrow 7/2_1$	37878.5335(50)	-0.0000	$3/2_2 \rightarrow 3/2_3$	34374.6758(50)•	0.0035
$7/2_3 \rightarrow 5/2_2$	37878.746(12)	-0.0016	$5/2_1 \rightarrow 3/2_2$	34374.8183(70)•	0.0021
$7/2_2 \rightarrow 9/2_1$	37878.817(12)	0.0022	$5/2_2 \rightarrow 3/2_3$	34375.0498(60)•	0.0037
$7/2_3 \rightarrow 7/2_2$	37879.0526(80)	-0.0032	$7/2_1 \rightarrow 7/2_2$	34375.1716(30)	-0.0000
$9/2_3 \rightarrow 9/2_1$	37879.1620(60)	0.0001	$5/2_2 \rightarrow 7/2_2$	34375.6808(30)	-0.0022
$5/2_2 \rightarrow 5/2_2$	37879.2327(60)	0.0008	$3/2_2 \rightarrow 5/2_3$	34375.7643(40)	0.0022
$3/2_1 \rightarrow 5/2_1$	37879.7351(80)	0.0014	$5/2_2 \rightarrow 5/2_3$	34376.1362(50)	0.0003
$5/2_2 \rightarrow 3/2_1$	37879.765(12)	-0.0021	$5/2_2 \rightarrow 3/2_2$	34376.412(10)	-0.0009
$7/2_3 \rightarrow 9/2_1$	37879.7921(50)	0.0008	$5/2_2 \rightarrow 5/2_2$	34376.6185(70)	-0.0006
Rotational transition $8_{1,7} \rightarrow 8_{1,8}$:			Rotational transition $2_{1,2} \rightarrow 3_{0,3}$:		
$21/2_1 \rightarrow 19/2_1$	14529.921(10)	-0.0008	$5/2_1 \rightarrow 5/2_3$	24502.6374(40)	0.0008
$17/2_2 \rightarrow 17/2_1$	14530.0875(80)	0.0002	$3/2_1 \rightarrow 5/2_3$	24502.8006(50)	-0.0020
$17/2_3 \rightarrow 19/2_1$	14530.4140(80)	-0.0021	$7/2_1 \rightarrow 5/2_3$	24502.9079(40)	-0.0011
$17/2_3 \rightarrow 15/2_1$	14530.6402(80)	0.0021	$7/2_1 \rightarrow 9/2_2$	24503.1015(30)	0.0005
$17/2_3 \rightarrow 17/2_1$	14530.871(10)	0.0005	$5/2_1 \rightarrow 7/2_3$	24503.4479(70)	0.0005
Rotational transition $9_{1,8} \rightarrow 9_{1,9}$:			$7/2_2 \rightarrow 9/2_2$	24503.6488(30)	0.0000
$19/2_2 \rightarrow 17/2_1$	18157.816(15)	0.0074	$5/2_1 \rightarrow 5/2_2$	24503.7345(50)	0.0007
$19/2_3 \rightarrow 21/2_1$	18158.291(10)	0.0037	$3/2_1 \rightarrow 5/2_2$	24503.9011(50)	0.0013
$17/2_3 \rightarrow 19/2_1$	18158.966(12)	-0.0069	$9/2_1 \rightarrow 9/2_2$	24504.0913(80)	-0.0038

$F_{\epsilon} \rightarrow F_{\epsilon}''$	Obs. frequency	Obs. -calc.	$F_{\epsilon} \rightarrow F_{\epsilon}''$	Obs. frequency	Obs. -calc.
$7/2_2 \rightarrow 7/2_3$	24504.270(10)	0.0025	$5/2_3 \rightarrow 5/2_2$	14442.9362(80)	0.0003
$5/2_1 \rightarrow 3/2_1$	24504.270(10)	0.0015	$7/2_1 \rightarrow 9/2_1$	14443.0087(80)	0.0021
$5/2_2 \rightarrow 7/2_3$	24504.4024(70)	-0.0015	$9/2_1 \rightarrow 9/2_2$	14443.0899(80)	-0.0004
Rotational transition $3_{1,3} \rightarrow 4_{0,4}$:			$5/2_2 \rightarrow 7/2_2$	14443.2030(80)	-0.0005
$5/2_1 \rightarrow 5/2_2$	14441.1875(80)	-0.0006	$5/2_3 \rightarrow 7/2_3$	14443.421(10)	0.0006
$5/2_1 \rightarrow 7/2_3$	14441.672(10)	-0.0003	$3/2_2 \rightarrow 3/2_1$	14443.421(10)	0.0039
$9/2_1 \rightarrow 11/2_2$	14441.7443(60)	-0.0039	$11/2_1 \rightarrow 13/2_1$	14443.5249(80)	-0.0008
$3/2_1 \rightarrow 5/2_2$	14441.8081(60)	0.0017	$7/2_2 \rightarrow 9/2_2$	14443.6438(80)	-0.0013
$5/2_1 \rightarrow 3/2_1$	14441.9136(60)	0.0008	$9/2_1 \rightarrow 11/2_1$	14443.7192(80)	-0.0018
$7/2_1 \rightarrow 9/2_3$	14442.0169(60)	0.0021	Rotational transition $7_{0,7} \rightarrow 6_{1,6}$:		
$7/2_2 \rightarrow 7/2_3$	14442.3243(60)	-0.0021	$15/2_1 \rightarrow 13/2_1$	16796.1599(70)	0.0028
$7/2_1 \rightarrow 7/2_2$	14442.3649(80)	0.0030	$11/2_2 \rightarrow 9/2_2$	16796.440(10)	0.0004
$9/2_2 \rightarrow 11/2_2$	14442.4577(60)	-0.0009	$15/2_2 \rightarrow 13/2_1$	16796.440(10)	-0.0042
$5/2_1 \rightarrow 7/2_2$	14442.6520(60)	0.0034	$17/2_2 \rightarrow 15/2_2$	16796.4972(90)	-0.0015
$7/2_1 \rightarrow 9/2_2$	14442.7013(60)	-0.0027			

Frequencies (in MHz) of the observed and calculated hyperfine transitions of $K^{13}CN$ in the ground vibrational state.

$F_{\epsilon} \rightarrow F_{\epsilon}''$	Obs. frequency	Obs. -calc.	$F_{\epsilon} \rightarrow F_{\epsilon}''$	Obs. frequency	Obs. -calc.
Rotational transition $2_{0,2} \rightarrow 1_{0,1}$:			$9/2_3 \rightarrow 9/2_2$	36911.6259(60)	0.0004
$3/2_2 \rightarrow 3/2_1$	18467.5640(80)	-0.0014	$7/2_3 \rightarrow 5/2_3$	36912.0581(80)	-0.0012
$5/2_3 \rightarrow 3/2_1$	18467.8374(80)	-0.0041	$5/2_2 \rightarrow 3/2_2$	36912.1550(60)	0.0010
$1/2_2 \rightarrow 1/2_1$	18468.1926(60)	0.0007	$11/2_2 \rightarrow 9/2_2$	36912.2704(80)	-0.0032
$3/2_3 \rightarrow 5/2_1$	18468.4213(40)	0.0011	$5/2_2 \rightarrow 5/2_3$	36912.5420(80)	0.0023
Rotational transition $4_{0,4} \rightarrow 3_{0,3}$:			$5/2_1 \rightarrow 5/2_1$	36912.7995(80)	0.0072
$3/2_1 \rightarrow 3/2_2$	36911.4342(60)	-0.0010	$7/2_3 \rightarrow 7/2_2$	36913.4567(60)	-0.0033

$F_{\epsilon} \rightarrow F_{\epsilon}''$	Obs. frequency	Obs. -calc.	$F_{\epsilon} \rightarrow F_{\epsilon}''$	Obs. frequency	Obs. -calc.
Rotational transition $8_{1,7} \rightarrow 8_{1,8}$:			$3/2_1 \rightarrow 3/2_3$	32697.2775(80)	0.0067
$11/2_1 \rightarrow 13/2_1$	14344.3906(80)	-0.0030	$5/2_1 \rightarrow 7/2_2$	32698.2708(80)	-0.0024
$17/2_2 \rightarrow 19/2_1$	14344.3906(80)	0.0037	$3/2_1 \rightarrow 5/2_3$	32698.3566(80)	-0.0012
$21/2_1 \rightarrow 19/2_1$	14344.6690(80)	-0.0031	Rotational transition $3_{1,3} \rightarrow 4_{0,4}$:		
$17/2_2 \rightarrow 17/2_1$	14344.833(10)	-0.0055	$5/2_1 \rightarrow 5/2_2$	13261.6273(70)	-0.0015
$15/2_3 \rightarrow 17/2_2$	14345.151(10)	0.0027	$3/2_1 \rightarrow 5/2_2$	13262.2442(60)	-0.0011
$17/2_3 \rightarrow 15/2_1$	14345.388(12)	0.0084	$5/2_1 \rightarrow 3/2_1$	13262.3422(60)	-0.0054
$17/2_3 \rightarrow 17/2_1$	14345.6115(70)	0.0003	$7/2_1 \rightarrow 9/2_3$	13262.4516(70)	0.0012
Rotational transition $9_{1,8} \rightarrow 9_{1,9}$:			$7/2_2 \rightarrow 7/2_3$	13262.7626(70)	0.0055
$19/2_1 \rightarrow 19/2_1$	17925.4546(90)	0.0010	$7/2_1 \rightarrow 7/2_2$	13262.8026(70)	0.0037
$19/2_2 \rightarrow 19/2_2$	17925.6094(80)	0.0022	Rotational transition $7_{0,7} \rightarrow 6_{1,6}$:		
$19/2_2 \rightarrow 17/2_2$	17925.7786(90)	0.0042	$15/2_1 \rightarrow 13/2_1$	17208.9254(60)	-0.0014
$13/2_1 \rightarrow 15/2_1$	17925.8398(90)	-0.0023	$11/2_2 \rightarrow 9/2_2$	17209.2094(80)	0.0031
$19/2_2 \rightarrow 21/2_1$	17925.8398(90)	0.0015	$15/2_2 \rightarrow 13/2_1$	17209.2094(80)	-0.0001
$17/2_2 \rightarrow 19/2_2$	17925.980(10)	-0.0066	$17/2_2 \rightarrow 15/2_2$	17209.2644(60)	-0.0003
$19/2_2 \rightarrow 17/2_1$	17926.0918(80)	0.0030	Rotational transition $11_{2,10} \rightarrow 12_{1,11}$:		
$23/2_1 \rightarrow 21/2_1$	17926.0918(80)	0.0011	$23/2_2 \rightarrow 25/2_3$	27986.170(20)	-0.0098
$17/2_2 \rightarrow 17/2_2$	17926.158(10)	0.0035	$23/2_2 \rightarrow 25/2_2$	27986.796(30)	0.0142
$17/2_3 \rightarrow 19/2_2$	17926.554(10)	0.0048	$21/2_3 \rightarrow 23/2_2$	27987.373(20)	0.0035
$19/2_3 \rightarrow 21/2_1$	17926.554(10)	-0.0054	Rotational transition $12_{2,11} \rightarrow 13_{1,12}$:		
$17/2_3 \rightarrow 19/2_1$	17927.2366(80)	-0.0057	$27/2_1 \rightarrow 27/2_2$	16267.747(20)	0.0049
$15/2_2 \rightarrow 15/2_1$	17927.7334(90)	0.0053	$27/2_2 \rightarrow 29/2_2$	16267.747(20)	-0.0104
$21/2_2 \rightarrow 21/2_1$	17927.7838(90)	-0.0036	$23/2_3 \rightarrow 25/2_2$	16268.937(30)	0.0124
$21/2_2 \rightarrow 19/2_1$	17928.2482(60)	-0.0016	Rotational transition $17_{1,16} \rightarrow 16_{2,15}$:		
Rotational transition $19_{2,17} \rightarrow 19_{2,18}$:			$33/2_2 \rightarrow 31/2_3$	32243.819(20)	-0.0053
$43/2_1 \rightarrow 43/2_1$	13059.228(20)	0.0049	$37/2_2 \rightarrow 35/2_2$	32244.932(20)	0.0053
$35/2_2 \rightarrow 35/2_2$	13059.955(20)	-0.0049	Rotational transition $21_{3,19} \rightarrow 22_{2,20}$:		
Rotational transition $20_{2,18} \rightarrow 20_{2,19}$:			$45/2_2 \rightarrow 47/2_2$	36812.477(20)	-0.0082
$45/2_1 \rightarrow 45/2_1$	15781.603(20)	-0.0056	$37/2_1 \rightarrow 39/2_1$	36813.202(20)	0.0082
$43/2_2 \rightarrow 43/2_2$	15782.416(20)	0.0056	Rotational transition $23_{3,21} \rightarrow 24_{2,22}$:		
Rotational transition $21_{2,19} \rightarrow 21_{2,20}$:			$49/2_2 \rightarrow 51/2_2$	12519.786(20)	0.0007
$43/2_1 \rightarrow 43/2_1$	18863.825(20)	0.0041	$45/2_3 \rightarrow 47/2_2$	12520.565(20)	-0.0007
$43/2_3 \rightarrow 43/2_2$	18864.724(20)	-0.0041	Rotational transition $26_{2,24} \rightarrow 25_{3,23}$:		
Rotational transition $1_{1,1} \rightarrow 2_{0,2}$:			$51/2_2 \rightarrow 49/2_3$	12823.963(20)	-0.0035
$3/2_1 \rightarrow 1/2_2$	32697.1706(80)	-0.0032	$55/2_2 \rightarrow 53/2_2$	12824.798(20)	0.0035

Frequencies (in MHz) of the observed and calculated hyperfine transitions of $KC^{15}N$ in the ground vibrational state.

$F_{\epsilon}^{\prime} \rightarrow F_{\epsilon}^{\prime\prime}$	Obs.frequency	Obs.-calc.	$F_{\epsilon}^{\prime} \rightarrow F_{\epsilon}^{\prime\prime}$	Obs.frequency	Obs.-calc.
Rotational transition $2_{0,2} \rightarrow 1_{0,1}$:			$13_1 \rightarrow 13_1$	26391.738(15)	-0.0040
$2_2 \rightarrow 2_2$	18564.3294(70)	0.0048	$10_1 \rightarrow 10_1$	26391.840(15)	0.0040
$2_1 \rightarrow 2_1$	18564.717(15)	-0.0072	$12_1 \rightarrow 12_1$	26391.840(15)	-0.0034
$3_2 \rightarrow 3_1$	18564.717(15)	-0.0074	Rotational transition $12_{1,11} \rightarrow 12_{1,12}$:		
$1_1 \rightarrow 1_1$	18565.728(12)	0.0006	$10_1 \rightarrow 10_1$	31174.623(15)	0.0005
$1_2 \rightarrow 1_1$	18567.1311(50)	-0.0009	$14_1 \rightarrow 14_1$	31174.623(15)	-0.0053
Rotational transition $3_{0,3} \rightarrow 2_{0,2}$:			$11_1 \rightarrow 11_1$	31174.728(15)	0.0053
$4_1 \rightarrow 4_1$	27839.4499(80)	-0.0067	$13_1 \rightarrow 13_1$	31174.728(15)	-0.0006
$1_1 \rightarrow 1_2$	27840.5122(50)	0.0000	Rotational transition $13_{1,12} \rightarrow 13_{1,13}$:		
$3_1 \rightarrow 3_1$	27840.8628(80)	0.0037	$11_1 \rightarrow 11_1$	36347.969(15)	-0.0005
$4_2 \rightarrow 4_1$	27840.8628(80)	0.0033	$15_1 \rightarrow 15_1$	36347.969(15)	-0.0049
$2_1 \rightarrow 2_1$	27841.5152(70)	-0.0003	$12_1 \rightarrow 12_1$	36348.075(15)	0.0049
Rotational transition $4_{0,4} \rightarrow 3_{0,3}$:			$14_1 \rightarrow 14_1$	36348.075(15)	0.0005
$3_1 \rightarrow 3_2$	37109.5313(40)	-0.0002	Rotational transition $19_{2,17} \rightarrow 19_{2,18}$:		
$2_1 \rightarrow 2_2$	37109.5313(40)	-0.0008	$17_1 \rightarrow 17_1$	13099.9300(80)	-0.0014
$4_1 \rightarrow 4_1$	37109.6955(50)	0.0014	$21_1 \rightarrow 21_1$	13099.9300(80)	-0.0005
$5_2 \rightarrow 5_1$	37109.6955(50)	0.0007	$18_1 \rightarrow 18_1$	13099.9624(80)	0.0005
$3_1 \rightarrow 3_1$	37110.1883(60)	-0.0001	$20_1 \rightarrow 20_1$	13099.9624(80)	0.0014
$2_1 \rightarrow 2_1$	37110.9368(80)	-0.0013	Rotational transition $20_{2,18} \rightarrow 20_{2,19}$:		
Rotational transition $8_{1,7} \rightarrow 8_{1,8}$:			$18_1 \rightarrow 18_1$	15832.1274(80)	0.0012
$6_1 \rightarrow 6_1$	14409.335(15)	0.0095	$22_1 \rightarrow 22_1$	15832.1274(80)	0.0025
$10_1 \rightarrow 10_1$	14409.335(15)	-0.0042	$19_1 \rightarrow 19_1$	15832.1568(80)	-0.0025
$7_1 \rightarrow 7_1$	14409.433(15)	0.0065	$21_1 \rightarrow 21_1$	15832.1568(80)	-0.0012
$9_1 \rightarrow 9_1$	14409.433(15)	-0.0073	Rotational transition $21_{2,19} \rightarrow 21_{2,20}$:		
$8_2 \rightarrow 8_1$	14409.6767(90)	-0.0017	$19_1 \rightarrow 19_1$	18925.8979(80)	-0.0012
Rotational transition $9_{1,8} \rightarrow 9_{1,9}$:			$23_1 \rightarrow 23_1$	18925.8979(80)	0.0005
$7_1 \rightarrow 7_1$	18007.261(15)	0.0040	$20_1 \rightarrow 20_1$	18925.9343(80)	-0.0005
$11_1 \rightarrow 11_1$	18007.261(15)	-0.0073	$22_1 \rightarrow 22_1$	18925.9343(80)	0.0012
$8_1 \rightarrow 8_1$	18007.365(15)	0.0073	Rotational transition $23_{2,21} \rightarrow 23_{2,22}$:		
$10_1 \rightarrow 10_1$	18007.365(15)	-0.0040	$21_1 \rightarrow 21_1$	26260.0877(80)	-0.0012
Rotational transition $11_{1,10} \rightarrow 11_{1,11}$:			$25_1 \rightarrow 25_1$	26260.0877(80)	0.0014
$9_1 \rightarrow 9_1$	26391.738(15)	0.0034	$22_1 \rightarrow 22_1$	26260.1280(80)	-0.0014

$F_{\epsilon} \rightarrow F_{\epsilon}''$	Obs. frequency	Obs. - calc.	$F_{\epsilon} \rightarrow F_{\epsilon}''$	Obs. frequency	Obs. - calc.
$24_1 \rightarrow 24_1$	26260.1280(80)	0.0012	$12_1 \rightarrow 12_1$	28330.364(12)	0.0024
Rotational transition $24_{2,22} \rightarrow 24_{2,23}$:			$11_2 \rightarrow 11_1$	28330.364(12)	-0.0049
$22_1 \rightarrow 22_1$	30524.6369(80)	0.0001	Rotational transition $12_{2,11} \rightarrow 13_{1,12}$:		
$26_1 \rightarrow 26_1$	30524.6369(80)	0.0032	$14_1 \rightarrow 14_2$	16548.359(12)	0.0058
$23_1 \rightarrow 23_1$	30524.6765(80)	-0.0032	$11_2 \rightarrow 11_1$	16548.359(12)	-0.0019
$25_1 \rightarrow 25_1$	30524.6765(80)	-0.0001	$13_1 \rightarrow 13_1$	16548.392(12)	0.0019
Rotational transition $1_{1,1} \rightarrow 2_{0,2}$:			$12_2 \rightarrow 12_1$	16548.392(12)	-0.0058
$0_1 \rightarrow 0_1$	32936.9888(40)	0.0000	Rotational transition $17_{1,16} \rightarrow 16_{2,15}$:		
$1_2 \rightarrow 1_2$	32938.1603(60)	0.0005	$16_1 \rightarrow 16_2$	32230.037(15)	0.0042
$3_1 \rightarrow 3_2$	32938.5115(40)	-0.0011	$15_1 \rightarrow 15_2$	32230.037(15)	0.0028
$2_2 \rightarrow 2_2$	32939.5648(50)	0.0008	$17_1 \rightarrow 17_1$	32230.037(15)	-0.0028
$2_2 \rightarrow 2_1$	32940.5680(40)	0.0003	$18_2 \rightarrow 18_1$	32230.037(15)	-0.0042
Rotational transition $7_{0,7} \rightarrow 6_{1,6}$:			Rotational transition $21_{3,19} \rightarrow 22_{2,20}$:		
$6_1 \rightarrow 6_2$	17235.1880(70)	0.0012	$23_1 \rightarrow 23_2$	37305.999(30)	0.0122
$7_1 \rightarrow 7_1$	17235.2213(70)	0.0011	$20_2 \rightarrow 20_1$	37305.999(30)	0.0094
$5_1 \rightarrow 5_2$	17235.2382(70)	-0.0024	$22_1 \rightarrow 22_1$	37305.999(30)	-0.0095
$8_2 \rightarrow 8_1$	17235.2746(70)	0.0005	$21_2 \rightarrow 21_1$	37305.999(30)	-0.0122
$6_1 \rightarrow 6_1$	17235.5144(80)	0.0027	Rotational transition $26_{2,24} \rightarrow 25_{3,23}$:		
$5_1 \rightarrow 5_1$	17236.5975(70)	-0.0024	$25_1 \rightarrow 25_2$	12615.515(15)	0.0023
Rotational transition $11_{2,10} \rightarrow 12_{1,11}$:			$24_1 \rightarrow 24_2$	12615.515(15)	0.0006
$13_1 \rightarrow 13_2$	28330.315(12)	0.0049	$26_1 \rightarrow 26_1$	12615.515(15)	-0.0006
$10_2 \rightarrow 10_1$	28330.315(12)	-0.0025	$27_2 \rightarrow 27_1$	12615.515(15)	-0.0023

REFERENCES

- ¹In this paper the alkali metal cyanides are denoted by MCN (where M represents the alkali metal), whatever the structure may be, and the atomic symbol designates the most abundant isotope, unless specified otherwise.
- ²P.E.S. Wormer, and J. Tennyson, *J. Chem. Phys.* **75**, 1245 (1981).
- ³M.L. Klein, J.D. Goddard, and D.G. Bounds, *J. Chem. Phys.* **75**, 3909 (1981); C.J. Marsden, *J. Chem. Phys.* **76**, 6451 (1982).
- ⁴R. Essers, J. Tennyson, and P.E.S. Wormer, *Chem. Phys. Lett.* **89**, 223 (1982).
- ⁵E. Clementi, H. Kistenmacher, and H. Popkie, *J. Chem. Phys.* **58**, 2460 (1973).
- ⁶Z.K. Ismail, R.H. Hauge, and J.L. Margrave, *J. Mol. Spectrosc.* **45**, 304 (1973).
- ⁷W.J. Pietro, B.A. Levi, W.J. Hehre, and R.F. Stewart, *Inorg. Chem.* **19**, 2225 (1980).
- ⁸P. Kuipers, T. Törring, and A. Dymanus, *Chem. Phys. Lett.* **42**, 423 (1976).
- ⁹T. Törring, J.P. Bekooy, W.L. Meerts, J. Hoef, E. Tiemann, and A. Dymanus, *J. Chem. Phys.* **73**, 4875 (1980).
- ¹⁰J.J. van Vaals, W.L. Meerts, and A. Dymanus, *Chem. Phys.*, in press (1983).
- ¹¹J.J. van Vaals, Ph.D. Thesis, Katholieke Universiteit Nijmegen, The Netherlands (1983).
- ¹²L.L. Simmons, L.F. Lowden, and T.C. Ehlert, *J. Phys. Chem.* **81**, 709 (1977).
- ¹³P. Thaddeus, L.C. Krisher, and J.H.N. Loubser, *J. Chem. Phys.* **40**, 257 (1964).
- ¹⁴All uncertainties stated in this paper represent three times the standard deviation as determined by the least-squares fit.
- ¹⁵The variance σ is defined as $[\chi^2/(n-m)]^{1/2}$ with χ^2 defined as usual in a least-squares fit, n the number of spectral lines and m the number of parameters in the fit.
- ¹⁶J.K.G. Watson, *J. Chem. Phys.* **46**, 1935 (1967); *J. Chem. Phys.* **48**, 4517 (1968).

- ¹⁷J.J. van Vaals, W.L. Meerts, and A. Dymanus, *34th Symposium on Molecular Spectroscopy* (Columbus, Ohio, 1980); *7th Colloquium on High Resolution Spectroscopy* (Reading, 1981).
- ¹⁸W.H. Kirchhoff, *J. Mol. Spectrosc.* *41*, 333 (1972).
- ¹⁹We used: $h=6.626176(36)\times 10^{-34}$ Js. This value is from: E.R. Cohen, and B.N. Taylor, *J. Phys. Chem. Ref. Data* *2*, 663 (1973).
- ²⁰J. Kraitchman, *Amer. J. Phys.* *21*, 17 (1953).
- ²¹D.R. Lide, Jr., in: *Molecular Structure and Properties, Physical Chemistry Series Two, Volume 2*, ed. A.D. Buckingham (Butterworths, London, 1975).
- ²²W. Gordy, and R.L. Cook, *Microwave Molecular Spectra* (Interscience, New York, 1970).
- ²³C.C. Costain, *J. Chem. Phys.* *29*, 864 (1958).
- ²⁴J.K.G. Watson, *J. Mol. Spectrosc.* *48*, 479 (1973).
- ²⁵C.J. Marsden, private communication.
- ²⁶J.J. van Vaals, W.L. Meerts, and A. Dymanus, *J. Chem. Phys.* *77*, 5245 (1982).
- ²⁷We employed $Q(^{39}\text{K}) = 0.059$ barn, and $Q(^{14}\text{N}) = 0.0166$ barn. These values are from: C.M. Lederer, and V.S. Shirley (eds.), *Table of Isotopes, Seventh Edition* (Wiley & Sons, New York, 1978).
- ²⁸D.W. Posener, *Austr. J. Phys.* *13*, 168 (1960).
- ²⁹This can be inferred from *ab initio* calculations (Refs. 2 and 3) and is confirmed by preliminary results for the electric dipole moments $\mu_a = 11(1)$ D and $\mu_b = 6(2)$ D, which we obtained from measurements in nonzero electric fields using the molecular beam electric resonance technique.
- ³⁰P.E.S. Wormer, private communication.
- ³¹P.R. Taylor, G.B. Bacskay, N.S. Hush, and A.C. Hurley, *J. Chem. Phys.* *70*, 4481 (1979).
- ³²J. Tennyson, and B.T. Sutcliffe, *Mol. Phys.* *46*, 97 (1982).
- ³³J. Tennyson, and A. van der Avoird, *J. Chem. Phys.* *76*, 5710 (1982); J. Tennyson, and B.T. Sutcliffe, *J. Chem. Phys.* *77*, 4061 (1982).
- ³⁴G.E. Leroi, and W. Klemperer, *J. Chem. Phys.* *35*, 774 (1961).
- ³⁵JANAF, *Thermochemical Tables*, 2nd ed. (U.S. Department of Commerce, National Bureau of Standards, Washington, D.C., 1971); J.N. Mulvihill, and L.F. Phillips, *Chem. Phys. Lett.* *33*, 608 (1975); B.V. L'vov, and L.A. Pelieva, *Prog. Analyt. Atom. Spectrosc.* *3*, 65 (1980); K. Skudlarski, and M. Miller, *Adv. Mass. Spectrom.* *8A*, 433 (1980); *High Temp. Sci.* *15*, 151 (1982).

³⁶V.A. Istomin, N.F. Stepanov, and B.I. Zhilinskii, *J. Mol. Spectrosc.* **67**, 265 (1977); B.I. Zhilinskii, V.A. Istomin, and N.F. Stepanov, *Chem. Phys.* **31**, 413 (1978); P.R. Bunker, and D.J. Howe, *J. Mol. Spectrosc.* **83**, 288 (1980); G. Brocks, and J. Tennyson, *J. Mol. Spectrosc.*, **99**, 263 (1983); O.S. van Roosmalen, F. Iachello, R.D. Levine, and A.E.L. Dieperink, preprint.

STRUCTURE OF SODIUM CYANIDE

BY MOLECULAR BEAM ELECTRIC RESONANCE SPECTROSCOPY

ABSTRACT

The results of the first successful observation of the microwave spectrum of sodium cyanide are presented. Twenty rotational transitions between 9.5 and 40 GHz were used to determine the rotational constants and the effective structure of the free molecule in the ground vibrational state. The structure was found to be T shaped and the results are: $r_{\text{CN}} = 1.169(6) \text{ \AA}$, $r_{\text{NaC}} = 2.366(29) \text{ \AA}$, $r_{\text{NaN}} = 2.243(27) \text{ \AA}$.

Until recently all gaseous alkali metal cyanides¹ were assumed to be linear. Quantum mechanical calculations² indicated that this is the case for lithium cyanide. The linear isocyanide configuration LiNC is expected to be the most stable. This structure was indeed deduced from vibrational isotope effects of lithium cyanide in inert gas matrices³. Using the same method Ismail *et al.*⁴ expected sodium and potassium cyanide to have a linear cyanide configuration. Pietro *et al.*⁵ calculated the equilibrium geometry of gaseous KCN using a STO-3G basis set and also found a linear cyanide configuration. Recently gas phase spectroscopy determined accurately and unambiguously the structure of KCN^{6,7}, which surprisingly was found to be T shaped. In this paper we report the experimentally determined structure of NaCN, which is found to be T shaped as well.

A report of the experimentally determined gas phase structure of potassium cyanide^{6,7} stimulated *ab initio* potential energy surface calculations on both potassium cyanide⁸⁻¹⁰ and sodium cyanide^{9,10}. As for LiCN, the M-CN bonding is found to be predominantly ionic: there is an almost complete charge transfer between the CN group and the alkali atom. The potential energy surface in the bending direction has very low barriers for internal rotation (0.3 eV or smaller). This implies that moderate thermal excitation of these molecules is sufficient to allow the M⁺ cation to move more or less freely around the CN⁻ anion. Clementi *et al.*² referred to this as a "polytopic bond", since in this case no structural formula is preferred. However, it is established that both KCN^{6,7} and NaCN (current work) can be considered rigid in the ground vibrational state. Yet the amplitudes of the zero-point bending motion in both molecules can range up to 10°, while for LiCN this amplitude is expected to be even larger².

In this communication we present the results of the first successful observation of the microwave spectrum of sodium cyanide. Earlier attempts by Kuijpers and Törring in our laboratory to observe microwave absorption of NaCN in the high temperature cell which was used for KCN¹¹ failed; probably due to polymerization of NaCN in combination with lack of sensitivity. Presently we employed the molecular beam electric resonance technique with essentially the same set-up as described before⁶. An argon seeded sodium cyanide beam was used. The temperatures of the supply chamber and the nozzle chamber of the stainless steel oven were typically held at 1100 K and 1300 K, respectively. The vapour

pressure of NaCN in the supply chamber at this temperature was of the order of 1 mbar, the stagnation pressure of the carrier gas argon was 1 bar. Maintaining a stable beam turned out to be more difficult than for KCN. Clogging occurred after a few hours and before each run the oven had to be cleaned thoroughly. The seeded beam technique was used in order to obtain strong translational, rotational and vibrational relaxation. Due to the vibrational cooling only transitions of molecules in the ground vibrational state were detected. This simplifies the microwave spectrum and makes identification of the observed transitions feasible. We observed 20 rotational transitions between 9.5 and 40 GHz. The quadrupole hyperfine structure was resolved for most transitions. The linewidth of a single component was about 30 kHz. The signal to noise ratio of the strongest lines was 10 using an integration time of 3 s. All the observed rotational transitions were identified as a-type (10) and b-type (10) transitions of a near-prolate asymmetric top rotor. The observed spectrum was fitted using Watson's reduced Hamiltonian¹². We determined the three rotational and the five quartic distortion constants. The τ -free rotational constants for sodium cyanide in the ground vibrational state are listed in Table I.

Assuming the CN bond lengths (r_{CN}) in NaCN and KCN to be equal within 0.006 Å and using the rotational constants from Table I, the structure of NaCN can be calculated. The result is presented in Table II. The effective CN bond length of KCN was determined by Vaals *et al.*⁷ using the results from three isotopic species. The assumption that within the quoted uncertainty r_{CN} is not affected by the change from potassium to sodium is justified by the following arguments. Both KCN and NaCN have similar T-shaped structures, the M-CN bonding in both molecules is almost completely ionic, and their bending vibrational frequencies ω_2 are about equal. The latter frequencies were estimated

Table I. The τ -free rotational constants for the ground vibrational state of NaCN.

Constant	Value (MHz)
A	57920.9 (11)
B	8368.48(17)
C	7272.37(17)

Table II. The effective structural parameters for the ground vibrational state of NaCN.

Constant	Value (Å)
r_{CN}^{a}	1.169 (6)
r_{NaC}	2.366(29)
r_{NaN}	2.243(27)

^aThe CN bond length has been fixed (see text).

from the inertial defects: $0.4295 \text{ amu}\text{\AA}^2$ for KCN and $0.3769 \text{ amu}\text{\AA}^2$ for NaCN, yielding¹³ $\omega_2 = 157(30) \text{ cm}^{-1}$ and $\omega_2 = 179(35) \text{ cm}^{-1}$, respectively. These values are in good agreement with those found by Ismail *et al.*⁴ in matrix-isolation studies: $\omega_2 = 139 \text{ cm}^{-1}$ for KCN and $\omega_2 = 169 \text{ cm}^{-1}$ for NaCN.

From the trend in ω_2 found in matrix-isolation studies of LiCN, NaCN and KCN, Törring *et al.*⁶ predicted a T-shaped structure for NaCN. Our present measurements have unambiguously confirmed this expectation. Recent *ab initio* computations of the potential energy surface of sodium cyanide^{9,10} also favour a T-shaped structure. The equilibrium structures derived from these calculations, however, have still relatively large uncertainties. This is illustrated by the disagreement among the calculated structures (5%) and isomerization energies (50%) that are obtained from various calculations using different basis sets or when electron correlation is included^{2,9,10}. The suggestion of Klein *et al.*⁹ that the difference between the computed equilibrium geometry and the experimentally determined effective structure r_0 ⁷ can be explained by the effect of vibrational averaging is not likely. Even for "floppy" molecules like KCN and NaCN these effects are much smaller than the discrepancies between the *ab initio* and experimental structures (e.g., 10% for the angle $\theta(\text{NaN})$). We have made an estimate for KCN⁷ of the differences between effective and substitution structural parameters to be less than 0.5% of r_0 . This implies that the expected differences between effective and equilibrium structural parameters are about 1% of r_0 .

A more accurate structure determination for NaCN, without assuming the CN bond length, will be possible after the evaluation of the rotational spectrum of the ^{13}C isotopically substituted species of sodium cyanide in the ground vibrational state. These experiments are currently underway. A full report of the present work will be published elsewhere.

The authors thank Dr. J.P. Bekooy for many stimulating discussions. This work is part of the research program of the Stichting voor Fundamenteel Onderzoek der Materie (F.O.M.) and has been made possible by financial support from the Nederlandse Organisatie voor Zuiver Wetenschappelijk Onderzoek (Z.W.O.).

REFERENCES

- ¹In this communication the alkali metal cyanides are denoted by MCN (where M represents the alkali metal), whatever the structure may be, unless specified otherwise.
- ²B. Bak, E. Clementi, and R.N. Kortzeborn, *J. Chem. Phys.* **52**, 764 (1970); E. Clementi, H. Kistenmacher, and H. Popkie, *J. Chem. Phys.* **58**, 2460 (1973); V.A. Istomin, N.F. Stepanov, and B.I. Zhilinskii, *J. Mol. Spectrosc.* **67**, 265 (1977); A. Schmiedekamp, C.W. Bock, and P. George, *J. Mol. Struct.* **67**, 107 (1980); L.T. Redmon, G.D. Purvis, III, and R.J. Bartlett, *J. Chem. Phys.* **72**, 986 (1980); R. Essers, J. Tennyson, and P.E.S. Wormer, *Chem. Phys. Lett.* **89**, 223 (1982).
- ³Z.K. Ismail, R.H. Hauge, and J.L. Margrave, *J. Chem. Phys.* **57**, 5137 (1972); K. Nakamoto, D. Tevault, and S. Tani, *J. Mol. Struct.* **43**, 75 (1978).
- ⁴Z.K. Ismail, R.H. Hauge, and J.L. Margrave, *J. Mol. Spectrosc.* **45**, 304 (1973).
- ⁵W.J. Pietro, B.A. Levi, W.J. Hehre, and R.F. Stewart, *Inorg. Chem.* **19**, 2225 (1980).
- ⁶T. Törring, J.P. Bekooy, W.L. Meerts, J. Hoeft, E. Tiemann, and A. Dymanus, *J. Chem. Phys.* **73**, 4875 (1980).
- ⁷J.J. van Vaals, W.L. Meerts, and A. Dymanus, *34th Symposium on Molecular Spectroscopy* (Columbus, Ohio, 1980); *7th Colloquium on High Resolution Spectroscopy* (Reading, 1981); manuscript in preparation.
- ⁸P.E.S. Wormer, and J. Tennyson, *J. Chem. Phys.* **75**, 1245 (1981).
- ⁹M.L. Klein, J.D. Goddard, and D.G. Bounds, *J. Chem. Phys.* **75**, 3909 (1981).
- ¹⁰C.J. Marsden, *J. Chem. Phys.* **76**, 6451 (1982).
- ¹¹P. Kuijpers, T. Törring, and A. Dymanus, *Chem. Phys. Lett.* **42**, 423 (1976).
- ¹²J.K.G. Watson, *J. Chem. Phys.* **46**, 1935 (1967); *J. Chem. Phys.* **48**, 4517 (1968).
- ¹³W. Gordy, and R.L. Cook, *Microwave Molecular Spectra* (Interscience, New York, 1970).

HIGH RESOLUTION MOLECULAR BEAM SPECTROSCOPY

OF NaCN AND Na¹³CN

ABSTRACT

The sodium cyanide molecule was studied by molecular beam electric resonance spectroscopy in the microwave region. We used the seeded beam technique to produce a supersonic beam with strong translational, rotational and vibrational cooling.

In the frequency range 9.5-40 GHz we observed and identified for NaCN 186 and for Na¹³CN 107 hyperfine transitions in 20 and 16 rotational transitions, respectively, all in the ground vibrational state. The rotational spectra could be fitted to an asymmetric rotor model, yielding the three rotational, the five quartic and three sextic centrifugal distortion constants for each isotopic species. The results for the rotational constants of NaCN are: $A'' = 57921.954(7)$ MHz, $B'' = 8369.312(2)$ MHz, $C'' = 7272.712(2)$ MHz. All quadrupole and several spin-rotation coupling constants for the hyperfine interaction were evaluated. The quadrupole coupling constants (in MHz) for NaCN are: $eQq_{aa}(\text{Na}) = -5.344(5)$, $eQq_{bb} = 2.397(7)$, $eQq_{aa}(\text{N}) = 2.148(4)$, $eQq_{bb}(\text{N}) = -4.142(5)$. From these constants and those of Na¹³CN we have determined the principal elements of the quadrupole coupling tensor for potassium and nitrogen.

The structure of sodium cyanide evaluated from the rotational constants of NaCN and Na¹³CN was found to be T shaped, similar to the structure of KCN but completely different from the linear isocyanide configuration of LiNC. The effective structural parameters for sodium cyanide in the ground vibrational state are: $r_{\text{CN}} = 1.170(4)$ Å, $r_{\text{NaC}} = 2.379(15)$ Å, $r_{\text{NaN}} = 2.233(15)$ Å, in gratifying agreement with *ab initio* calculations. Both the geometrical structure and the hyperfine coupling justify the conclusion that the CN group in gaseous sodium cyanide approximately can be considered as a free CN⁻ ion.

1. INTRODUCTION

The molecular structure of alkali metal cyanides¹ is difficult to predict. Since the first successful determination of the structure of gaseous potassium cyanide, which was found to be T shaped², several *ab initio* calculations of the potential energy surface and equilibrium structure of KCN were performed³⁻⁵. Recently, two *ab initio* calculations of the structure of NaCN became available^{4,5}. Both calculations predicted a T-shaped structure for sodium cyanide. However, as is illustrated by Marsden⁵, the quality of the basis sets used in the SCF calculations and the inclusion of electron correlation influences the calculated potential energy surface and the estimated equilibrium geometries drastically.

Ismail *et al.*⁶ concluded from vibrational isotope effects of sodium cyanide in inert gas matrices that the molecule has a linear cyanide configuration.

Earlier we reported preliminary results⁷ for the first successful observation of the rotational spectrum of the most abundant isotopic species of sodium cyanide. The structure was found to be T shaped, and under the assumption of a fixed CN bond length an effective structure for the ground vibrational state was calculated.

In the current work we discuss a more elaborate study of the rotational and hyperfine spectra of NaCN and Na¹³CN. We used the molecular beam electric resonance (MBER) spectrometer to observe for NaCN 186 and for Na¹³CN 107 hyperfine transitions in 20 and 16 rotational transitions, respectively. The hyperfine structure was analysed and for each isotopic species we evaluated the quadrupole coupling constants and some spin-rotation constants. All rotational transitions, measured in the frequency range 9.5-40 GHz, originated in the ground vibrational state of the molecule and could be fitted to an asymmetric rotor model. We determined the three rotational and eight distortion constants for NaCN and Na¹³CN.

Since spectroscopic information from two isotopic species is now available, a more accurate structure can be calculated without assuming a CN bond length of 1.169 Å, as was done before⁷. The result is in very good agreement with the preliminary structure⁷.

The molecular parameters established experimentally are compared with the results of *ab initio* calculations^{4,5}. The agreement is gratifying.

The principal elements of the quadrupole coupling tensor for sodium and nitrogen were evaluated from the results for the two isotopic species. These val-

ues and the structure indicate that the CN group in sodium cyanide can be considered as an almost unperturbed CN^- ion.

2. EXPERIMENTAL RESULTS

The sodium cyanide molecule was studied by molecular beam electric resonance spectroscopy at microwave frequencies. This method furnishes high sensitivity at very high resolution, in the order of 10 kHz. The spectrometer has been described elsewhere^{2,7-9}.

The molecular beam was produced in a supersonic expansion of a mixture of sodium cyanide diluted in argon through a 130 μm nozzle at a backing pressure of 1 bar. The temperature of the supply chamber of the stainless steel oven was held at 1100 K, which corresponds according to Ingold¹⁰ and Porter¹¹ to a vapour pressure of monomeric sodium cyanide of 0.8-1.0 mbar. The nozzle chamber temperature was kept at 1300 K, to avoid clogging. Maintaining a stable molecular beam at the high temperatures necessary to obtain sufficient vapour pressure of monomeric NaCN, was handicapped by the instability of the cyanide

Table 1. Hyperfine coupling constants¹⁴ for the ground vibrational state of NaCN and Na^{13}CN .

Constant	NaCN	Na^{13}CN	Unit
$eQq_{aa}(\text{Na})$	-5.344(5)	-5.328(12)	MHz
$eQq_{bb}(\text{Na})$	2.397(7)	2.387(15)	MHz
$eQq_{aa}(\text{N})$	2.148(4)	2.130(7)	MHz
$eQq_{bb}(\text{N})$	-4.142(5)	-4.122(8)	MHz
$c_{bb}(\text{Na})$	1.09(20)	-	kHz
$c_{cc}(\text{Na})$	0.96(31)	-	kHz
$c_{aa}(\text{N})$	13.7(3.5)	13.6(6.5)	kHz
$c_{cc}(\text{N})$	1.88(42)	-	kHz
$d_{aa}(\text{Na-N})$	-0.3714	-0.3674	kHz
$d_{bb}(\text{Na-N})$	0.1651	0.1610	kHz

Table II. Frequencies (in MHz) of the observed^a and calculated hyperfine-free origins of the rotational transitions of NaCN and Na¹³CN in the ground vibrational state.

Isotope	J'	K ₋₁ '	K ₁ '	J''	K ₋₁ ''	K ₁ ''	Type	Obs. frequency	Obs. - calc.
NaCN	1	0	1	0	0	0	a	15640.3280(30)	0.0006
	2	0	2	1	0	1	a	31262.3341(30)	-0.0003
	4	1	3	4	1	4	a	10962.9463(20)	-0.0012
	5	1	4	5	1	5	a	16439.8314(30)	0.0020
	6	1	5	6	1	6	a	23005.2519(30)	0.0004
	7	1	6	7	1	7	a	30652.1941(40)	-0.0014
	8	1	7	8	1	8	a	39369.7637(50)	0.0007
	11	2	9	11	2	10	a	12153.1380(30)	-0.0001
	12	2	10	12	2	11	a	16691.9700(50)	0.0007
	13	2	11	13	2	12	a	22246.513(14)	-0.0028
	1	1	1	2	0	2	b	18289.3222(20)	-0.0002
	4	0	4	3	1	3	b	15497.1375(20)	-0.0009
	5	0	5	4	1	4	b	33010.2203(30)	0.0014
	6	2	5	7	1	6	b	25796.2003(50)	-0.0002
	9	1	8	8	2	7	b	14251.7157(40)	0.0008
	10	1	9	9	2	8	b	34919.1656(40)	-0.0008
	12	3	10	13	2	11	b	30238.988(22)	0.0206
	13	3	11	14	2	12	b	9783.5098(30)	-0.0007
15	2	13	14	3	12	b	11402.6720(50)	-0.0011	
16	2	14	15	3	13	b	33303.6225(40)	0.0001	
Na ¹³ CN	1	0	1	0	0	0	a	15304.7785(70)	0.0019
	2	0	2	1	0	1	a	30590.6388(60)	-0.0025
	4	1	3	4	1	4	a	10908.6373(50)	-0.0021
	5	1	4	5	1	5	a	16358.0861(40)	0.0002
	6	1	5	6	1	6	a	22890.1355(70)	0.0013
	11	2	9	11	2	10	a	12507.2515(50)	-0.0006
	12	2	10	12	2	11	a	17156.985(10)	0.0043
	13	2	11	13	2	12	a	22834.293(19)	-0.0069
	1	1	1	2	0	2	b	16883.9590(60)	0.0014
	4	0	4	3	1	3	b	16209.3468(40)	-0.0002
	5	0	5	4	1	4	b	33365.0025(40)	0.0008
	6	2	5	7	1	6	b	22000.8898(50)	-0.0001
	9	1	8	8	2	7	b	17302.5009(50)	0.0005
	10	1	9	9	2	8	b	37585.577(10)	-0.0023
	12	3	10	13	2	11	b	23823.073(10)	0.0003
15	2	13	14	3	12	b	17281.945(10)	0.0002	

^aThe observed frequencies¹⁴ are evaluated in the least-squares fit of the observed hyperfine spectrum.

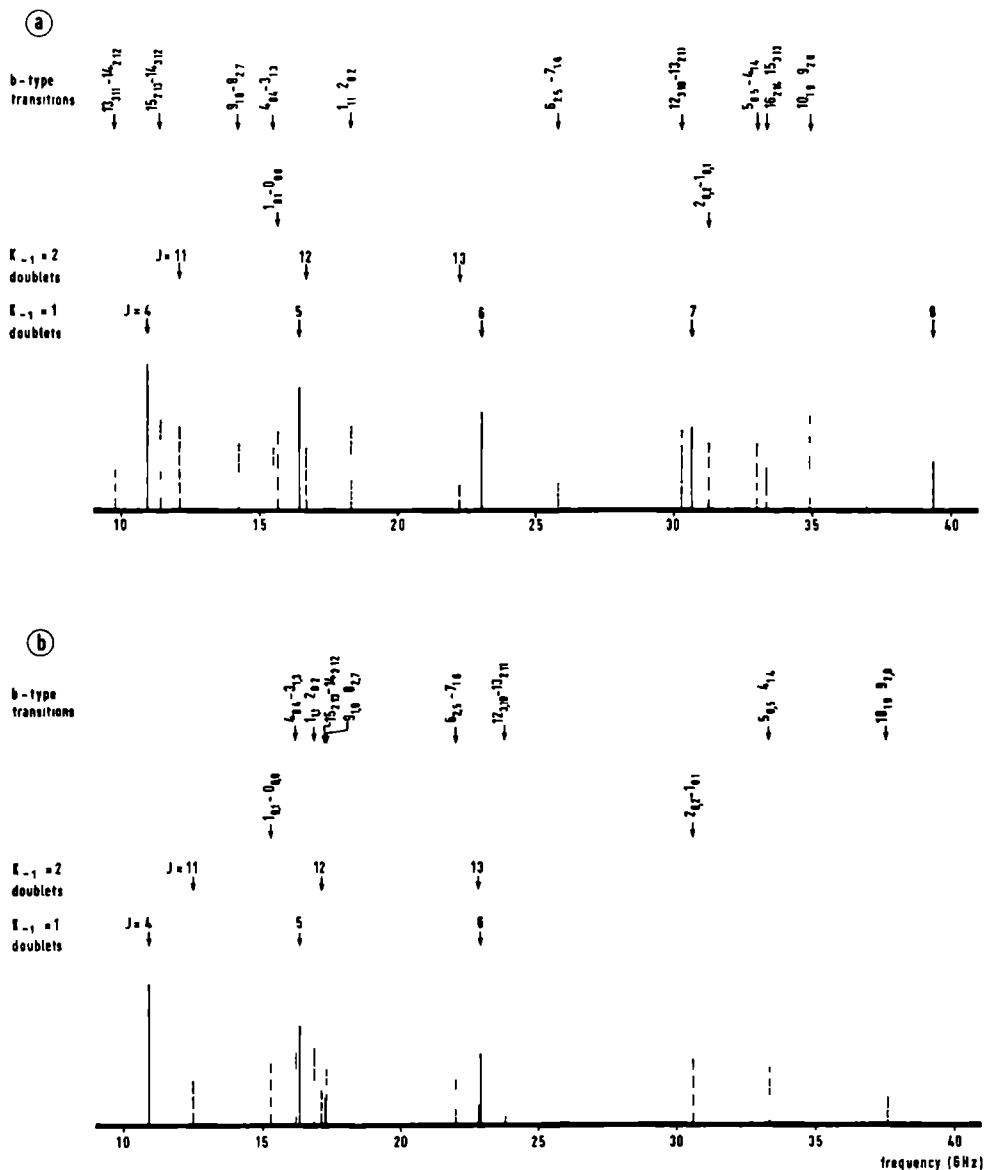


Fig. 1. Observed rotational transitions of NaCN (a) and Na¹³CN (b) in the ground vibrational state in the frequency region 9.5-40 GHz. The rotational transitions are indicated by $J_{K_{-1}, K_1} \rightarrow J_{K_{-1}, K_1}$. $K_{-1}=1$ doublets are transitions $J_{1, J-1} \rightarrow J_{1, J}$ and $K_{-1}=2$ doublets are transitions $J_{2, J-2} \rightarrow J_{2, J-1}$.

Table III. Rotational constants¹⁴ for the ground vibrational state of NaCN and Na¹³CN.

Constant	NaCN	Na ¹³ CN	Unit
A''	57921.954(7)	55674.366(14)	MHz
B''	8369.312(2)	8198.767(3)	MHz
C''	7272.712(2)	7107.582(3)	MHz
τ_{aaaa}	-4.026(10)	-4.084(16)	MHz
τ_{bbbb}	-0.0833(2)	-0.0833(3)	MHz
τ_{cccc}	-0.0459(2)	-0.0445(3)	MHz
τ_1	-3.3283(43)	-3.0809(65)	MHz
τ_2	-0.3670(6)	-0.3454(9)	MHz
H _{JK}	-15.6(6)	-14.2(1.2)	Hz
H _{KJ}	285(13)	270(22)	Hz
h _{JK}	-10.8(3.2)	-6.6(5.8)	Hz
$\Delta\tau$	-3.74(4)	-3.52(10)	kHz

molecule due to decomposition of the compound by wall reactions in the double chamber oven and thermal dissociation. The spectrum of Na¹³CN was obtained with a 90% isotopically enriched sample.

As a consequence of the seeded beam technique, the internal temperatures of the sodium cyanide molecules were decreased strongly, concentrating the population in the low J states of the ground vibrational state. The intensity of the measured transitions was hereby enhanced and the rotational spectra were simplified drastically because no molecules in excited vibrational states were observed, facilitating analysis and identification considerably.

The rotational transitions of both isotopic species were identified by the observed hyperfine structure, the optimum voltages for the state selector field of the MBER spectrometer, and the optimum microwave radiation power irradiated to induce the transitions^{2, 12}.

The hyperfine structure of the rotational transitions was analysed with a computer program including quadrupole, spin-rotation and spin-spin interaction based on the hyperfine Hamiltonian and representation outlined in the paper on KCN¹². The energy states obtained from diagonalization of the Hamiltonian matrix are labeled by the quantum numbers J and F, and by a pseudo spin quan-

Table IV. Derived molecular constants for the ground vibrational state of NaCN and Na¹³CN.

Constant	NaCN	Na ¹³ CN	Unit
From τ_1 and τ_2 , assuming planarity:			
A	57921.006	55673.470	MHz
B	8368.463	8197.977	MHz
C	7272.386	7107.294	MHz
τ_{aaaa}	-4.026	-4.084	MHz
τ_{bbbb}	-0.0833	-0.0833	MHz
τ_{aabb}	0.2664	0.2910	MHz
τ_{abab}	-1.8369	-1.7331	MHz
ΔI	0.3767	0.3827	amuÅ ²
From τ_1 and τ_{cccc} , assuming planarity:			
A	57921.075	55673.533	MHz
B	8368.473	8197.986	MHz
C	7272.342	7107.254	MHz
τ_{aaaa}	-4.026	-4.084	MHz
τ_{bbbb}	-0.0833	-0.0833	MHz
τ_{aabb}	0.1095	0.1474	MHz
τ_{abab}	-1.6979	-1.6062	MHz
ΔI	0.3772	0.3832	amuÅ ²
From the τ -free rotational constants:			
I_a	8.72531(5)	9.07755(5)	amuÅ ²
I_b	60.3909(25)	61.6468(25)	amuÅ ²
I_c	69.4931(25)	71.1073(25)	amuÅ ²

tum number ϵ , where J is the molecular rotational angular momentum and F is the total angular momentum. For a given J and F , the state lowest in energy is denoted with $\epsilon=1$; the higher states are labeled by $\epsilon=2,3,\dots$ in the order of increasing energy.

Starting values for the quadrupole coupling constants were obtained¹³ from the *ab initio* field gradients calculated by Klein *et al.*⁶, with a correction applied on these values corresponding to the difference between the *ab initio*⁶ and the experimental¹² results for the quadrupole interaction in KCN. In a step by step

calculation we succeeded in analysing the hyperfine structure of NaCN. All observed hyperfine transitions were identified. The quadrupole coupling constants $eQq_{aa}(\text{Na})$, $eQq_{bb}(\text{Na})$, $eQq_{aa}(\text{N})$ and $eQq_{bb}(\text{N})$, and four spin-rotation coupling constants: $c_{bb}(\text{Na})$, $c_{cc}(\text{Na})$, $c_{aa}(\text{N})$ and $c_{cc}(\text{N})$ were determined in a least-squares fit of the hyperfine splittings.

The hyperfine spectrum of Na^{13}CN was analysed by a similar approach. For this molecule we started with the quadrupole coupling constants evaluated for NaCN. The contribution of the nuclear spin ($I=\frac{1}{2}$) of ^{13}C to the hyperfine structure has been neglected in the analysis because no additional splitting or broadening of the sodium-nitrogen hyperfine lines could be observed. From the analysis of the hyperfine spectrum all quadrupole coupling constants and the spin-rotation coupling constant $c_{aa}(\text{N})$ have been obtained.

For both molecules we fixed the remaining spin-rotation coupling constants at zero in the fit, since these could not be determined significantly. The spin-spin coupling constants $d_{aa}(\text{Na-N})$ and $d_{bb}(\text{Na-N})$ were constrained in the fit at the values calculated¹² from the geometry.

All observed hyperfine transitions (186 and 107 in 20 and 16 rotational transitions for NaCN and Na^{13}CN , respectively) are listed in the Appendix. The results for the hyperfine coupling constants¹⁴ for both isotopic species in the ground vibrational state are presented in Table I. The values of eQq_{cc} and d_{cc} can be obtained by using Laplace's equation¹². The variance¹⁵ for the least-squares fit of the hyperfine structure was $\sigma=0.32$ for NaCN and $\sigma=0.44$ for Na^{13}CN . The quadrupole coupling constants are discussed in detail in Section 4.

The hyperfine-free origins of the rotational transitions, established in the fit of the hyperfine spectra for NaCN and Na^{13}CN , are given in Table II. An impression of the observed rotational spectra in the frequency region 9.5-40 GHz of the two isotopic species in the ground vibrational state is presented in Fig. 1. Both a-type and b-type transitions have been observed. The hyperfine-free rotational transition frequencies ν_0 were fitted for both molecules to an asymmetric rotor model^{12,16} without invoking the planarity conditions for the τ 's^{12,17}. The quality of the fit of the rotational structure is good ($\sigma=0.53$ for NaCN and $\sigma=0.44$ for Na^{13}CN)¹⁵. We obtained for both isotopic species the rotational constants (A'' , B'' and C''), the quartic centrifugal distortion constants (τ_{aaaa}' , τ_{bbbb}' , τ_{cccc}' , τ_1 and τ_2), and three sextic centrifugal distortion constants (H_{JK} , H_{KJ} and h_{JK}). The best fit values¹⁴ are listed in Table III. The remaining four sextic distortion constants (H_J , H_K , h_J and h_K) could not well

be determined in the fit and were fixed at zero. Table III is also gives the τ -planarity defect¹⁷ $\Delta\tau$.

Table IV lists the τ -free rotational constants A, B and C, the centrifugal distortion constants τ_{aaaa} , τ_{bbbb} , τ_{aabb} and τ_{abab} , and the inertial defect¹² ΔI for NaCN and Na¹³CN in the ground vibrational state, evaluated by imposing the planarity condition¹⁷, and the effective moments of inertia (I_a , I_b and I_c), derived¹⁸ from the τ -free rotational constants.

3. STRUCTURE

An exact evaluation of the structure requires rotational information of at least two isotopic species, which is now available. The effective moments of inertia for NaCN and Na¹³CN, listed in Table IV, were used to calculate the structural parameters of sodium cyanide in the ground vibrational state. The resulting T-shaped structure presented¹⁴ in Table V is in close agreement with the structure we reported earlier⁷. This shows that the assumption $r_{CN}(\text{NaCN})=r_{CN}(\text{KCN})$ used to obtain a preliminary structure in that communication⁷ was correct.

The values of the calculated structural parameters are well within the uncertainties given in Table V, if the geometry of sodium cyanide is computed from any combination of four moments of inertia of the two isotopic species, with the limitation that I_a always has to be taken into account. This limitation can be explained from the same considerations as discussed for potassium cyanide¹².

Table V. The effective structural parameters¹⁴ for the ground vibrational state of sodium cyanide.

Constant	Value (Å)
r_{CN}	1.170(4)
r_{NaC}	2.379(15)
r_{NaN}	2.233(15)

4. DISCUSSION

The large τ -planarity defect $\Delta\tau$ and inertial defect ΔI indicate that sodium cyanide is a floppy molecule, i.e. shows large amplitude motions in the bending direction. The bending vibrational frequency ω_2 evaluated¹⁹ from the inertial defect is $179(35) \text{ cm}^{-1}$ for NaCN and $176(35) \text{ cm}^{-1}$ for Na^{13}CN . This is in good agreement with the frequency 168 cm^{-1} , obtained by Ismail *et al.*⁶ for NaCN using the matrix-isolation technique. As with potassium cyanide, the value measured by Leroi and Klemperer²⁰ in an infrared absorption cell ($\omega_2=239(10) \text{ cm}^{-1}$) does not agree very well with the other results. An explanation as argued for KCN^{6,12} may also be applicable here: the infrared absorption frequency should be assigned to another molecule, possibly NaOCN.

A summary of results of *ab initio* calculations for the structure and hyperfine quadrupole coupling constants is given in Table VI. There is fair agreement between the *ab initio* and experimental structures. The quadrupole coupling constants were obtained¹³ by transforming the field gradient matrices calculated by Klein *et al.*⁴ to the principal inertia axes system of the *ab initio* structure, and of the experimental structure, respectively. The results for the transformation to the principal axes system of the experimental structure are in better agreement with the accurate experimental values listed in Table I than the results with respect to the *ab initio* structure.

The principal elements of the quadrupole coupling tensors for sodium ($eQq_x(\text{Na})$ and $eQq_z(\text{Na})$) and nitrogen ($eQq_x(\text{N})$ and $eQq_z(\text{N})$) in sodium cyanide were determined by the method of Posener²¹. The results, including the asymmetry parameter for the quadrupole coupling $\eta=(eQq_x-eQq_y)/eQq_z$ and the angles $\theta(a,z)$ and $\theta(z,C-N)$, defined in Fig. 2, are presented in Table VII. The axes of the principal inertial and principal quadrupole systems are denoted a,b,c and x,y,z , respectively. The principal axis z is chosen as the axis for which the coupling of the nucleus has nearly axial symmetry.

Since $\theta(z_{\text{N}},C-N)$ and η_{N} are small, the field gradient at the nitrogen nucleus is approximately symmetric about the bond axis between the carbon and the nitrogen nucleus. The experimental values of r_{CN} and $eQq_z(\text{N})$ are in close agreement with the results of *ab initio* calculations for the free CN^- ion: the equilibrium value of $r_{\text{CN}}=1.173(2) \text{ \AA}^{22}$ and $eQq(\text{N})=-4.090 \text{ MHz}^{23}$. From these arguments we conclude that in sodium cyanide, like in KCN¹², the CN group can be considered as an almost unperturbed CN^- ion.

Table VI. Summary of results^a of *ab initio* calculations on NaCN. The hyperfine coupling constants¹³ are given for the *ab initio* structure, and in brackets for the experimental structure (see text).

Constant	Klein <i>et al.</i> ⁴	Marsden ⁵	Unit
E(NaCN)	1640	1090	cm ⁻¹
E(NaNC)	280	1340	cm ⁻¹
r _{CN}	1.152	1.175	Å
r _{NaC}	2.470	2.376	Å
r _{NaN}	2.195	2.252	Å
eQq _{aa} (Na)	-5.491(-6.295)	-	MHz
eQq _{bb} (Na)	1.828(2.632)	-	MHz
eQq _{aa} (N)	1.674(2.001)	-	MHz
eQq _{bb} (N)	-3.517(-3.844)	-	MHz

^aThe quantities E(NaCN) and E(NaNC) are the energies relative to the T-shaped configuration of the linear cyanide and isocyanide configurations, respectively.

Table VII. Principal hyperfine quadrupole coupling constants¹⁴ for sodium cyanide in the ground vibrational state.

Constant	Sodium	Nitrogen	Unit
eQq _x	2.429(10)	2.225(7)	MHz
eQq _z	-5.375(9)	-4.219(7)	MHz
η	0.096(4)	0.055(4)	
θ(a, z)	-3.6(8)	83.7(3)	degree
θ(z, C-N)	86.3(8)	-1.0(3)	degree

The large anharmonicity and the low barriers of the potential energy surface in the bending direction^{4,5} are most likely the origin of the disagreement among the available thermodynamic data^{6,11,24} for sodium cyanide. To remove those discrepancies it will be imperative to take the exact potential energy surface into account.

Table VI shows that the differences between the *ab initio* calculated values of $E(\text{NaCN})$ and $E(\text{NaNc})$ are very large. This implies that the reliability of the computed potentials is rather questionable. With the accurate experimental determination of the T-shaped structure of NaCN in the ground vibrational state, the bottom of the intermolecular potential is now well located. Recently we have started experiments in which the excited vibrational states of the alkali metal

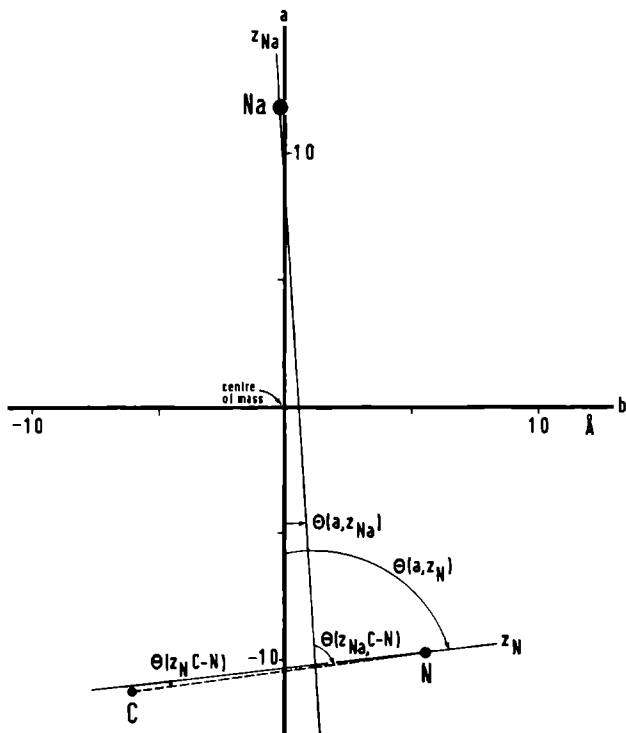


Fig. 2. Orientation of the principal axes of inertia (a,b,c) and the principal axes of the field gradient (x,y,z) in the sodium cyanide molecule. The c and y axes coincide and are perpendicular to the molecular plane. The subscripts Na and N are added to clarify the distinction between the sodium and the nitrogen quadrupole principal axes

cyanides are investigated. These studies will hopefully provide a more accurate picture of the potential energy surface and a better understanding of the weak internal interactions in floppy molecules.

ACKNOWLEDGMENT

The authors wish to express their gratitude to Dr. P.E.S. Wormer for calculating the field gradient at the nitrogen nucleus in the CN^- ion, and to Dr. C.J. Marsden for communicating his result on the *ab initio* structure of NaCN. They thank Dr. J.P. Bekooy for the many fruitful discussions that we have enjoyed with him. This work is part of the research program of the Stichting voor Fundamenteel Onderzoek der Materie (F.O.M.) and has been made possible by financial support from the Nederlandse Organisatie voor Zuiver Wetenschappelijk Onderzoek (Z.W.O.).

APPENDIX

Frequencies (in MHz) of the observed and calculated hyperfine transitions of NaCN in the ground vibrational state.

$F_{\epsilon}^{\prime} \rightarrow F_{\epsilon}^{\prime\prime}$	Obs.frequency	Obs.-calc.	$F_{\epsilon}^{\prime} \rightarrow F_{\epsilon}^{\prime\prime}$	Obs.frequency	Obs.-calc.
Rotational transition $1_{0,1} \rightarrow 0_{0,0}$:			Rotational transition $5_{1,4} \rightarrow 5_{1,5}$:		
$7/2_1 \rightarrow 5/2_1$	15640.4907(70)	0.0003	$11/2_2 \rightarrow 13/2_1$	16440.034(10)	-0.0021
$5/2_2 \rightarrow 5/2_1$	15640.9925(40)	0.0000	$5/2_1 \rightarrow 7/2_1$	16440.034(10)	-0.0094
$1/2_2 \rightarrow 1/2_1$	15641.6909(50)	0.0002	$9/2_3 \rightarrow 7/2_2$	16440.2233(80)	0.0041
$3/2_3 \rightarrow 3/2_1$	15641.8645(40)	-0.0003	$11/2_3 \rightarrow 13/2_2$	16440.274(10)	0.0048
Rotational transition $2_{0,2} \rightarrow 1_{0,1}$:			$9/2_2 \rightarrow 11/2_2$	16440.274(10)	-0.0027
$5/2_3 \rightarrow 3/2_2$	31262.7269(70)	-0.0015	$11/2_2 \rightarrow 11/2_1$	16440.4187(70)	0.0000
$7/2_2 \rightarrow 7/2_1$	31263.0095(70)	-0.0006	$9/2_2 \rightarrow 9/2_1$	16440.7467(80)	-0.0001
$5/2_3 \rightarrow 5/2_1$	31263.7463(60)	0.0005	$11/2_3 \rightarrow 9/2_2$	16441.0094(70)	0.0034
$3/2_3 \rightarrow 3/2_2$	31263.7463(60)	-0.0005	$9/2_3 \rightarrow 11/2_2$	16441.1173(90)	0.0008
$1/2_2 \rightarrow 1/2_1$	31264.5149(80)	0.0013	$9/2_3 \rightarrow 9/2_2$	16441.3295(90)	0.0026
$3/2_3 \rightarrow 5/2_1$	31264.7650(60)	0.0009	$11/2_3 \rightarrow 11/2_1$	16441.546(10)	0.0016
Rotational transition $4_{1,3} \rightarrow 4_{1,4}$:			$9/2_3 \rightarrow 9/2_1$	16441.583(10)	-0.0038
$7/2_1 \rightarrow 9/2_1$	10962.4800(80)	-0.0008	$9/2_3 \rightarrow 11/2_1$	16441.863(10)	-0.0017
$11/2_1 \rightarrow 9/2_1$	10962.9114(50)	-0.0035	$13/2_2 \rightarrow 13/2_1$	16442.1532(70)	-0.0012
$3/2_1 \rightarrow 5/2_1$	10963.0483(60)	-0.0048	$13/2_2 \rightarrow 11/2_1$	16442.5376(90)	0.0008
$7/2_3 \rightarrow 7/2_3$	10963.0483(60)	-0.0035	$7/2_2 \rightarrow 9/2_1$	16442.5376(90)	-0.0019
$9/2_1 \rightarrow 9/2_1$	10963.1907(60)	0.0012	Rotational transition $6_{1,5} \rightarrow 6_{1,6}$:		
$9/2_2 \rightarrow 9/2_1$	10963.4168(70)	0.0010	$15/2_1 \rightarrow 15/2_2$	23003.8375(70)	0.0024
$7/2_2 \rightarrow 7/2_2$	10963.5017(80)	-0.0004	$13/2_1 \rightarrow 15/2_1$	23004.9912(60)	0.0009
$13/2_1 \rightarrow 11/2_1$	10963.5843(60)	0.0007	$13/2_1 \rightarrow 13/2_1$	23005.3872(80)	-0.0013
$9/2_3 \rightarrow 7/2_2$	10964.0700(80)	0.0016	$13/2_2 \rightarrow 11/2_2$	23005.4328(80)	0.0018
$7/2_2 \rightarrow 9/2_1$	10964.1214(80)	0.0029	$13/2_2 \rightarrow 13/2_1$	23005.9321(60)	-0.0006
$9/2_3 \rightarrow 11/2_1$	10964.3212(80)	0.0055	$11/2_2 \rightarrow 11/2_1$	23006.1968(70)	0.0022
$7/2_3 \rightarrow 9/2_1$	10965.0533(50)	0.0015	$13/2_3 \rightarrow 15/2_1$	23006.5478(90)	0.0027
$11/2_2 \rightarrow 11/2_1$	10965.1937(70)	0.0020	$11/2_3 \rightarrow 11/2_2$	23006.7162(90)	-0.0047
$5/2_2 \rightarrow 7/2_2$	10965.2681(80)	0.0040	$11/2_3 \rightarrow 13/2_1$	23007.2224(60)	-0.0002
$11/2_2 \rightarrow 9/2_1$	10965.562(15)	0.0016	$15/2_2 \rightarrow 15/2_1$	23007.6132(70)	0.0025
$5/2_2 \rightarrow 7/2_1$	10965.588(20)	-0.0068	$15/2_2 \rightarrow 13/2_1$	23008.0056(50)	-0.0032

$F_{\epsilon} \rightarrow F_{\epsilon}''$	Obs. frequency	Obs. -calc.	$F_{\epsilon} \rightarrow F_{\epsilon}''$	Obs. frequency	Obs. -calc.
Rotational transition $7_{1,6} \rightarrow 7_{1,7}$:			Rotational transition $13_{2,11} \rightarrow 13_{2,12}$:		
$15/2_2 \rightarrow 15/2_1$	30652.9544(80)	0.0042	$23/2_1 \rightarrow 23/2_1$	22246.190(20)	0.0017
$15/2_3 \rightarrow 15/2_2$	30653.174(10)	-0.0033	$25/2_1 \rightarrow 25/2_1$	22246.190(20)	-0.0017
$11/2_2 \rightarrow 13/2_3$	30653.174(10)	-0.0032	Rotational transition $1_{1,1} \rightarrow 2_{0,2}$:		
$15/2_3 \rightarrow 13/2_1$	30653.6290(90)	0.0000	$3/2_1 \rightarrow 1/2_2$	18286.4453(60)	0.0010
$13/2_3 \rightarrow 15/2_1$	30654.115(10)	0.0017	$3/2_1 \rightarrow 3/2_3$	18286.5604(60)	-0.0006
$17/2_2 \rightarrow 15/2_1$	30654.981(10)	-0.0017	$1/2_1 \rightarrow 1/2_2$	18286.8512(60)	-0.0015
Rotational transition $8_{1,7} \rightarrow 8_{1,8}$:			$1/2_1 \rightarrow 3/2_3$	18286.9688(60)	-0.0006
$15/2_1 \rightarrow 17/2_3$	39367.5894(80)	0.0027	$5/2_1 \rightarrow 7/2_2$	18287.4524(40)	0.0002
$19/2_1 \rightarrow 21/2_1$	39367.841(10)	-0.0017	$3/2_1 \rightarrow 5/2_3$	18287.5793(80)	-0.0001
$17/2_3 \rightarrow 17/2_3$	39369.589(12)	0.0019	$1/2_2 \rightarrow 3/2_3$	18287.939(10)	0.0010
$17/2_1 \rightarrow 15/2_1$	39369.626(12)	-0.0034	$3/2_2 \rightarrow 1/2_2$	18288.035(12)	0.0009
$19/2_2 \rightarrow 17/2_1$	39372.569(12)	-0.0021	$3/2_2 \rightarrow 3/2_3$	18288.1499(60)	-0.0006
Rotational transition $11_{2,9} \rightarrow 11_{2,10}$:			$5/2_2 \rightarrow 3/2_3$	18288.4936(80)	0.0020
$23/2_2 \rightarrow 23/2_3$	12152.770(12)	0.0027	$7/2_1 \rightarrow 7/2_2$	18288.5798(80)	0.0004
$21/2_2 \rightarrow 21/2_3$	12152.797(10)	0.0028	$5/2_2 \rightarrow 7/2_2$	18289.046(12)	-0.0003
$19/2_1 \rightarrow 19/2_1$	12152.8815(80)	0.0032	$7/2_1 \rightarrow 9/2_1$	18289.177(10)	-0.0022
$21/2_1 \rightarrow 21/2_1$	12152.8815(80)	0.0007	$1/2_2 \rightarrow 3/2_2$	18289.2392(80)	0.0000
$23/2_1 \rightarrow 23/2_1$	12152.9328(80)	-0.0008	$5/2_2 \rightarrow 5/2_3$	18289.5111(60)	0.0012
$21/2_3 \rightarrow 21/2_3$	12153.085(10)	0.0000	$3/2_2 \rightarrow 5/2_2$	18289.699(10)	-0.0010
$23/2_3 \rightarrow 23/2_3$	12153.126(10)	-0.0023	Rotational transition $4_{0,4} \rightarrow 3_{1,3}$:		
$23/2_2 \rightarrow 23/2_2$	12153.3684(70)	0.0000	$9/2_1 \rightarrow 7/2_2$	15496.588(10)	0.0016
$21/2_2 \rightarrow 21/2_2$	12153.4574(80)	-0.0013	$11/2_1 \rightarrow 9/2_1$	15496.799(10)	0.0014
$19/2_2 \rightarrow 19/2_2$	12153.608(12)	0.0000	$9/2_2 \rightarrow 7/2_2$	15496.8812(90)	-0.0019
$25/2_2 \rightarrow 25/2_2$	12153.608(12)	-0.0063	$13/2_1 \rightarrow 11/2_1$	15496.976(10)	-0.0004
$23/2_3 \rightarrow 23/2_2$	12153.737(20)	0.0078	$7/2_2 \rightarrow 5/2_2$	15497.3310(60)	0.0017
$21/2_3 \rightarrow 21/2_2$	12153.737(20)	-0.0115	$9/2_2 \rightarrow 9/2_1$	15497.4113(80)	-0.0003
Rotational transition $12_{2,10} \rightarrow 12_{2,11}$:			$9/2_1 \rightarrow 7/2_1$	15497.4686(80)	0.0020
$21/2_1 \rightarrow 21/2_1$	16691.681(12)	0.0040	$9/2_2 \rightarrow 7/2_1$	15497.7611(90)	-0.0020
$23/2_1 \rightarrow 23/2_1$	16691.681(12)	0.0011	$7/2_2 \rightarrow 5/2_1$	15497.8324(60)	0.0009
$25/2_1 \rightarrow 25/2_1$	16691.733(10)	-0.0007	$11/2_2 \rightarrow 9/2_2$	15498.0074(60)	-0.0015
$21/2_2 \rightarrow 21/2_2$	16692.510(15)	0.0023	$7/2_2 \rightarrow 7/2_1$	15498.0987(80)	-0.0014
$27/2_2 \rightarrow 27/2_2$	16692.510(15)	-0.0043	$7/2_3 \rightarrow 7/2_2$	15498.1309(80)	-0.0003
$25/2_3 \rightarrow 25/2_2$	16692.618(20)	0.0008	$9/2_3 \rightarrow 7/2_1$	15498.4144(70)	0.0014
$23/2_3 \rightarrow 23/2_2$	16692.618(20)	-0.0084	$5/2_2 \rightarrow 3/2_1$	15498.6488(70)	0.0015

$F_{\epsilon} \rightarrow F_{\epsilon}''$	Obs. frequency	Obs. -calc.	$F_{\epsilon} \rightarrow F_{\epsilon}''$	Obs. frequency	Obs. -calc.
$5/2_2 \rightarrow 5/2_2$	15498.7263(60)	-0.0018	$19/2_1 \rightarrow 17/2_1$	34918.704(15)	0.0002
$5/2_2 \rightarrow 5/2_1$	15499.2294(80)	-0.0010	$19/2_2 \rightarrow 17/2_3$	34918.782(15)	0.0010
Rotational transition $5_0, \epsilon \rightarrow 4_1, \epsilon$:			$21/2_1 \rightarrow 19/2_1$	34918.782(15)	-0.0028
$7/2_1 \rightarrow 7/2_2$	33009.9400(80)	-0.0040	$25/2_1 \rightarrow 23/2_1$	34918.8694(80)	-0.0019
$9/2_3 \rightarrow 7/2_3$	33010.0532(80)	0.0052	$21/2_2 \rightarrow 19/2_2$	34919.254(10)	-0.0010
$11/2_2 \rightarrow 9/2_2$	33010.0532(80)	0.0008	$19/2_2 \rightarrow 17/2_2$	34919.3997(80)	0.0007
$11/2_2 \rightarrow 11/2_1$	33010.4874(70)	-0.0007	$17/2_2 \rightarrow 15/2_2$	34919.954(15)	0.0042
$9/2_2 \rightarrow 7/2_2$	33010.5478(80)	-0.0014	$19/2_3 \rightarrow 17/2_2$	34919.954(15)	-0.0012
$7/2_2 \rightarrow 7/2_3$	33010.5478(80)	0.0054	Rotational transition $12_3, \epsilon \rightarrow 13_2, \epsilon$:		
$11/2_1 \rightarrow 9/2_1$	33010.5977(70)	-0.0012	$21/2_2 \rightarrow 23/2_2$	30238.434(50)	0.0070
$9/2_2 \rightarrow 9/2_1$	33011.1633(80)	-0.0023	$27/2_2 \rightarrow 29/2_2$	30238.434(50)	0.0101
$9/2_3 \rightarrow 9/2_2$	33011.2464(90)	0.0032	$25/2_3 \rightarrow 27/2_2$	30239.272(50)	0.0013
$11/2_3 \rightarrow 9/2_1$	33011.5669(80)	-0.0012	$25/2_1 \rightarrow 27/2_1$	30239.272(50)	-0.0094
$7/2_2 \rightarrow 5/2_1$	33011.717(12)	0.0006	$27/2_1 \rightarrow 29/2_1$	30239.272(50)	-0.0090
$9/2_3 \rightarrow 7/2_1$	33011.760(12)	-0.0022	Rotational transition $13_3, \epsilon \rightarrow 14_2, \epsilon$:		
$13/2_2 \rightarrow 11/2_1$	33011.8269(80)	0.0006	$29/2_2 \rightarrow 31/2_2$	9782.927(12)	0.0015
$7/2_2 \rightarrow 7/2_2$	33011.924(10)	-0.0025	$23/2_2 \rightarrow 25/2_2$	9782.927(12)	-0.0039
$7/2_2 \rightarrow 7/2_1$	33012.2559(80)	-0.0009	$27/2_2 \rightarrow 29/2_3$	9782.956(10)	-0.0008
Rotational transition $6_2, \epsilon \rightarrow 7_1, \epsilon$:			$25/2_2 \rightarrow 27/2_3$	9782.956(10)	-0.0015
$17/2_1 \rightarrow 17/2_2$	25794.752(20)	0.0038	$27/2_3 \rightarrow 29/2_3$	9783.3040(90)	0.0022
$13/2_1 \rightarrow 13/2_3$	25794.845(25)	-0.0112	$25/2_3 \rightarrow 27/2_3$	9783.3680(80)	0.0005
$15/2_1 \rightarrow 15/2_3$	25794.900(25)	-0.0084	$25/2_2 \rightarrow 27/2_2$	9783.3680(80)	-0.0016
$13/2_1 \rightarrow 15/2_3$	25795.103(10)	0.0013	$27/2_2 \rightarrow 29/2_2$	9783.463(12)	0.0000
$9/2_2 \rightarrow 11/2_2$	25795.223(15)	-0.0005	$31/2_1 \rightarrow 33/2_1$	9783.723(12)	0.0034
$11/2_2 \rightarrow 13/2_3$	25795.328(10)	0.0013	$25/2_3 \rightarrow 27/2_2$	9783.777(15)	-0.0026
$13/2_3 \rightarrow 13/2_3$	25795.552(15)	0.0006	$27/2_1 \rightarrow 29/2_1$	9783.8080(90)	0.0009
$9/2_1 \rightarrow 9/2_1$	25795.637(25)	-0.0122	$25/2_1 \rightarrow 27/2_1$	9783.841(12)	0.0008
$13/2_3 \rightarrow 13/2_2$	25796.268(25)	0.0092	$23/2_1 \rightarrow 25/2_1$	9783.841(12)	0.0001
Rotational transition $9_1, \epsilon \rightarrow 8_2, \epsilon$:			Rotational transition $15_2, \epsilon \rightarrow 14_3, \epsilon$:		
$23/2_1 \rightarrow 21/2_1$	14251.4295(90)	0.0000	$25/2_1 \rightarrow 23/2_1$	11402.391(12)	-0.0074
$19/2_2 \rightarrow 17/2_2$	14251.7595(70)	0.0035	$35/2_1 \rightarrow 33/2_1$	11402.442(14)	0.0029
$17/2_3 \rightarrow 15/2_3$	14251.9318(60)	-0.0035	$31/2_2 \rightarrow 29/2_2$	11402.711(14)	0.0063
$19/2_3 \rightarrow 17/2_3$	14252.0135(70)	0.0013	$29/2_2 \rightarrow 27/2_2$	11402.792(14)	-0.0021
Rotational transition $10_1, \epsilon \rightarrow 9_2, \epsilon$:			$29/2_3 \rightarrow 27/2_3$	11402.847(14)	0.0025
$17/2_1 \rightarrow 15/2_1$	34918.704(15)	0.0049	$31/2_3 \rightarrow 29/2_3$	11402.916(14)	0.0060

$F_{\epsilon} \rightarrow F_{\epsilon}''$	Obs. frequency	Obs. -calc.	$F_{\epsilon} \rightarrow F_{\epsilon}''$	Obs. frequency	Obs. -calc.
$27/2_2 \rightarrow 25/2_2$	11403.268(15)	0.0003	$35/2_1 \rightarrow 33/2_1$	33303.328(14)	0.0069
$33/2_2 \rightarrow 31/2_2$	11403.268(15)	-0.0066	$27/2_1 \rightarrow 25/2_1$	33303.328(14)	-0.0025
Rotational transition $16_{2,14} \rightarrow 15_{3,13}$:			$29/2_2 \rightarrow 27/2_2$	33304.2361(60)	0.0044
$33/2_1 \rightarrow 31/2_1$	33303.310(12)	-0.0065	$35/2_2 \rightarrow 33/2_2$	33304.2361(60)	-0.0036

Frequencies (in MHz) of the observed and calculated hyperfine transitions of Na^{13}CN in the ground vibrational state.

$F_{\epsilon} \rightarrow F_{\epsilon}''$	Obs. frequency	Obs. -calc.	$F_{\epsilon} \rightarrow F_{\epsilon}''$	Obs. frequency	Obs. -calc.
Rotational transition $1_{0,1} \rightarrow 0_{0,0}$:			$11/2_2 \rightarrow 11/2_1$	10910.8728(80)	0.0007
$7/2_1 \rightarrow 5/2_1$	15304.941(10)	0.0029	Rotational transition $5_{1,4} \rightarrow 5_{1,5}$:		
$5/2_2 \rightarrow 3/2_1$	15305.4394(90)	0.0014	$13/2_1 \rightarrow 13/2_2$	16356.7424(80)	-0.0034
$1/2_2 \rightarrow 3/2_1$	15306.137(10)	-0.0017	$9/2_1 \rightarrow 9/2_1$	16357.3796(80)	0.0045
$3/2_3 \rightarrow 1/2_1$	15306.3091(90)	-0.0024	$7/2_1 \rightarrow 9/2_2$	16357.4559(80)	-0.0008
Rotational transition $2_{0,2} \rightarrow 1_{0,1}$:			$13/2_1 \rightarrow 11/2_1$	16358.0093(70)	-0.0020
$5/2_1 \rightarrow 5/2_2$	30589.042(12)	0.0012	$11/2_2 \rightarrow 9/2_2$	16358.1327(90)	0.0083
$5/2_3 \rightarrow 3/2_2$	30591.0338(90)	0.0038	$11/2_1 \rightarrow 11/2_1$	16358.2787(80)	0.0018
$1/2_1 \rightarrow 1/2_1$	30591.122(10)	-0.0092	$11/2_2 \rightarrow 11/2_1$	16358.6742(60)	0.0016
$1/2_2 \rightarrow 1/2_1$	30592.8166(90)	0.0007	$9/2_2 \rightarrow 9/2_2$	16358.7384(90)	0.0017
$3/2_3 \rightarrow 5/2_1$	30593.0662(80)	0.0018	$15/2_1 \rightarrow 13/2_1$	16358.7384(90)	-0.0016
Rotational transition $4_{1,3} \rightarrow 4_{1,4}$:			$9/2_2 \rightarrow 9/2_1$	16358.9986(70)	-0.0044
$7/2_1 \rightarrow 7/2_2$	10907.563(10)	0.0073	$11/2_3 \rightarrow 9/2_1$	16359.5128(70)	0.0031
$5/2_1 \rightarrow 7/2_2$	10907.9660(90)	-0.0038	$9/2_3 \rightarrow 9/2_2$	16359.5717(90)	0.0012
$9/2_1 \rightarrow 9/2_2$	10908.073(12)	-0.0078	$9/2_3 \rightarrow 11/2_1$	16360.1130(80)	-0.0057
$7/2_1 \rightarrow 9/2_1$	10908.1789(90)	-0.0006	$7/2_2 \rightarrow 7/2_1$	16360.282(10)	-0.0013
$9/2_1 \rightarrow 9/2_1$	10908.8840(80)	0.0001	$13/2_2 \rightarrow 13/2_1$	16360.3962(70)	-0.0016
$9/2_2 \rightarrow 9/2_1$	10909.1062(90)	-0.0005	$13/2_2 \rightarrow 11/2_1$	16360.782(14)	0.0078
$7/2_2 \rightarrow 7/2_2$	10909.188(10)	-0.0007	$7/2_2 \rightarrow 9/2_1$	16360.782(14)	-0.0067
$13/2_1 \rightarrow 11/2_1$	10909.2701(70)	-0.0009	Rotational transition $6_{1,5} \rightarrow 6_{1,6}$:		
$9/2_3 \rightarrow 9/2_1$	10910.3717(80)	0.0030	$11/2_1 \rightarrow 13/2_1$	22889.7345(80)	-0.0036
$7/2_3 \rightarrow 7/2_1$	10910.4526(80)	0.0006	$11/2_3 \rightarrow 13/2_1$	22892.1012(70)	-0.0052

$F_{\epsilon} \rightarrow F_{\epsilon}''$	Obs.frequency	Obs.-calc.	$F_{\epsilon} \rightarrow F_{\epsilon}''$	Obs.frequency	Obs.-calc.
15/2 ₂ →15/2 ₁	22892.4825(90)	0.0001	7/2 ₂ →5/2 ₁	16210.0361(80)	-0.0010
9/2 ₂ →11/2 ₁	22892.8795(90)	0.0077	11/2 ₂ →9/2 ₂	16210.2112(60)	0.0013
15/2 ₂ →13/2 ₁	22892.8795(90)	0.0054	9/2 ₃ →7/2 ₁	16210.625(10)	0.0061
Rotational transition 11 _{2,9} →11 _{2,10} :			5/2 ₂ →3/2 ₁	16210.847(10)	-0.0028
19/2 ₁ →19/2 ₁	12506.9890(90)	0.0076	5/2 ₂ →5/2 ₁	16211.426(12)	-0.0097
21/2 ₁ →21/2 ₁	12506.9890(90)	0.0053	Rotational transition 5 _{0,5} →4 _{1,4} :		
23/2 ₁ →23/2 ₁	12507.0403(70)	-0.0049	11/2 ₂ →11/2 ₁	33365.2705(80)	-0.0015
21/2 ₃ →21/2 ₃	12507.1975(80)	-0.0069	9/2 ₂ →7/2 ₂	33365.3241(80)	0.0026
23/2 ₃ →23/2 ₃	12507.2450(80)	-0.0017	7/2 ₂ →7/2 ₃	33365.3241(80)	-0.0002
23/2 ₂ →23/2 ₂	12507.4828(80)	0.0049	11/2 ₁ →9/2 ₁	33365.3807(80)	-0.0008
Rotational transition 12 _{2,10} →12 _{2,11} :			13/2 ₂ →11/2 ₂	33365.7676(70)	0.0022
21/2 ₁ →21/2 ₁	17156.683(12)	0.0025	9/2 ₂ →9/2 ₁	33365.9441(80)	-0.0013
23/2 ₁ →23/2 ₁	17156.683(12)	-0.0002	9/2 ₃ →9/2 ₂	33366.0299(80)	0.0000
25/2 ₂ →25/2 ₂	17157.219(12)	-0.0023	11/2 ₃ →9/2 ₁	33366.353(10)	0.0040
Rotational transition 13 _{2,11} →13 _{2,12} :			7/2 ₂ →7/2 ₁	33367.028(10)	-0.0066
23/2 ₁ →23/2 ₁	22833.954(20)	-0.0018	Rotational transition 6 _{2,5} →7 _{1,6} :		
29/2 ₁ →29/2 ₁	22834.034(20)	0.0018	13/2 ₂ →13/2 ₃	21999.814(10)	0.0049
Rotational transition 1 _{1,1} →2 _{0,2} :			15/2 ₂ →17/2 ₂	21999.930(10)	-0.0033
3/2 ₁ →1/2 ₂	16881.092(10)	0.0025	11/2 ₂ →13/2 ₃	22000.018(12)	-0.0003
3/2 ₁ →3/2 ₃	16881.209(10)	0.0027	13/2 ₂ →15/2 ₃	22000.060(12)	-0.0023
1/2 ₁ →1/2 ₂	16881.499(12)	0.0029	13/2 ₃ →15/2 ₃	22000.491(10)	-0.0004
1/2 ₁ →3/2 ₃	16881.612(12)	-0.0013	11/2 ₃ →13/2 ₃	22000.552(10)	-0.0023
5/2 ₁ →7/2 ₂	16882.0966(80)	-0.0056	11/2 ₂ →13/2 ₂	22000.7233(90)	0.0055
3/2 ₁ →5/2 ₃	16882.222(10)	-0.0039	13/2 ₂ →15/2 ₂	22000.9714(80)	-0.0025
3/2 ₂ →3/2 ₃	16882.788(14)	0.0009	Rotational transition 9 _{1,6} →8 _{2,7} :		
3/2 ₁ →1/2 ₁	16882.788(14)	0.0132	15/2 ₁ →13/2 ₁	17301.9974(80)	-0.0013
7/2 ₁ →9/2 ₁	16883.817(14)	-0.0016	17/2 ₁ →15/2 ₁	17301.9974(80)	-0.0002
Rotational transition 4 _{0,4} →3 _{1,3} :			19/2 ₂ →17/2 ₃	17302.036(10)	0.0057
11/2 ₁ →9/2 ₁	16209.011(12)	0.0021	23/2 ₁ →21/2 ₁	17302.2148(80)	-0.0023
9/2 ₃ →7/2 ₃	16209.011(12)	-0.0007	19/2 ₂ →17/2 ₂	17302.543(10)	0.0021
9/2 ₂ →7/2 ₂	16209.090(10)	-0.0038	17/2 ₃ →15/2 ₃	17302.713(10)	-0.0019
13/2 ₁ →11/2 ₁	16209.187(10)	0.0020	Rotational transition 10 _{1,9} →9 _{2,8} :		
7/2 ₂ →5/2 ₂	16209.532(10)	0.0006	25/2 ₁ →23/2 ₁	37585.280(12)	-0.0054
9/2 ₁ →7/2 ₁	16209.677(10)	0.0016	17/2 ₂ →15/2 ₂	37586.363(12)	0.0064
9/2 ₂ →7/2 ₁	16209.972(10)	0.0000	23/2 ₂ →21/2 ₂	37586.363(12)	-0.0010

$F_{\epsilon}' \rightarrow F_{\epsilon}''$	Obs.frequency	Obs.-calc.	$F_{\epsilon}' \rightarrow F_{\epsilon}''$	Obs.frequency	Obs.-calc.
Rotational transition $12_{3,10} \rightarrow 13_{2,11}$:			Rotational transition $15_{2,13} \rightarrow 14_{3,12}$:		
$21/2_2 \rightarrow 23/2_2$	23822.504(14)	0.0021	$25/2_1 \rightarrow 23/2_1$	17281.667(14)	0.0012
$27/2_2 \rightarrow 29/2_2$	23822.504(14)	0.0001	$27/2_2 \rightarrow 25/2_2$	17282.549(12)	0.0005
$25/2_1 \rightarrow 27/2_1$	23823.365(14)	-0.0004	$33/2_2 \rightarrow 31/2_2$	17282.549(12)	-0.0013
$27/2_1 \rightarrow 29/2_1$	23823.365(14)	-0.0017			

REFERENCES

- ¹In this paper the alkali metal cyanides are denoted by MCN (where M represents the alkali metal), whatever the structure may be, and the atomic symbol designates the most abundant isotope, unless specified otherwise.
- ²T. Törring, J.P. Bekooy, W.L. Meerts, J. Hoeft, E. Tiemann, and A. Dymanus, *J. Chem. Phys.* **73**, 4875 (1980).
- ³P.E.S. Wormer, and J. Tennyson, *J. Chem. Phys.* **75**, 1245 (1981).
- ⁴M.L. Klein, J.D. Goddard, and D.G. Bounds, *J. Chem. Phys.* **75**, 3909 (1981).
- ⁵C.J. Marsden, *J. Chem. Phys.* **76**, 6451 (1982); private communication.
- ⁶Z.K. Ismail, R.H. Hauge, and J.L. Margrave, *J. Mol. Spectrosc.* **45**, 304 (1973).
- ⁷J.J. van Vaals, W.L. Meerts, and A. Dymanus, *J. Chem. Phys.* **77**, 5245 (1982).
- ⁸J.J. van Vaals, W.L. Meerts, and A. Dymanus, *Chem. Phys.*, in press (1983).
- ⁹J.J. van Vaals, Ph D. Thesis, Katholieke Universiteit Nijmegen, The Netherlands (1983).
- ¹⁰C.K. Ingold, *J. Chem. Soc.* **123**, 885 (1923).
- ¹¹R.F. Porter, *J. Chem. Phys.* **35**, 318 (1961).
- ¹²J.J. van Vaals, W.L. Meerts, and A. Dymanus, *J. Mol. Spectrosc.*, submitted (1983).
- ¹³We employed $Q(^{23}\text{Na}) = 0.116$ barn, and $Q(^{14}\text{N}) = 0.0166$ barn. These values are from: C.M. Lederer, and V.S. Shirley (eds.), *Table of Isotopes*, Seventh Edition (Wiley & Sons, New York, 1978).
- ¹⁴All uncertainties stated in this paper represent three times the standard deviation as determined by the least-squares fit.
- ¹⁵The variance σ is defined as $[\chi^2/(n-m)]^{\frac{1}{2}}$ with χ^2 defined as usual in a least-squares fit, n the number of spectral lines and m the number of parameters in the fit.
- ¹⁶J.K.G. Watson, *J. Chem. Phys.* **46**, 1935 (1967); *J. Chem. Phys.* **48**, 4517 (1968).
- ¹⁷W.H. Kirchhoff, *J. Mol. Spectrosc.* **41**, 333 (1972).
- ¹⁸We employed: $h=6.626176(36)\times 10^{-34}$ Js. This value is from E.R. Cohen, and B.N. Taylor, *J. Phys. Chem. Ref. Data* **2**, 663 (1973).

- ¹⁹W. Gordy, and R.L. Cook, *Microwave Molecular Spectra* (Interscience, New York, 1970).
- ²⁰G.E. Leroi, and W. Klemperer, *J. Chem. Phys.* **35**, 774 (1961).
- ²¹D.W. Posener, *Austr. J. Phys.* **13**, 168 (1960).
- ²²P.R. Taylor, G.B. Bacskay, N.S. Hush, and A.C. Hurley, *J. Chem. Phys.* **70**, 4481 (1979).
- ²³This result was evaluated (Ref. 13) from the field gradient computed by P.E.S. Wormer (private communication) in a SCF calculation using 54 contracted Gaussian type orbitals at $r_{\text{CN}} = 1.174 \text{ \AA}$.
- ²⁴E.W. Guernsey, and M.S. Sherman, *J. Am. Chem. Soc.* **48**, 695 (1926); JANAF, *Thermochemical Tables*, 2nd ed. (U.S. Department of Commerce, National Bureau of Standards, Washington, D.C., 1971); J.N. Mulvihill, and L.F. Phillips, *Chem. Phys. Lett.* **33**, 608 (1975); B.V. L'vov, and L.A. Pelieva, *Prog. Analyt. Atom. Spectrosc.* **3**, 65 (1980); K. Skudlarski, and M. Miller, *Adv. Mass. Spectrom.* **8A**, 433.br;(1980); *High Temp. Sci.* **15**, 151 (1982).

ROTATIONAL SPECTRUM, HYPERFINE SPECTRUM, AND STRUCTURE
OF LITHIUM ISOCYANIDE

ABSTRACT

The rotational spectrum of LiNC has been measured for the first time. We succeeded in producing a supersonic molecular beam (~1% LiNC in Ar). The molecular beam electric resonance technique has been employed to obtain high resolution microwave spectra. Two rotational transitions ($J=1\rightarrow 0$ and $J=2\rightarrow 1$) of $^7\text{LiNC}$ in the ground vibrational state were observed. The hyperfine structure was resolved and identified with the help of microwave-microwave double resonance. The rotational constants B_0 and D_0 and the hyperfine coupling constants $eQq(\text{Li})$, $eQq(\text{N})$, and $c(\text{Li})$ could be deduced. The $J=1\rightarrow 0$ rotational transition of $^6\text{LiNC}$ was observed in natural abundance.

From this we conclude that LiNC has a *linear* isocyanide structure. The results for the effective structural parameters are: $r_{\text{LiN}} = 1.760 \text{ \AA}$, and $r_{\text{NC}} = 1.168 \text{ \AA}$. We did not observe transitions in excited vibrational states or from LiCN. The agreement between the experimental results and recent *ab initio* calculations is good.

1. INTRODUCTION

The molecular structures of the alkali metal cyanides¹ are very sensitive to a subtle balance between a short-range and a long-range component of the interaction energy, as is pointed out by Essers *et al.*². This leads to different effective structures, which we determined experimentally to be T shaped for KCN^{3,4} and NaCN⁵, and linear isocyanide for LiNC (current work). Therefore, an experimental determination of the most stable geometries of the alkali metal cyanides is a good test of the predictive power of a variety of increasingly sophisticated *ab initio* methods for calculation of molecular structure.

The structure of gaseous lithium cyanide has been the subject of numerous *ab initio* studies^{2,6-10}. These studies indicate that a state of minimum energy exists for both linear LiCN and LiNC with a marginal energy difference of less than 0.3 eV, and with the lithium isocyanide configuration the more stable one. However, there exists a rather large spread among the calculated structures and isomerization energies (i.e. the difference in energy between the two linear configurations), as can be seen in Table I. This is mainly due to the effects of different basis sets in the SCF *ab initio* calculations and whether or not correlation energy was included. Not only for LiCN, but also for HCN^{9,11}, NaCN^{12,13} and KCN¹²⁻¹⁴, inclusion of correlation stabilizes the cyanide structure more than the isocyanide structure. In the case of NaCN, the relative stability of the cyanide and isocyanide isomer even reverses¹³. Since no full potential energy surface calculation including correlation is available for LiNC, the possibility of a T-shaped structure cannot be ruled out.

The cyanides are very floppy molecules with bending vibrational frequencies $\omega_2 = 139, 170,$ and 120 cm^{-1} for KCN, NaCN and LiNC, respectively, according to matrix-isolation studies¹⁵, and with large zero-point bending motion amplitudes of up to 15° , predicted by *ab initio* calculations^{2,13,14}. Yet, we established³⁻⁵ that the rotational spectra of both KCN and NaCN in the ground vibrational state can be described properly by an asymmetric rotor model. The bending vibrational frequencies are in the region $110\text{-}180 \text{ cm}^{-1}$ which is an intermediate case¹⁴ between typical values of $\omega_2 = 519 \text{ cm}^{-1}$ for a covalent bonded molecule like SO_2 ¹⁶ and $\omega_2 = 20 \text{ cm}^{-1}$ for a van der Waals molecule like Ar-N_2 ¹⁷. In case of the alkali metal cyanides, the M-CN bonding is predominantly ionic and moderate vibrational excitation will be sufficient to overcome the marginal potential energy barrier in the bending direction so that the M^+ cation can orbit

Table 1. Summary of theoretical predictions for LiCN and LiNC.

	Cyanide structure			Isocyanide structure	
	$r_{\text{LiC}}(\text{\AA})$	$r_{\text{CN}}(\text{\AA})$	$\Delta E(\text{cm}^{-1})^{\text{a}}$	$r_{\text{CN}}(\text{\AA})$	$r_{\text{LiN}}(\text{\AA})$
Bak <i>et al.</i> ⁶	1 922	1 160	3100	1.157	1 765
Clementi <i>et al.</i> ⁷	1.931	1 132	2420	1 154	1 773
Redmon <i>et al.</i> ⁸	-	-	1360	-	-
Schmiedekamp <i>et al.</i> ⁹	1.930	1.154	2130-3120	1.169-8	1.780-1
Essers <i>et al.</i> ²	2.003	1 157	2270	1 157	1 768
Marsden ¹⁰	-	-	<2270	1 174	1 817

^aThe isomerization energy ΔE is the energy difference $E(\text{LiCN})-E(\text{LiNC})$

around the CN^- anion. Clementi *et al.*⁷ called this a "polytopic" bonding, since no unique structure can be assigned.

In the current work we present the results of the first successful observation of the microwave spectrum of LiNC. The LiNC molecule has been prepared by two totally different chemical reactions. We succeeded in producing a supersonic molecular beam (1% LiNC in Ar) using a tantalum oven. We measured two rotational transitions ($J=1\rightarrow 0$ and $J=2\rightarrow 1$) of $^7\text{LiNC}$ and one rotational transition ($J=1\rightarrow 0$) of $^6\text{LiNC}$ in the ground vibrational state. The hyperfine structure was resolved and identified. The rotational constants B_0 and D_0 , and the hyperfine coupling constants $eQq(\text{Li})$, $eQq(\text{N})$, and $c(\text{Li})$ have been determined for $^7\text{LiNC}$. The rotational constant B_0 of $^6\text{LiNC}$ could be deduced. We established that LiNC has a *linear* isocyanide structure.

2. EXPERIMENTAL

The spectra were obtained using the molecular beam electric resonance (MBER) technique. The spectrometer has been described in detail elsewhere^{3,10}. For this experiment we introduced a few modifications on the apparatus. Only some features relevant to the current work are discussed here.

The LiNC beam intensity was monitored by a surface ionization detector, with an effective aperture of 3x3 mm. The iridium ribbon of the surface ionization detector was oxygenated before each run to achieve 100% efficiency for Li compounds. The C-field of the spectrometer, where molecular transitions are induced, consists of two parallel plates. Microwave power is irradiated from a transmitting horn¹⁹ between these two plates, perpendicular to the molecular beam axis. The transmission line is terminated by an absorber in order to avoid standing waves. The resulting spectral linewidth is determined by the beam velocity and the length of the transition region and is 20-30 kHz. To enable searching over a wide frequency range (9.5-40 GHz) within a reasonable sweep time we artificially broadened the instrumental linewidth to about 3 MHz by white noise frequency modulation²⁰ of the radiation sources [backward wave oscillators (BWO) or klystrons]. In this way the peak intensity of the spectral lines is not affected and a frequency region of 1 GHz could be covered in one scan of 30 minutes. After preliminary location of a transition, an accurate frequency determination was performed at normal resolution. To make such a detailed scan, the radiation sources were frequency stabilized by phase locking techniques to a Hewlett-Packard 8660B or 5105A synthesizer. For frequencies higher than 40 GHz, an intermediate X-band oscillator was used to facilitate locking. The microwave power was modulated at 20 Hz and phase sensitive detection was applied. In all measurements, the integration time of the lock-in was set at 1 s. The signal-to-noise ratio of the strongest lines was 30. Because of the low signal-to-noise ratio for many of the spectral lines, it was necessary to use signal averaging techniques. For this purpose a Hewlett-Packard 5480B signal analyser was interfaced with the scan control unit. Double resonance measurements were performed by irradiating simultaneously between the parallel plates microwave power at two discrete frequencies, obtained from two separate sources, independently phase locked by two synthesizers.

Very little information is available on the properties of (gaseous) lithium isocyanide²¹. The chemical stability of LiNC, however, is known to be very poor, especially in the presence of sample impurities or under moist atmosphere. In the latter case LiOH and HCN are formed by hydrolysis. From the experience we obtained with the production of KCN and NaCN molecular beams we learned that wall reactions in a stainless steel oven are responsible for part of the problems to maintain a stable beam of alkali metal cyanides. It is also known that LiNC, heated in the presence of Fe, will form Li_2CN_2 and C. Facing these problems, we decided to develop a new double chamber oven, made of tantalum. A schematic view is shown in Fig. 1. Because leak tight welding of tantalum is

very difficult, wedged clamp fittings without gaskets were applied for all assembled parts. Sealing is accomplished by tightening the screws which results in plastic deformation of the contact surface of the two parts. The lid could be removed easily by means of screws in the auxiliary screw-holes. It could be reused many times without any remachining and leakage never occurred. The nozzle with a diameter of $130\ \mu\text{m}$ has been made by scintillating through the tantalum with a tungsten wire. The heating and the temperature monitoring is handled by a method similar to the one described by Törring *et al.*³. In a test run, rotational spectral lines of NaCN were obtained already after 15 minutes of operation on the required oven and nozzle temperatures. With a stainless steel oven as used before, it took us several weeks of running until the beam conditions were adequate to observe any transition⁵. Furthermore, the signal-to-noise ratio for the tantalum oven was a factor of four higher than for the stainless steel oven.

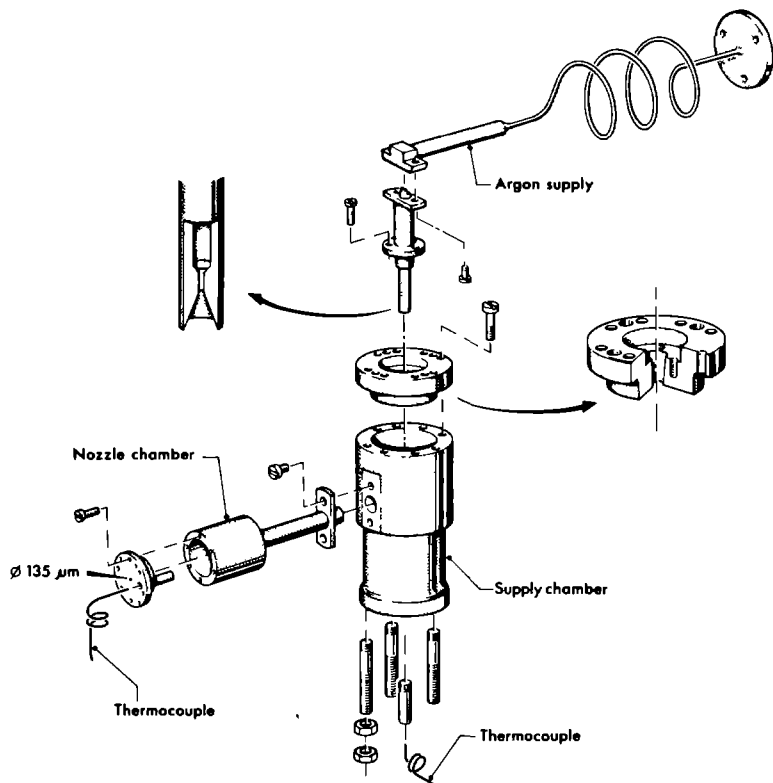


Fig. 1. Exploded view of the tantalum double chamber oven.

At the start of the experiment, the required oven temperature to obtain sufficient LiNC vapour pressure to produce a molecular beam was unknown. We found out that the supply chamber temperature should be kept at 1040 K to acquire LiNC vapour pressure of about 1 mbar. To avoid clogging, the nozzle chamber temperature was kept at 1240 K. These are approximately the same temperatures as needed for NaCN (1100 K and 1300 K, respectively⁵) and KCN (1150 K and 1350 K, respectively⁴). During each start up, clogging impeded and pressure bursts occurred. However, once stable beam conditions at an elevated temperature were attained, runs of more than 24 hours were possible. If the supply chamber temperature was raised above 1040 K, the signal-to-noise ratio of the spectral lines deteriorated and the molecular beam became instable.

The seeded beam technique was used to concentrate the population in the lower rotational and vibrational levels. The stagnation pressure of the carrier gas argon was 1 bar. The velocity distribution of a pure argon beam has been measured by Meerts *et al.*²² under identical conditions. These measurements yielded a translational temperature $T_t = 30(5)$ K. From the relative intensities of the observed transitions and the dependence of the LiNC beam intensity on the state selector voltage we estimated the rotational temperature of the LiNC molecules in the beam to be $T_r = 30(5)$ K. Since no excited vibrational states were observed, the vibrational relaxation of the LiNC molecules is expected to be strong.

Because of the high pyrophoricity of reactants such as powdered lithium metal, and the extreme toxicity of hydrogen cyanide gas, which is formed easily since LiNC is highly hydrolysis sensitive, the preparation of lithium isocyanide is hazardous and precautionary measures have to be taken. In all cases we started with chemical compounds which were dried and heated at an appropriate temperature in vacuum for a few hours. The solvents we utilized were first dried by refluxing over calcium hydride in the case of dimethylformamide (DMF) and lithium tetrahydridoaluminate in the case of tetrahydrofuran (THF), and by subsequent distillation. In order to produce and preserve anhydrous LiNC and for safety reasons, it was necessary to maintain a dry nitrogen atmosphere over the surface of the reaction mixtures and products. This was persevered during filtering off the reaction precipitate and filling the oven. The reaction product was stored under vacuum conditions.

Lithium isocyanide has been obtained by two totally different chemical reactions. The first method, adapted from Hoffman *et al.*²³, consisted of heating up to 950 K for 30 minutes an evacuated quartz cell filled with equimolar amounts of LiCl (6.4 g) and NaCN (7.4 g). After cooling and grinding, the sol-

ids were leached with 150 ml of dried DMF at reflux for 20 hours. Next, the hot solution was filtered, and upon standing and cooling a crystalline precipitate was filtered off. The filtrate, about 3.8 g of the adduct LiNC.DMF, was then vacuum dried at 420 K for 5 hours, and 2.6 g of DMF was removed. With the resulting solid we managed to produce a molecular beam of lithium isocyanide and measured for the first time microwave transitions of the molecule. However, the molecular beam was not very stable, probably due to residual impurities in the sample. The second method by which we prepared lithium isocyanide is basically the one described by Rossmanith²⁴. We distilled 400 ml dried THF over into a flask containing 17.5 g of AgCN, 1 g of powdered Li metal and 10 g of naphthalene. The resulting solution was refluxed for six hours and filtered when still hot. After cooling the solvent was filtered off, leaving the product as a greyish solid. This solid was washed with dried petroleum ether until the washings were clear, yielding 3.6 g of the adduct LiNC.THF. The product was dried by heating in vacuum, providing 1.4 g of solid lithium isocyanide. With this sample we checked our previous measurements and performed all the succeeding experiments. Material consumption was very low as a consequence of the seeded beam technique. A sample of about 0.25 g was sufficient to maintain a molecular beam during 20 hours.

Other methods were also tried to produce lithium isocyanide. The tantalum oven was loaded with equimolar amounts of two chemical compounds: Li and NaCN, LiCl and NaCN, or Li and AgCN, respectively. Neither of these efforts resulted in the synthesis of LiNC at elevated temperatures under proper molecular beam conditions.

3. RESULTS

The frequencies of the observed microwave transitions of lithium isocyanide in the ground vibrational state are listed in Table II. We measured three hyperfine transitions of the $J=1\rightarrow 0$ rotational transition of $^7\text{LiNC}$. The $J=2\rightarrow 1$ transition was observed as a many MHz's wide feature with hardly any structure. By applying microwave-microwave double resonance we were able to resolve and identify unambiguously seven hyperfine components of this rotational transition. The double resonance signals were observed by monitoring the intensity of a specific hyperfine component of the $J=1\rightarrow 0$ rotational transition, while simultane-

Table II. Frequencies (in MHz) of the observed and calculated transitions of LiNC in the ground vibrational state.

Isotope	J'→J''	F _ε '→F _ε ''	Obs. frequency	Obs.-calc.	Calc. ν ₀ ^a
⁷ LiNC	1→0	3/2 ₂ →1/2 ₁	26586.5982(50)	-0.0010	26586.4532(40)
		5/2 ₂ →3/2 ₁	26586.6480(30)	0.0008	
		3/2 ₃ →1/2 ₁	26587.9252(40)	-0.0008	
	2→1	1/2 ₂ →3/2 ₃	53171.3428(30)	-0.0002	53172.1271(25)
		5/2 ₃ →3/2 ₃	53171.3832(40)	0.0003	
		3/2 ₃ →3/2 ₃	53171.4258(30)	-0.0004	
		5/2 ₃ →5/2 ₂	53172.6615(40)	-0.0002	
		1/2 ₂ →3/2 ₂	53172.6749(70)	0.0051	
		3/2 ₃ →5/2 ₂	53172.7039(50)	-0.0011	
⁶ LiNC	1→0	2 ₂ →1 ₁	29183.0291(60)	0.0020	29182.8796(60)
		1 ₃ →0 ₁	29184.3479(60)	-0.0020	

^aν₀ is the frequency of the pure rotational transition corrected for nuclear hyperfine displacements.

ously another microwave radiation source was scanned around the frequency of the J=2→1 rotational transition. The two hyperfine components of the J=1→0 transition of the isotopic species ⁶LiNC have been observed in natural abundance. An example of the observed spectra is shown in Figs. 2 and 3.

The observed transition frequencies from Table II were fitted by a least-squares method using a computer program for the hyperfine interaction in molecules with two nuclei possessing couplings of comparable strength. This program⁶ employs the general expressions derived by Thaddeus *et al.*²⁵ for the matrix elements of the hyperfine Hamiltonian including quadrupole, spin-rotation and spin-spin interaction. In the representation used, the nucleus with spin indicated by I₁ couples first to the molecular rotational angular momentum J to form a resultant F₁; then the nucleus with spin I₂ couples with F₁ to form the total angular momentum F. After diagonalization, the energy states are labeled by the quantum numbers J and F, and by a pseudo spin quantum number ε. For a given J and F, the state lowest in energy is denoted with ε=1; the states higher in energy are labeled ε=2,3,... consecutively. In the case of ⁶LiNC,

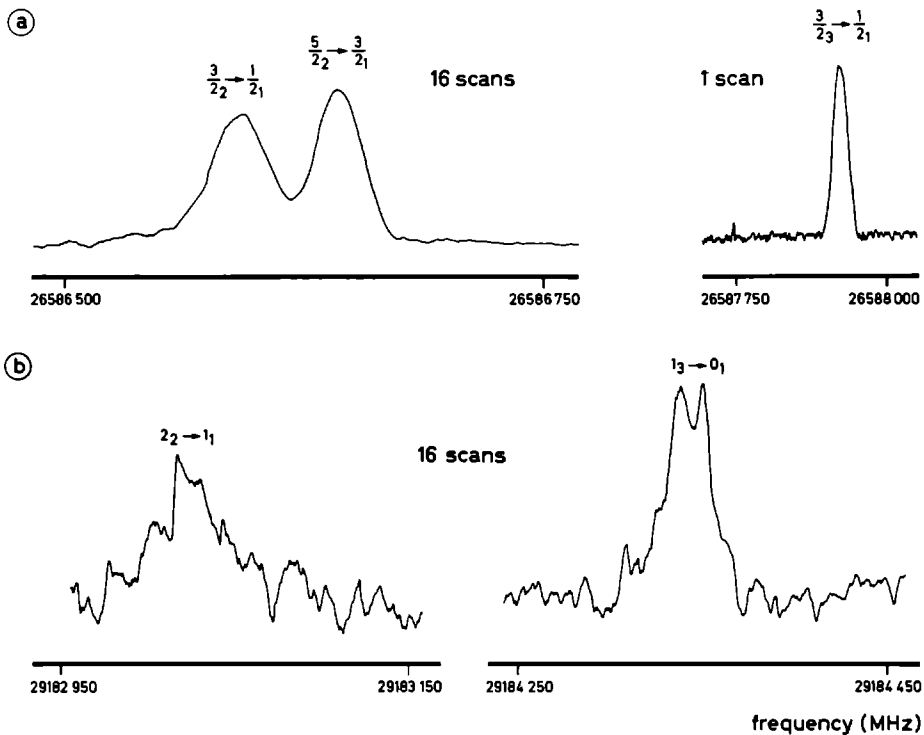


Fig. 2. Spectral recording of the $J=1 \rightarrow 0$ rotational transitions of ${}^7\text{LiNC}$ (a) and ${}^6\text{LiNC}$ (b) in the ground vibrational state. The full linewidth at half height is 30 kHz. The hyperfine structure transitions are indicated as $F_{\epsilon}' \rightarrow F_{\epsilon}''$.

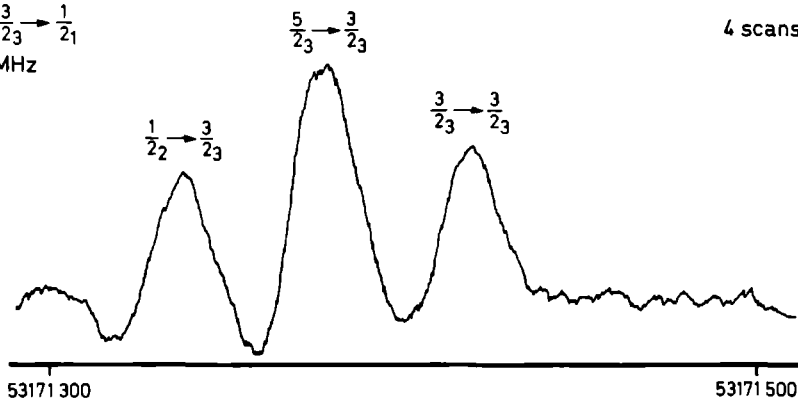
where the energy of the quadrupole interaction of the lithium nucleus is only ~ 2 kHz, we used the same labelling for reasons of consistency.

The best fit values²⁶ for the frequencies ν_0 of the hyperfine-free origins of the rotational transitions, the quadrupole coupling constants $eQq(\text{Li})$ and $eQq(\text{N})$, and the spin-rotation coupling constant $c(\text{Li})$ of ${}^7\text{LiNC}$ in the ground vibrational state are given in Tables II and III. The spin-rotation coupling of the nitrogen nucleus could not be determined and has been fixed at zero. In the least-squares fit, the spin-spin coupling constant $d(\text{Li-N})$ has been constrained at the value calculated from the geometry using the relation:

$$d = g_1 g_2 \mu_N^2 r_{12}^{-3}, \quad (1)$$

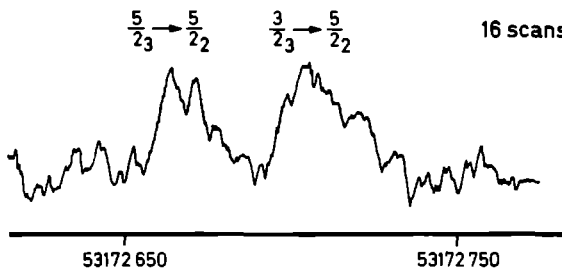
$J=1 \rightarrow 0, F_{\epsilon} = \frac{3}{2_3} \rightarrow \frac{1}{2_1}$
 $\nu = 26587925 \text{ MHz}$

4 scans



$J=1 \rightarrow 0, F_{\epsilon} = \frac{5}{2_2} \rightarrow \frac{3}{2_1}$
 $\nu = 26586648 \text{ MHz}$

16 scans



$J=1 \rightarrow 0, F_{\epsilon} = \frac{3}{2_2} \rightarrow \frac{1}{2_1}$
 $\nu = 26586598 \text{ MHz}$

16 scans

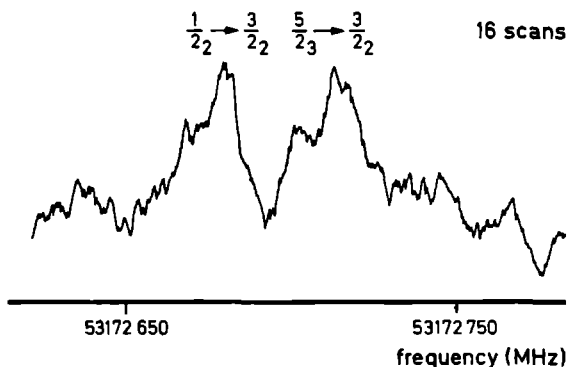


Fig 3. Spectral recording of the $J=2 \rightarrow 1$ rotational transition of ${}^7\text{LiNC}$ in the ground vibrational state by means of microwave double resonance spectroscopy. The full linewidth at half height is 20 kHz. The hyperfine structure transitions are indicated as $F_{\epsilon}' \rightarrow F_{\epsilon}''$. The quantum numbers and frequencies of the hyperfine transitions of the rotational transition $J=1 \rightarrow 0$ used for double resonance are stated.

where g_1 and g_2 are the nuclear g -factors, μ_N is the nuclear magneton, and $r_{12} = r_{\text{LiN}} = 1.760 \text{ \AA}$ (this work). For ${}^6\text{LiNC}$, the hyperfine coupling constants were constrained in the fit at the values obtained for ${}^7\text{LiNC}$, corrected²⁷ for the change of the nuclear electric quadrupole moment Q and the nuclear g -factor of Li.

Using the relation²⁷ for the frequencies of rotational transitions $J+1 \rightarrow J$ for linear molecules:

$$\nu = 2B_0(J+1) - 4D_0(J+1)^3, \quad (2)$$

we can determine the rotational constants B_0 and D_0 for the ground vibrational state of lithium isocyanide. The results are presented in Table III.

Table III. Hyperfine coupling constants^a and rotational constants for the ground vibrational state of LiNC.

Isotope	Constant	Value	Unit
${}^7\text{LiNC}$	$eQq(\text{Li})$	0.364(20)	MHz
	$eQq(\text{N})$	-2.941(9)	MHz
	$c(\text{Li})$	1.0(8)	kHz
	$d(\text{Li-N})^b$	0.61864	kHz
	B_0	13293.292(3)	MHz
	D_0	32.5(4)	kHz
${}^6\text{LiNC}$	B_0^c	14591.505(20)	MHz
	D_0^d	32.5	kHz

^aThe following convention has been used: $eQq \equiv eQq_{aa} = -2eQq_{bb} = -2eQq_{cc}$, $c \equiv c_{cc} = c_{bb}$, $d \equiv d_{cc} = d_{bb} = -\frac{1}{2}d_{aa}$. The a axis is the molecular symmetry axis.

^bThe spin-spin coupling constant $d(\text{Li-N})$ has been constrained at the value determined from the structure with $r_{\text{LiN}} = 1.760 \text{ \AA}$.

^cThe uncertainty in B_0 is based on an assumed uncertainty of 30% in the fixed value of D_0 .

^dThe D_0 constant of ${}^6\text{LiNC}$ has been constrained at the value of the D_0 constant of ${}^7\text{LiNC}$.

Table IV. The effective structural parameters for the ground vibrational state of LiNC.

Constant	Value (Å)
r_{LiN}^a	1.760(6)
r_{CN}	1.168(6)

^aThe uncertainty in the CN bond length has been assumed to be twice the uncertainty in the case of KCN⁴ and NaCN¹⁰.

A T-shaped structure for LiNC can be excluded, since this would give rise to a spectrum of an asymmetric top molecule with many transitions below 40 GHz. Searches in the region of 9.5-40 GHz for such a spectrum were negative. It is not possible to determine unambiguously the structure of a nonsymmetric, triatomic linear molecule from the rotational constants of only two isotopic species. However, the vibrational isotope effects of lithium isocyanide as observed in inert gas matrices clearly indicate^{15,28} that under the assumption of a linear structure the isocyanide configuration is lower in energy than the cyanide configuration. So, in the case of lithium isocyanide there is experimental evidence to remove the ambiguity in the structure and to justify the conclusion that LiNC is more stable than LiCN. The effective structural parameters for the ground vibrational state of lithium isocyanide were calculated using the rotational constants B_0 of ⁷LiNC and ⁶LiNC from Table III. The results are given in Table IV.

Two additional arguments against the cyanide configuration as the most stable structure can be inferred from *ab initio* calculations^{2,6-10}. Under the assumption of a linear cyanide configuration, the rotational constants B_0 from Table III yield the following structural parameters: $r_{\text{LiC}} = 1.670$ Å, $r_{\text{CN}} = 1.168$ Å. The *ab initio* cyanide structures, listed in Table I, predict $r_{\text{LiC}} \geq 1.92$ Å. Inclusion of correlation, essential for more accurate predictions^{9,10,11,29}, even consistently increases the bond length predictions²⁹, which makes the disagreement between the *ab initio* bond length r_{LiC} and the value obtained from the experiment when assuming a cyanide configuration even larger. The hyperfine quadrupole coupling constants (in MHz) evaluated³⁰ from the *ab initio* calculation by Essers *et al.*² are: $eQq(\text{Li}) = 0.405$, $eQq(\text{N}) = -2.891$ for LiNC, and $eQq(\text{Li}) = 0.403$, $eQq(\text{N}) = -4.983$ for LiCN, re-

spectively. Table III shows, that the calculated $eQq(N)$ for LiNC is in close agreement with the experimental value, while the calculated $eQq(N)$ for LiCN is off by almost a factor of two. The calculated $eQq(Li)$ is about the same for LiNC and LiCN and is in gratifying agreement with the experimental value.

4. DISCUSSION

The current study presents the first experimental investigation of the structure of gaseous lithium isocyanide by means of high resolution molecular beam electric resonance spectroscopy. The agreement between our experimental results and the *ab initio* calculations is good, confirming that the most stable structure is the linear isocyanide configuration. An unambiguous structure determination from the rotational constants is possible by measuring more isotopic species of LiNC. Since the nitrogen nucleus is located very close to the centre of mass, no structural information can be obtained from the isotopic species $Li^{15}NC$. More can be learned from the rotational spectrum of $LiN^{13}C$. An effort to measure this isotopic species in natural abundance was unsuccessful due to lack of sensitivity. An attempt to increase the abundance of $LiN^{13}C$ in the molecular beam by loading the tantalum oven with equimolar amounts of LiNC and $K^{13}CN$ also failed.

A search for transitions of the LiNC molecule in an excited vibrational state was performed. However, due to the strong relaxation in the seeded supersonic beam, these states are not sufficiently populated to observe their spectrum. Since no transitions of the molecule LiCN were observed, less than 3% of the cyanide molecules in the beam was LiCN, the rest being LiNC. From this result a lower limit for the isomerization energy can be calculated: $\Delta E \geq 120 \text{ cm}^{-1}$.

Information on the excited vibrational states will reveal more about the electronic structure of lithium isocyanide. A MBER study might be possible if the vibrational relaxation of the cyanide molecules in the seeded molecular beam is reduced, e.g. by using a different carrier gas. Microwave absorption in a high temperature cell, as used for KCN by Kuijpers *et al.*³¹, is another method to observe the rotational transitions of LiNC in excited vibrational states. Far infrared ($100\text{-}800 \text{ cm}^{-1}$) Fourier spectroscopy is the appropriate method to measure directly the vibrational frequencies of the gaseous LiNC molecule. Such experiments, currently underway, will provide a further check for *ab initio* cal-

culations of the shape and depth of the potential energy surface^{2,6-10}, the force constants⁹, and the ro-vibrational spectrum^{2,32} of LiNC.

ACKNOWLEDGMENT

The authors like to thank Dr. C.J. Marsden for communicating his results prior to publication. The excellent technical assistance of Mr. F. van Rijn is gratefully acknowledged. One of us (JJvV) wishes to thank Dr. A.B. Voet for many fruitful discussions. This work is part of the research program of the Stichting voor Fundamenteel Onderzoek der Materie (F.O.M.) and has been made possible by financial support from the Nederlandse Organisatie voor Zuiver Wetenschappelijk Onderzoek (Z.W.O.).

REFERENCES

- ¹In this paper the alkali metal cyanides are denoted by MCN (where M represents the alkali metal), whatever the structure may be, and the atomic symbol designates the most abundant isotope, unless specified otherwise.
- ²R. Essers, J. Tennyson, and P.E.S. Wormer, *Chem. Phys. Lett.* **89**, 223 (1982); G.H.L.A. Brocks, and J. Tennyson, *J. Mol. Spectrosc.* **99**, 263 (1983).
- ³T. Törring, J.P. Bekooy, W.L. Meerts, J. Hoeft, E. Tiemann, and A. Dymanus, *J. Chem. Phys.* **73**, 4875 (1980).
- ⁴J.J. van Vaals, W.L. Meerts, and A. Dymanus, *34th Symposium on Molecular Spectroscopy* (Columbus, Ohio, 1980); *7th Colloquium on High Resolution Spectroscopy* (Reading, 1981); *J. Mol. Spectrosc.*, submitted (1983).
- ⁵J.J. van Vaals, W.L. Meerts, and A. Dymanus, *J. Chem. Phys.* **77**, 5245 (1982).
- ⁶B. Bak, E. Clementi, and R.N. Kortzeborn, *J. Chem. Phys.* **52**, 764 (1970).
- ⁷E. Clementi, H. Kistenmacher, and H. Popkie, *J. Chem. Phys.* **58**, 2460 (1973).
- ⁸L.T. Redmon, G.D. Purvis, III, and R.J. Bartlett, *J. Chem. Phys.* **72**, 986 (1980).
- ⁹A. Schmiedekamp, C.W. Bock, and P. George, *J. Mol. Struct.* **67**, 107 (1980).
- ¹⁰C.J. Marsden, private communication.
- ¹¹C.E. Dykstra, and D. Secrest, *J. Chem. Phys.* **75**, 3967 (1981).
- ¹²M.L. Klein, J.D. Goddard, and D.G. Bounds, *J. Chem. Phys.* **75**, 3909 (1981).
- ¹³C.J. Marsden, *J. Chem. Phys.* **76**, 6451 (1982).
- ¹⁴P.E.S. Wormer, and J. Tennyson, *J. Chem. Phys.* **75**, 1245 (1981); J. Tennyson, and B.T. Sutcliffe, *Mol. Phys.* **46**, 97 (1982); J. Tennyson, and A. van der Avoird, *J. Chem. Phys.* **76**, 5710 (1982); J. Tennyson, and B.T. Sutcliffe, *J. Chem. Phys.* **77**, 4061 (1982).
- ¹⁵Z.K. Ismail, R.H. Hauge, and J.L. Margrave, *J. Chem. Phys.* **57**, 5137 (1972); Z.K. Ismail, R.H. Hauge, and J.L. Margrave, *J. Mol. Spectrosc.* **45**, 304 (1973).
- ¹⁶G. Herzberg, *Electronic Spectra and Electronic Structure of Polyatomic Molecules* (Van Nostrand Reinhold, New York, 1966).
- ¹⁷G. Henderson, and G.E. Ewing, *Mol. Phys.* **27**, 903 (1974).

- ¹⁸J.J. van Vaals, Thesis, Katholieke Universiteit Nijmegen (1983).
- ¹⁹H. Dijkerman, W. Flegel, G. Gräff, and B. Mönter, *Z. Naturforsch.* **27a**, 100 (1972).
- ²⁰W.L. Meerts, J.P. Bekooy, and A. Dymanus, *Mol. Phys.* **37**, 425 (1979).
- ²¹A. Perret, and R. Perrot, *Comptes Rendus* **194**, 95 (1932); *Helv. Chim. Acta* **15**, 1165 (1932); *Comptes Rendus* **196**, 268 (1933); A. Perret, and J. Riethmann, *Helv. Chim. Acta* **26**, 740 (1943); *Gmelins Handbuch der anorganischen Chemie* nr. 20, Lithium, Ergänzungsband (Verlag Chemie, Weinheim, 1960).
- ²²W.L. Meerts, G. ter Horst, J.M.L.J. Reinartz, and A. Dymanus, *Chem. Phys.* **35**, 253 (1978).
- ²³D.K. Hoffman, and R.O. Bach, U.S. Patent 3,846,494 (1974).
- ²⁴K. Rossmannith, *Monatsh. Chem.* **96**, 1690 (1965).
- ²⁵P. Thaddeus, L.C. Krisher, and J.H.N. Loubser, *J. Chem. Phys.* **40**, 257 (1964).
- ²⁶All uncertainties stated in this paper represent three times the standard deviation as determined by the least-squares fit.
- ²⁷W. Gordy, and R.L. Cook, *Microwave Molecular Spectra* (Interscience, New York, 1970).
- ²⁸K. Nakamoto, D. Tevault, and S. Tani, *J. Mol. Struct.* **43**, 75 (1978).
- ²⁹C.E. Dykstra, *Ann. Rev. Phys. Chem.* **32**, 25 (1981).
- ³⁰We used $Q(^7\text{Li}) = -0.0366$ barn, and $Q(^{14}\text{N}) = 0.0166$ barn. These values are from: C.M. Lederer, and V.S. Shirley (eds.), *Table of Isotopes*, Seventh Edition (Wiley & Sons, New York, 1978).
- ³¹P. Kuijpers, T. Törring, and A. Dymanus, *Chem. Phys. Lett.* **42**, 423 (1976).
- ³²V.A. Istomin, N.F. Stepanov, and B.I. Zhilinskii, *J. Mol. Spectrosc.* **67**, 265 (1977); B.I. Zhilinskii, V.A. Istomin, and N.F. Stepanov, *Chem. Phys.* **31**, 413 (1978); P.R. Bunker, and D.J. Howe, *J. Mol. Spectrosc.* **83**, 288 (1980).

HOGE RESOLUTIE MOLECULAIRE BUNDEL ONDERZOEK
VAN
ALKALICYANIDES

Het proefschrift beschrijft een onderzoek naar fundamentele fysische eigenschappen, zoals de internucleaire afstanden, de rotatiestructuur en de hyperfijnstructuur van kaliumcyanide, natriumcyanide en lithiumisocyanide en hun isotopen.

Hiertoe werd gebruik gemaakt van moleculaire-bundel elektrische-resonantie (MBER) spectroscopie in het microgolfgebied. Met deze techniek is het mogelijk de moleculen over een groot frequentiegebied te onderzoeken (in dit onderzoek 9-54 GHz), met een hoge gevoeligheid die onafhankelijk is van de grootte van de waargenomen energiever verschillen (doordat het *aantal* deeltjes dat een overgang maakt wordt gedetecteerd met een 100% efficiënte detector), en een zeer hoog oplossend vermogen (in de orde van 10 kHz).

De "seeded beam"-techniek is toegepast, waarbij de bundel gevormd wordt door middel van een supersone expansie door een "nozzle" van een mengsel van een edelgas en het te onderzoeken molecuul in een lage concentratie (0.1-1%). Op deze wijze wordt een bundel met een zeer lage interne rotatie- en vibratietemperatuur verkregen. Ten gevolge van deze koeling in de bundel zijn aanzienlijk minder rotatie- en vibratietoestanden bezet, waardoor de gevoeligheid vergroot en de identificatie van het spectrum mogelijk wordt. Bij de hoge temperatuur (1000 °C) van de bron, een dubbele-kameroven, noodzakelijk om voldoende hoge dampdruk (ongeveer 1 mbar) van de alkalicyanidemoleculen te verkrijgen, wordt het vormen van een stabiele molecuulbundel bemoeilijkt door reacties tussen de moleculen en het materiaal van de ovenwand, thermische dissociatie, polymerisatie en het verstopt raken van de "nozzle".

Tot voor kort werd algemeen aangenomen dat de moleculaire structuur van de alkalicyanides lineair is, net als het geval is bij de andere drie-atomige cyanides zoals HCN, FCN, ClCN, BrCN en ICN. Na recente experimentele resultaten werd duidelijk dat de structuur van kaliumcyanide T-vormig is. Aangezien echter slechts aan één isotoop was gemeten, bleek het niet mogelijk een eénduidig resultaat voor de geometrie te geven.

In het proefschrift wordt beschreven hoe dit probleem is opgelost door het bestuderen van de isotopisch gesubstitueerde moleculen $K^{13}CN$ en $KC^{15}N$. Bij de identificatie van de zeer gecompliceerde hyperfijnspectra werd met veel succes de microgolf-microgolf dubbel-resonantie techniek toegepast. De kennis van de hyperfijnopsplitsingen geeft informatie over de elektronische ladingsverdeling en maakte een nauwkeurige analyse van de rotatiespectra, beschreven met het asymmetrische-rotormodel, van KCN, $K^{13}CN$ en $KC^{15}N$ mogelijk. De hyperfijn- en rotatieconstanten werden bepaald. Uit de laatste konden de effectieve- en de substitutiestructuur van kaliumcyanide in de grond-vibratietoestand nauwkeurig worden berekend, waarbij éénduidig de T-vormige geometrie werd bevestigd.

Hierna werd de bestudering van het NaCN-molecuul ter hand genomen. Nadat de aanvankelijke problemen met de bundelproductie, die samenhangen met de instabiliteit bij $1000\text{ }^{\circ}C$ van het natriumcyanidemolecuul in de roestvast stalen oven, waren opgelost, zijn de hyperfijn- en rotatiespectra gemeten van NaCN en $Na^{13}CN$. Analyse en identificatie van de spectra, waarbij de rotatiestructuur aan het asymmetrische-rotormodel voldeed, resulteerde in de nauwkeurige bepaling van hyperfijn- en rotatieconstanten. Ook voor natriumcyanide werd een voorheen niet verwachte T-vormige effectieve structuur gevonden.

Het LiNC is zelfs bij kamertemperatuur instabiel, zodat het niet commercieel verkrijgbaar is. Een tweetal geheel verschillende chemische produktiemethoden werd gebruikt om het LiNC te vervaardigen. Voor dit molecuul werd een oven van het minder reactieve tantaal ontworpen. Hierdoor werd het mogelijk ook van LiNC een moleculaire bundel te produceren. De rotatie- en hyperfijnspectra van 7LiNC en 6LiNC werden waargenomen. De analyse van de hyperfijnstructuur werd uitgevoerd met behulp van microgolf-microgolf dubbel-resonantie metingen. De hyperfijn-, rotatie- en structuurparameters werden bepaald. Het LiNC-molecuul is in tegenstelling tot KCN en NaCN *lineair* met het lithiatoom aan de kant van het stikstofatoom, dus lithiumisocyanide.

Vast is komen te staan dat de alkalicyanides onderling sterk verschillende structuren hebben die niet eenvoudig te voorspellen zijn. De moleculen zijn "floppy": het alkali-atoom kan grote interne bewegingen beschrijven ten opzichte van de CN-groep. In KCN en NaCN kan de cyanidegroep beschouwd worden als een vrijwel ongestoord CN^{-} -ion. De wisselwerking tussen het in het proefschrift beschreven experiment en hierdoor geïnitieerde *ab initio* berekeningen heeft reeds geresulteerd in een beter begrip van dergelijke moleculen, die een klasse apart vormen tussen de moleculen met een stevige covalente binding en de los gebonden Van der Waals-complexen.

CURRICULUM VITAE

Op 6 februari 1955 ben ik geboren te Gilze en Rijen. De middelbare schoolopleiding volgde ik aan het Sint-Montfortcollege te Rotterdam en het Mgr. Frencken College te Oosterhout (N.Br.), alwaar ik in 1972 het diploma H.B.S.-B behaalde. Aansluitend werd de studie natuurkunde gevolgd aan de Katholieke Universiteit te Nijmegen. De kandidaatsexamens natuurkunde (N1) en sterrenkunde (A1) werden behaald in oktober 1975 en na een afstudeerstage op de afdeling Atoom- en Molecuulfysica volgde het doctoraal examen experimentele natuurkunde met groot bijvak capita uit de experimentele natuurkunde in november 1979. Na mijn afstuderen bleef ik, als wetenschappelijk medewerker in F.O.M.-verband, aan deze groep verbonden. Hier heb ik mijn promotieonderzoek verricht onder leiding van Prof.dr. A. Dymanus en Dr. W.L. Meerts. De resultaten van dit onderzoek zijn beschreven in het proefschrift.

Van 1976 tot 1979 ben ik als student-assistent werkzaam geweest bij de werkgroep Sociale Systemen van de subfaculteit Psychologie, in de functie van computerprogrammeur.

Van 1978 tot 1983 heb ik, eerst als student-assistent en later in het kader van mijn onderwijsstaak als wetenschappelijk medewerker, geassisteerd bij practica en werkcolleges voor natuurkunde- en scheikundestudenten.

STELLINGEN

1. In de interpretatie van de botsingsgeïnduceerde rotatieovergangen voor formaldehyde door Chardon *et al.* dienen de effecten van de broncondities en de toestandsselectoren niet verwaarloosd te worden.
J.-C. Chardon, C. Gentry, E.K. Hill, et J.-C. Labrune, J. Physique 44, 1149 (1983).
2. De eerste blauw-verschoven lijn in het ν_3 -CARS spectrum van SF₆ is waarschijnlijk niet de ν_4 , maar de $\nu_4 + \nu_6$.
S.S. Alimpiev, B.O. Zikrin, L. Holz, S.M. Nikiforov, V.V. Smirnov, B.G. Sartakov, V.I. Fabelinskii, and A.L. Shtarkov, Laser Spectroscopy VI, eds. H.P. Weber, and W. Lüthy (Springer-Verlag, Berlin, 1983).
3. De S₀-S₁ overgang in pyrazine moet gekarakteriseerd worden als een singlet-triplet overgang.
B.J. van der Meer, H.Th. Jonkman, J. Kommandeur, W.L. Meerts, and W.A. Majewski, Chem. Phys. Lett. 92, 565 (1982).
4. De bepaling van de T-vormige structuur van KCN zal de resultaten voor de thermodynamische functies, berekend onder de aanname van een "polytopic" structuur, zeker veranderen.
K. Skudlarski, and M. Miller, High Temp. Sci. 15, 151 (1982).
5. De opmerking van L'vov en Pelieva dat Leroi en Klemperer de rotatiestructuur van KCN en NaCN hebben onderzocht is onjuist.
B.V. L'vov, and L.A. Pelieva, Prog. Analyt. Atom. Spectrosc. 3, 65 (1980).
G.E. Leroi, and W. Klemperer, J. Chem. Phys. 35, 774 (1961).
6. Eenvoudige goniometrische berekeningen zijn soms moeilijker dan ingewikkelde *ab initio* SCF berekeningen, zoals blijkt uit de foutieve waarden voor θ_e (KNC) berekend door Klein *et al.*.
M.L. Klein, J.D. Goddard, and D.G. Bounds, J. Chem. Phys. 75, 3909 (1981).

7. Het bepalen van het aantal bladzijden gemaakt met een geavanceerde printer aangesloten op een grote computer met behulp van een brievenweger leidt tot onnodige onnauwkeurigheid.

8. Er is slechts een kwantitatief verschil tussen rokers, die er verantwoordelijk voor zijn dat niet-rokers in dezelfde ruimte aanwezig bijna evenveel schadelijke stoffen binnenkrijgen als zichzelf, en bedrijven die soortgelijke stoffen in het milieu lozen.

